The Bell System Technical Journal

July, 1929

Magnetic Alloys of Iron, Nickel, and Cobalt [1]

By G. W. ELMEN

SYNOPSIS: Recent investigations of magnetic properties of alloys of iron, nickel and cobalt have resulted in the discovery of materials of remarkable magnetic properties previously unknown. In a brief review, early experiments that led to the discovery of these materials and the magnetic properties of the entire field are discussed. Those groups of alloys of outstanding scientific and technical importance such as the permalloys and the perminvars and special heat treatment required for development of special magnetic properties are taken up in detail. A theory is suggested to account for some of the magnetic characteristics, and a few of the practical applications of these materials are described.

IF the three ferromagnetic metals—iron, nickel and cobalt—are melted together in various proportions, all of the resultant alloys are magnetic when the materials used are reasonably pure. The magnetic properties of the alloys, however, vary greatly with composition and heat treatment. Some alloys have been found to be nearly non-magnetic; others have higher permeability than any hitherto known magnetic material and may be magnetically saturated in the earth's field. Still others are superior at high field strengths or excel in constancy of permeability at low fields.

In the Bell Telephone Laboratories we have been especially interested in these alloys and have made a fairly complete survey of the magnetic properties of the whole field of compositions of these metals. In this address I wish to tell you how our interest in those alloys was aroused, what our procedure was in carrying out the investigation, and what some of the principal results were. I shall also refer to some of the particular applications which we have made as a result of our discoveries.

I first became interested in these alloys in 1913. At that time I was looking for a magnetic material which would be more suitable for certain uses in the electrical communication field than the iron then used. Of the large number of alloys investigated, several contained principally iron and nickel. One of these was particularly interesting. The composition of this alloy was approximately 70 per cent nickel and 30 per cent iron; it was a commercial alloy used as a special resistance material. In the hard worked condition in which it was

[1] *Journal of the Franklin Institute,* Vol. 207, May, 1929, pp. 583–617.

supplied, its magnetic properties were not even as good as iron in a similar magnetic condition, but when heat treated it was superior to the iron at low field strengths, the region in which I was especially interested.

This alloy differed from iron in another important characteristic. Experience with iron had shown that the best magnetic quality was obtained when the material was heated to a high temperature, and then cooled slowly to room temperature. It was considered particularly important to cool slowly in order to give the iron time to pass through its transformations and to allow it to build up a large grain structure. When the nickel-iron alloy was heat treated in this manner, it was found to have lower permeability than it has when cooled fairly rapidly.

The discovery that rapid cooling was required for this alloy to give the best magnetic quality was one of the major contributions from our early work. It showed us that one of the important factors in developing the magnetic properties of new alloys was the determination of the rate of cooling for the best magnetic quality for each alloy.

Another difference between this alloy and iron relates to the energy loss caused by the hysteresis at low flux densities. In this range iron has lower hysteresis loss when it is in a mechanically hard condition than when it is well annealed. As the flux density increases, however, the hysteresis loss of the hard material increases more rapidly than does that of the annealed and at medium and high flux density, the mechanically hard iron is much inferior. Tests on the nickel-iron alloy show that both for high and low flux densities the hysteresis loss was a great deal higher for the mechanically hard material than for the one heat treated to give the best magnetic quality.

The discovery of the unusual magnetic properties of this 70–30 per cent nickel-iron alloy gave us the lead that we were looking for, and started our investigation of the magnetic properties of the whole series of nickel-iron alloys. We found, as we had reason to expect, that the 70–30 per cent alloy was one of a large group of alloys in the same series which had similar magnetic properties. In fact substantially all of the alloys containing more than 30 per cent nickel had similar characteristics except that some of them were not as sensitive to heat treatment as the first alloy we had tested.

Because of the technical possibilities of the nickel-iron alloys, we spent several years in their investigation and their commercial application. We were especially concerned with increasing the resistivity of a number of these alloys, and with this in view we added other elements to the iron and nickel in order to determine their effect both on the resistivity and the magnetic properties. Copper, chromium, molybdenum, tungsten, and tantalum are a few of those we added; also the magnetic element cobalt. The striking results obtained with the addition of cobalt to the iron-nickel alloys led us to make a com-

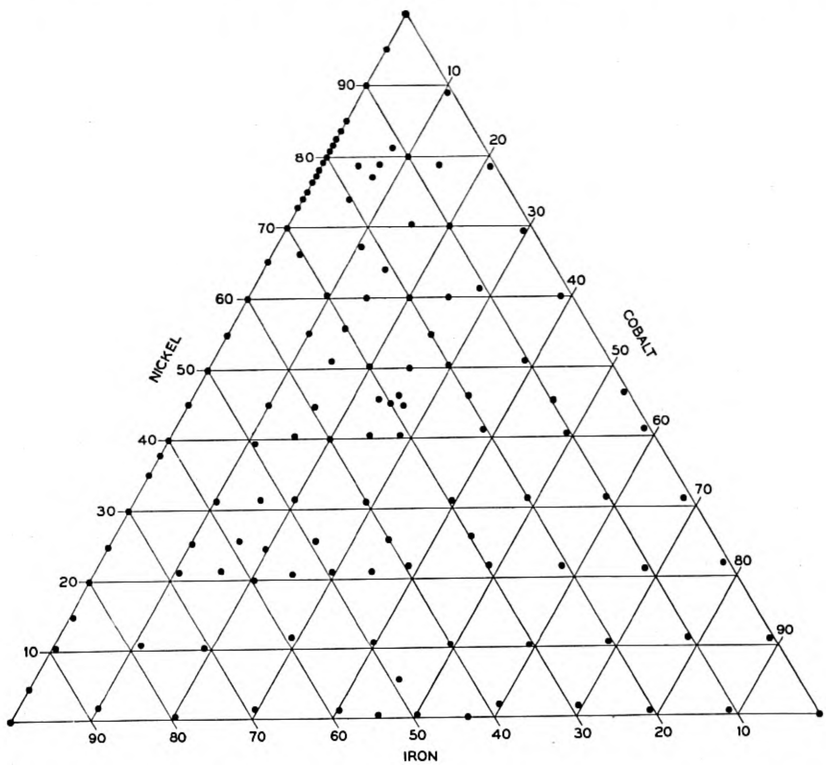

Fig. 1—Composition diagram—Ni-Fe-Co series. Dots show compositions tested.

plete survey of the whole field of alloys containing the three magnetic metals.

A convenient way of showing graphically the number of alloys we investigated and the distribution of compositions of these alloys is afforded by the equilateral composition triangle in Fig. 1. In this triangle the metals—iron, nickel, and cobalt—are represented by the corners; the binary alloys by points on the three sides, and the ternary alloys by points within the area of the triangle. Each alloy we investigated is indicated by a dot and the location of each dot indicates the proportion in per cent of the three metals in the alloy. A glance at the diagram will give you an appreciation of the completeness with which the field was covered.

In preparing these alloys we used the best commercial materials available. These contained small amounts of impurities, some of which affect unfavorably the magnetic properties. It was considered beyond the scope of this investigation, in which such a large number of alloys were required, to attempt to remove these impurities completely or even partially. Moreover we were especially interested in alloys which could be reproduced on a commercial scale, without too great cost due to refinements of raw materials or to methods of preparing the alloys.

Throughout the investigation we have followed a standard procedure for preparing our samples. We have also followed a standard procedure for heat treating and in magnetic measurements. The result is that we have accumulated a large mass of data over a number of years, all of which may be significantly compared.

The alloys were cast from Armco iron, electrolytic nickel, and a very high grade of commercial cobalt containing only small amounts of impurities. They were melted together in the desired proportions in a silica crucible in a high frequency induction furnace. The metal was cast into bars 18 in. long and ¾ in. in diameter. The bars were rolled or swaged into ¼ in. rods; then they were drawn into wire and flattened and trimmed into ⅛ in. by .006 in. tape. The material was annealed several times in the reduction process, for the cold working hardened the alloys rapidly and made them difficult to work.

To prepare the tape for heat treatment and subsequent magnetic measurements, about 30 ft. of it was wound spirally into a ring of 3 in. inside diameter, the ends being spot welded to the adjacent turns. Care was taken to wind the rings loosely to prevent the turns from sticking to each other during annealing.

For convenient comparison of the magnetic properties of the alloys with those of the metals from which the alloys were cast, sample lots of the iron, nickel, and cobalt which we used in making the alloys, were melted, cast, and prepared in the same manner as the alloy test samples.

In Fig. 2 the various steps through which the alloys had to pass in the mechanical reduction to tape are shown. Between each step in the reduction, as indicated by a sample, the alloy had to be annealed to remove the mechanical hardness. A sample ring wound from the finished tape, ready for heat treatment, is also shown in the figure.

The next step in the process of preparing these alloys for magnetic measurements is the heat treatment. Early experience with the nickel-iron alloys indicated the need for a variety of such treatments, but of course it was impossible to apply to every alloy such a complete variety of heat treatments, that all of the combinations of heat treatment and composition could be known. Our procedure was to apply three types of heat treatment.

A number of rings of a given composition were packed in a nichrome pot. The pot was placed in an electrical resistance furnace, the temperature of the furnace raised to between 900° and 1,000° C. and held at that temperature for one hour. The current was then turned

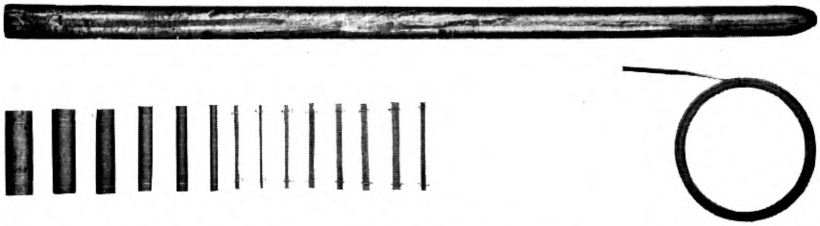

Fig. 2—Cast alloy bar and intermediate stages of samples in reduction to tape. Also ring from tape ready for heat treatment.

off and the pot cooled with the furnace. Ten hours were required for the furnace to cool to the temperature of the room. Between 700° C. and 400° C. the rate of cooling was approximately 1.5° C. per minute.

At least two rings of each composition were always annealed together. One of these rings received no further heat treatment. The second ring was heated for 15 minutes in a furnace held at 600° C., then removed and cooled rapidly on a copper plate in the air. With this cooling the rate was approximately 20° C. per second. In some cases a third annealed ring was heated 24 hours at 425° C.

In the discussions and in the figures, the rings which received the first heat treatment only are referred to as "annealed," those reheated to 600° C. and rapidly cooled as "air quenched," and those held for a long time at 425° C. as "baked." The magnetic measurements were made on these rings.

The magnetic induction, or flux density, was determined for a large number of magnetizing forces, beginning at a few thousandths of a gauss and increasing in uniform steps up to 100 gauss. Magnetization curves were plotted from these measurements. The induction was also determined for each composition at a magnetizing force of 1,500 gauss.

The permeabilities were computed from the induction measurements, and were plotted either against the flux density or the magnetizing force, depending on which graph illustrated best the characteristics of the material. At the lower ends these curves were extended to zero field strengths. Their intercepts on the permeability axis are the initial permeabilities. The maximum permeabilities were also obtained from these curves.

For determining hysteresis loss, two methods were used. In some cases hysteresis loops were plotted from ballistic measurements, and in other cases a direct determination of hysteresis loss was made from the apparent alternating-current resistance of a winding wrapped around the sample. Ordinarily the hysteresis loop was obtained for one condition only in which the flux density was varied between plus and minus 5,000 gauss. For some of the alloys of special interest, a large number of loops were obtained for different magnetizations, the maximum flux densities varying from 100 or less to 5,000 gauss.

In illustrating the magnetic properties I will be forced to limit the discussion to a few outstanding values for each alloy, and by comparing these, obtain a general view of the relation of the magnetic properties to composition. The values I have selected are the intrinsic inductions for two magnetizing forces, 50 and 1,500 gauss respectively, the initial and the maximum permeabilities and the hysteresis loss for a maximum flux density of 5,000 gauss. For a number of alloys which represent regions of composition with magnetic properties of special interest, curves for magnetization and permeability will be shown. A number of hysteresis loops for different maximum flux densities will also be given.

In illustrating graphically the relations between the magnetic properties and compositions of ternary alloys, it is convenient to plot these quantities in the form of solid diagrams. Such a diagram is shown in Fig. 3 constructed for initial permeabilities of the alloys in the annealed condition. In this figure the composition triangle, Fig. 1, is used as the base. On this triangle, verticals are erected proportional to the numerical values of the initial permeability. The ends of these verticals give a contour of the upper face of the figure. With a sufficient number of alloys this surface represents fairly accurately the values of the initial permeabilities for all compositions. The edges of the surface give the initial permeabilities of the binary alloys and the rest of the surface those of the ternaries.

The coordinates of the composition triangle, the intersections of which give the compositions of the alloys in 10 per cent variations, are projected to the surface and are represented by the narrow black lines. The heavy black lines on this surface are contours such as you see on topographical maps and represent the intersections with the surface of planes parallel to the base at definite elevations. Each line locates the compositions of those alloys which have equal values of initial permeability.

In this solid diagram of the initial permeabilities for the alloys in annealed conditions, there are three regions of composition which are

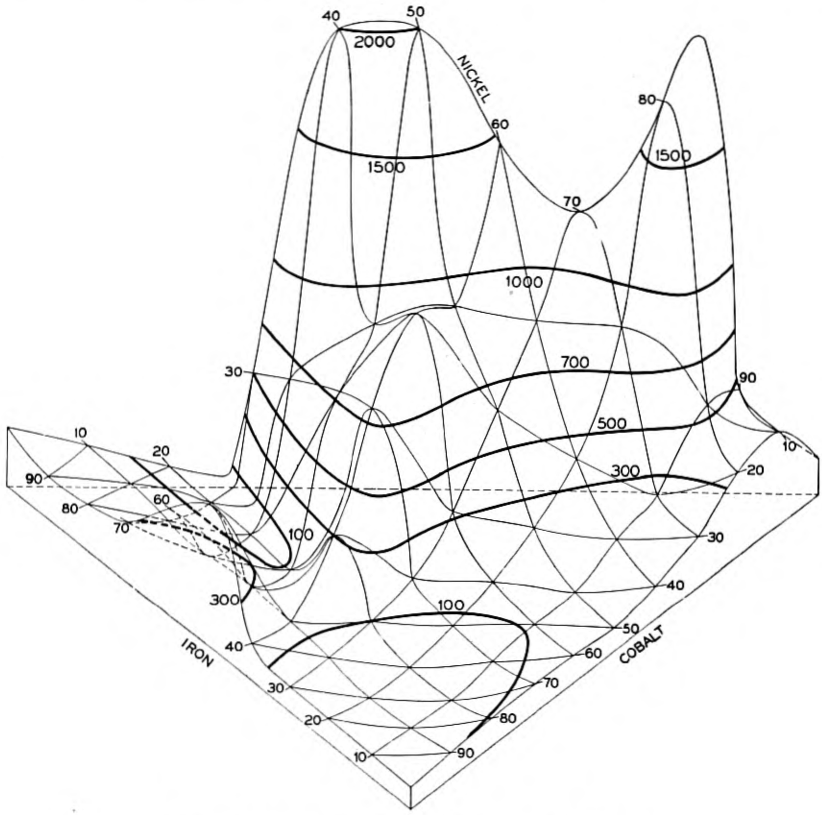

Fig. 3—Initial permeabilities for annealed alloys.

of special interest. The first of these is in the binary iron-nickel series represented by the back face of the diagram, which may be referred to as the nickel-iron plane. The nickel percentage is indicated by the numbers at the intersections of the permeability coordinates with the surface. The left-hand corner represents 100 per cent iron and the right-hand corner 100 per cent nickel, with initial permeabilities of 250 and 200, respectively. Between these limits of composition the initial permeability varies from approximately 100 to more than 2,000. With small additions of nickel to iron, the permeability drops gradually until the added amount is approximately 28 per cent of the composition. From that point there is a rapid rise in the permeability

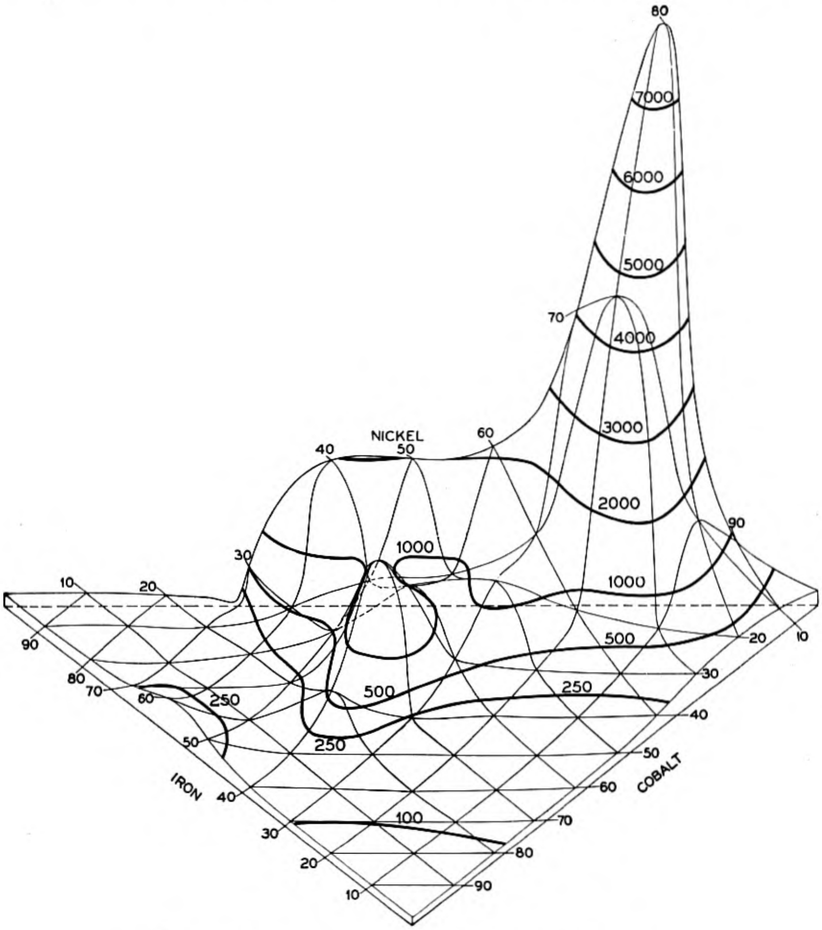

Fig. 4—Initial permeabilities for air-quenched alloys.

with the increase in the nickel content reaching a maximum of over 2,000 for the alloy containing approximately 45 per cent nickel. It then decreases as more nickel is added, reaching a second minimum of about 1,200 for 70 per cent nickel and increases again reaching a second maximum of approximately 1,900 at 83 per cent nickel.

Another region of special interest is found in the ternary series in front of the first maximum in the nickel-iron series. If you follow the coordinate from 40 per cent nickel, you will note an elevation between the 700 and 1,000 permeability contour lines. The ternary alloys of this region are remarkable, not because of their high permeabilities although they are higher than for the surrounding region, but because of the constancy of permeability and low hysteresis loss at low magnetizing forces.

Another region of interest is located in the iron-cobalt plane between 40 per cent and 70 per cent iron. This is the plane in the figure on which the iron percentages are marked. The initial permeability for the highest point is over 600, more than twice the initial permeability of Armco iron.

When the alloys are air quenched, the initial permeabilities change in some regions very materially and give us an entirely different looking solid diagram as shown in Fig. 4. Because of the very high values of the permeabilities a different scale was used in this figure from that used in Fig. 3. It is interesting to note how the rapid cooling has affected some of the binaries in the iron-nickel plane. The rise in permeability begins at about 28 per cent, the same as for the annealed alloys, and the initial permeabilities are substantially the same, up to about 45 per cent nickel. Between 45 per cent and about 90 per cent nickel, the permeabilities have increased to a remarkable degree. The valley we saw in the region 45–75 per cent nickel for the annealed alloys has disappeared, and from 55 per cent upward there is a rapid increase reaching a peak value of approximately 8,000 for the composition containing 78½ per cent nickel, an increase of over four times the permeability of the annealed alloy of the same composition.

Air quenching also increases the initial permeabilities of the group of ternary alloys which in the annealed condition showed a maximum characterized by a low hysteresis loss and a substantially constant permeability. This increase in permeability, however, is accompanied by a material increase in the hysteresis loss at low flux densities and a decrease in the constancy of permeability.

In contrast to the alloys just discussed, the iron-cobalt series in the neighborhood of 50 per cent iron gives a lower permeability upon rapid cooling. In this respect they behave the same as iron and cobalt.

The maximum permeabilities for the annealed alloys shown in Fig. 5 give a surface very similar to that for the initial permeabilities. The most interesting difference is the rapid decrease in permeability of iron as indicated at the left-hand corner of the diagram by the addition of small amounts of cobalt or nickel, 10 per cent of either being sufficient to reduce the maximum permeability 85 per cent. All of the iron-nickel alloys between 35 per cent and 85 per cent nickel have as high or higher permeability than Armco iron.

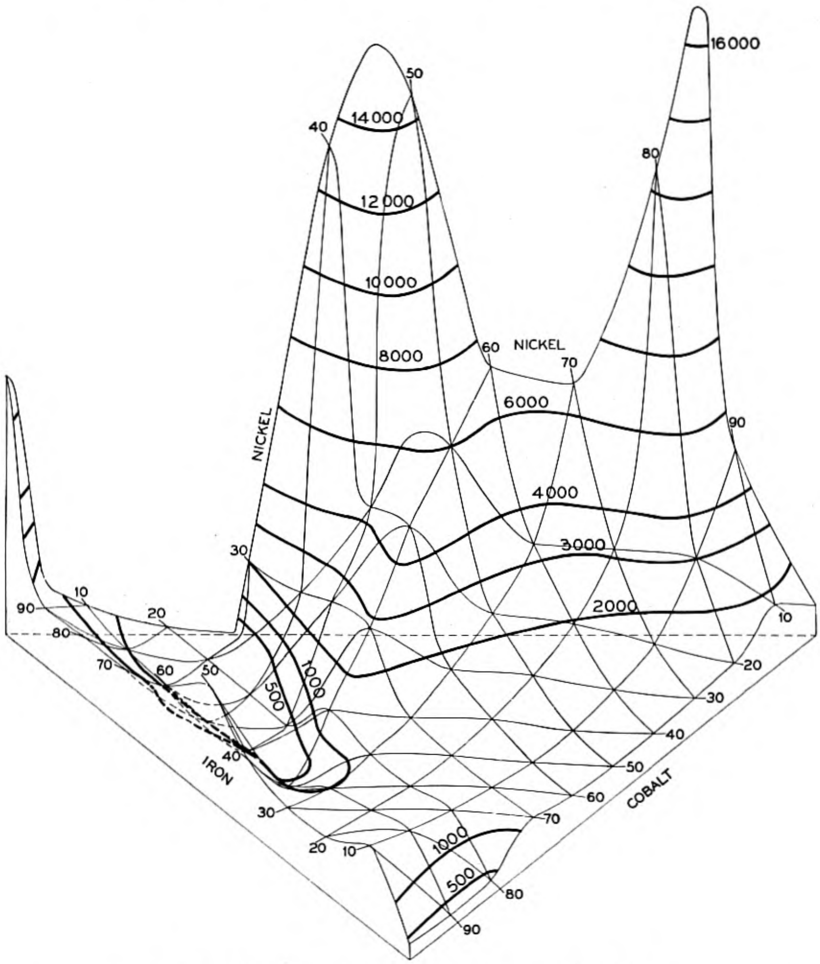

Fig. 5—Maximum permeabilities for annealed alloys.

I have not prepared a diagram for the maximum permeabilities for the air-quenched alloy. However, I can say that the surface obtained resembles the one shown for the initial permeabilities for the rapidly cooled alloys, although, of course, the maximum permeabilities are of different magnitudes. As high as 120,000 has been obtained for the alloy containing 78.5 per cent nickel.

The group of alloys of high permeability for low magnetizing forces in the iron-nickel series we have named permalloy.[2] The permalloys, therefore, include nickel-iron alloys containing more than approximately 30 per cent nickel. In referring to specific compositions in this group we have found it convenient to use as a distinguishing prefix for each composition its nickel content. For example, 78.5 permalloy is the alloy containing 78.5 per cent nickel and 21.5 per cent iron. When other elements are added to the permalloys, the chemical symbol and the percentage of the added element are also added to

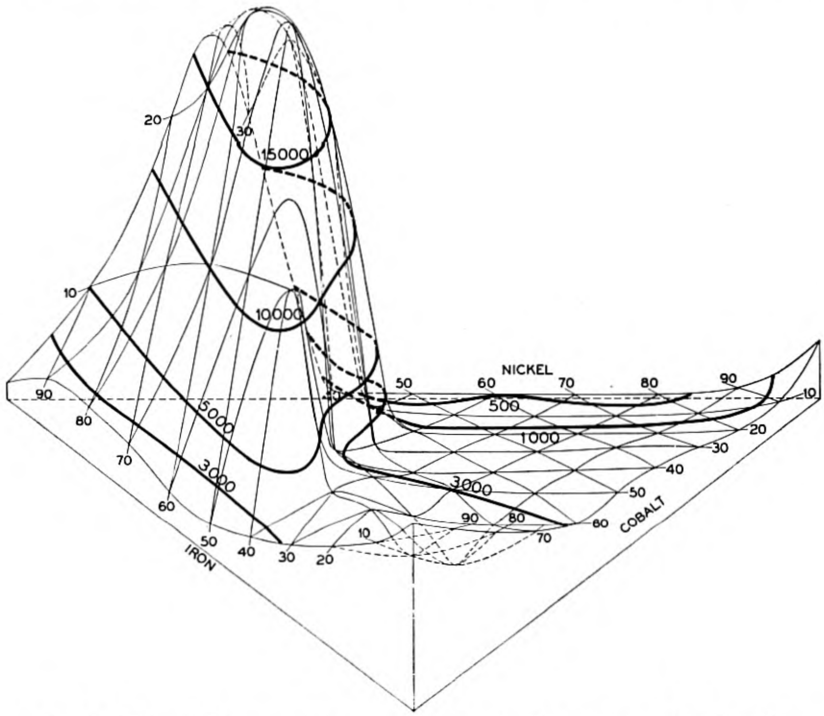

Fig. 6—Hysteresis losses, ergs per cm.[3] per cycle, for maximum flux density of 5,000 gauss for annealed alloys.

the prefix. For example, 3.5–78.5 Mo-permalloy is an alloy containing 3.5 per cent molybdenum, 78.5 per cent nickel, and 18 per cent iron.

The ternary alloys of constant permeability and extremely low hysteresis loss at low flux densities we have also grouped together under a common name, perminvar.[3] The limits of composition for the perminvars are less easily defined than for the permalloys, because the transition in magnetic properties is not as marked with small

[2] H. D. Arnold and G. W. Elmen, *Journal of Franklin Inst.*, May, 1923, p. 621.
[3] G. W. Elmen, *Journal of Franklin Inst.*, Sept., 1928, p. 317.

changes in composition. We have found that compositions between 10 per cent and 40 per cent iron, 10 per cent and 80 per cent nickel, and 10 per cent and 80 per cent cobalt have marked perminvar characteristics.

The hysteresis losses of the alloys in the annealed condition are plotted in Fig. 6 for a maximum flux density of 5,000 gauss. This

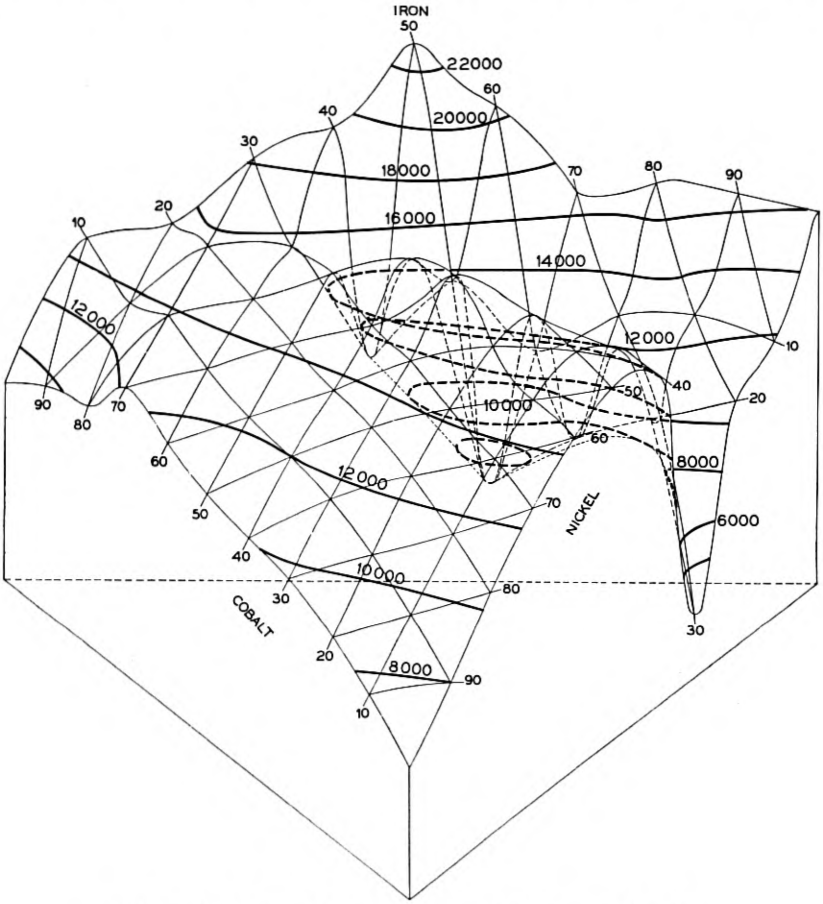

Fig. 7—Intrinsic inductions for annealed alloys at $H = 50$.

diagram illustrates again the abrupt change in the magnetic properties as we pass from alloys with large iron content to those in which nickel predominates. In this figure the lowest energy losses are those for alloys in the neighborhood of the 78.5 permalloy composition. In the iron-cobalt series the 50 per cent cobalt alloy has the lowest hysteresis loss.

The intrinsic inductions, which are those parts of the inductions contributed by the magnetic material, are shown in Fig. 7 for a magnetizing force of 50 gauss. In the figure the triangle has been turned through 120° clockwise from its position in the previous figures, placing the iron-cobalt alloys in the back of the diagram. For this

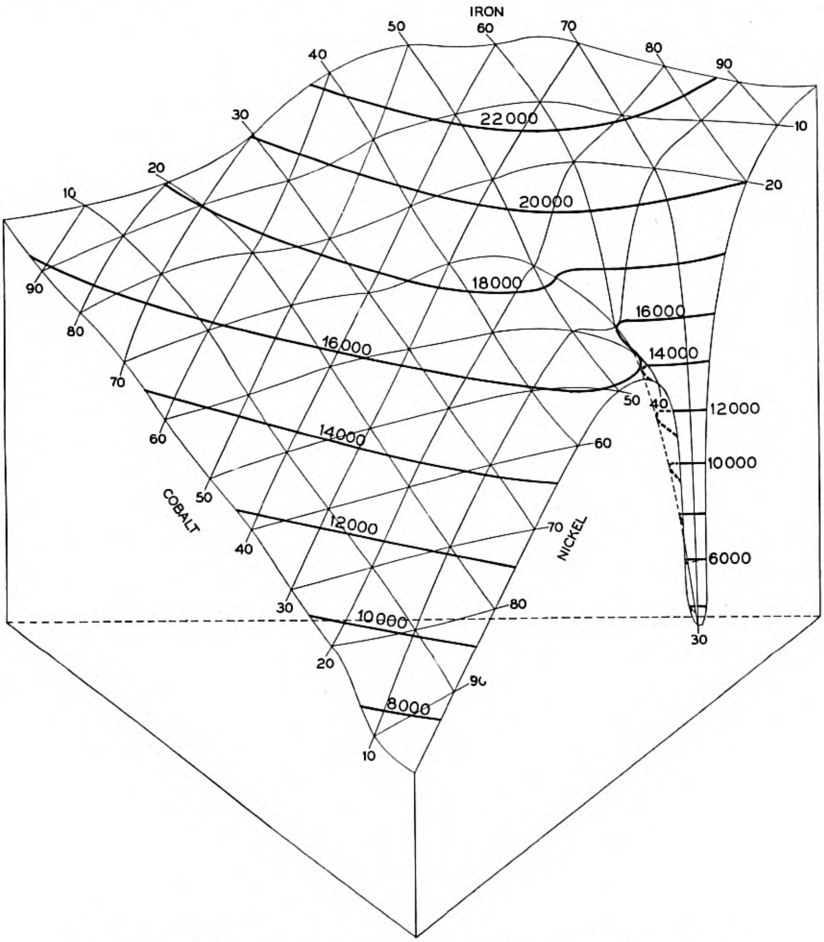

Fig. 8—Intrinsic inductions for annealed alloys at H = 1,500.

magnetization the 50 per cent iron-cobalt alloy is superior to any of the others.[4] Another interesting part of this diagram is the deep depression at about 30 per cent nickel, in the iron-nickel plane—now the right-hand front face of the diagram. This depression extends back for some distance into the ternary alloys.

[4] This was also found by Ellis, Engineering and Science Series No. 16, June, 1927, Rensselaer Polytechnic Institute.

The intrinsic inductions are also shown for a magnetizing force of 1,500 gauss in Fig. 8. Here we find that the irregularities of the surface in the previous figure have largely disappeared and the surface has become fairly flat. The inductions for the alloys in the neighborhood of 34 per cent cobalt and 66 per cent iron have now increased so that they are practically the same as for the 50 per cent composition.

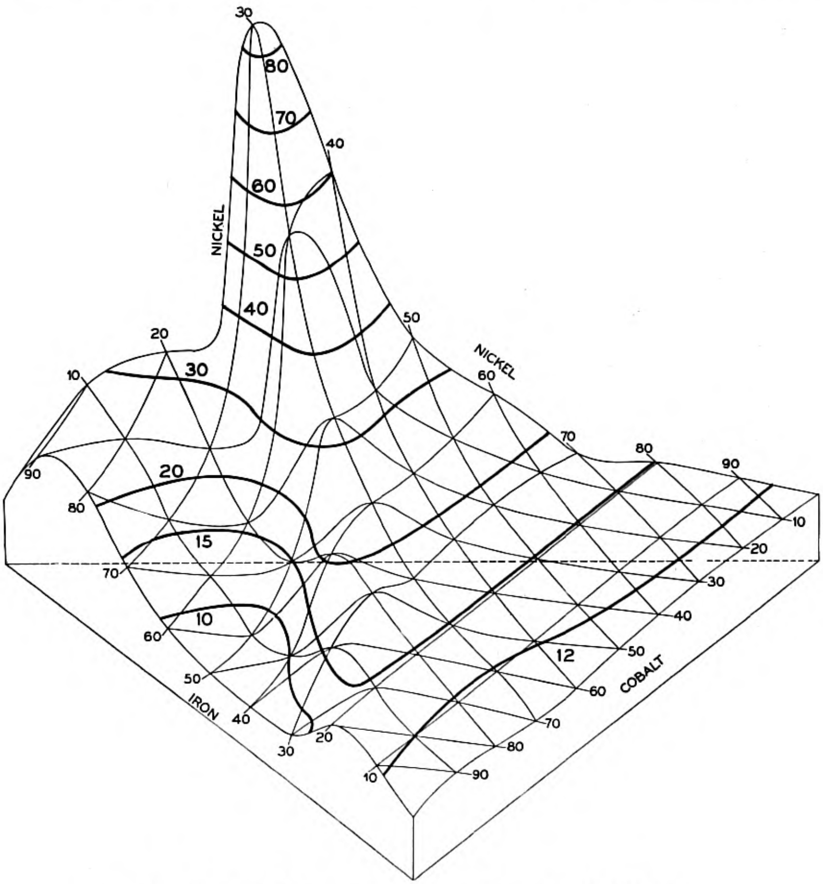

Fig. 9—Resistivities, microhm-cm., for annealed alloys.

The valley in the neighborhood of 30 per cent nickel has largely disappeared except for the alloys without cobalt which are much harder to saturate.

In Fig. 9 a solid diagram has also been constructed for the resistivity of these alloys in the annealed condition. It is interesting to note the high resistivities of some of the nickel-iron alloys—again in the back of the diagram—and the low values for some of the cobalt-iron alloys in the 45–70 per cent cobalt range of compositions.

In the discussion of the magnetic properties of these alloys, I have pointed out that there are three regions of composition which are of special interest from the standpoint of applications because of their unusual magnetic properties. One of these is in the iron-cobalt series. A representative alloy of this group is the 50 per cent cobalt composition. In Fig. 10 the magnetization curves for this alloy and for

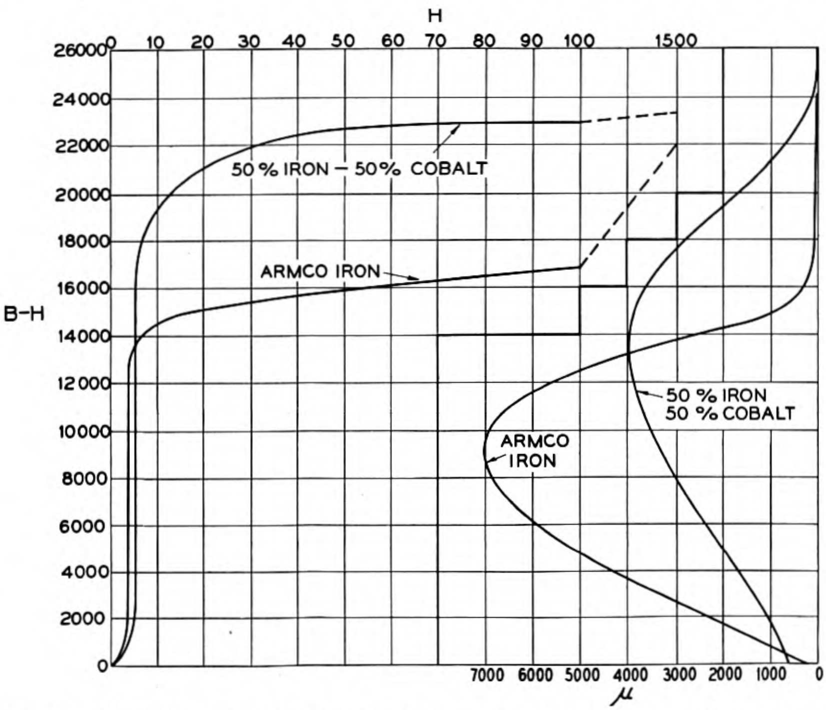

Fig. 10—Magnetization and permeability curves for the 50 per cent iron, 50 per cent cobalt composition and for Armco iron.

a sample of iron are shown on the left and the permeability curves plotted against the same scale of intrinsic inductions on the right. The scale for the magnetizing force of the magnetization curve is at the top of the figure. Below an induction of 1,000 and above 13,000 the permeability of the alloy is higher than for iron. Its initial permeability is 600 and the maximum permeability is 4,000. For a magnetizing force of 100 gauss the intrinsic induction is nearly 23,000 gauss. For Armco iron the initial and maximum permeabilities are 250 and 7,000, respectively, and the intrinsic induction for a magnetizing force of 100 gauss is 17,000.

The perminvars are the next group with interesting characteristics. Their remarkable constancy of permeability at low magnetizing forces and their extremely low hysteresis loss at low flux densities make them of unusual interest. The composition 45 per cent nickel, 25 per cent cobalt and 30 per cent iron is a typical alloy for this group. Permeability curves for this alloy for three types of heat treatment are plotted against magnetizing force in Fig. 11. The insert in the upper right-hand corner shows the lower parts of these curves plotted to a larger scale. For the baked alloy the permeability is constant at 300 with

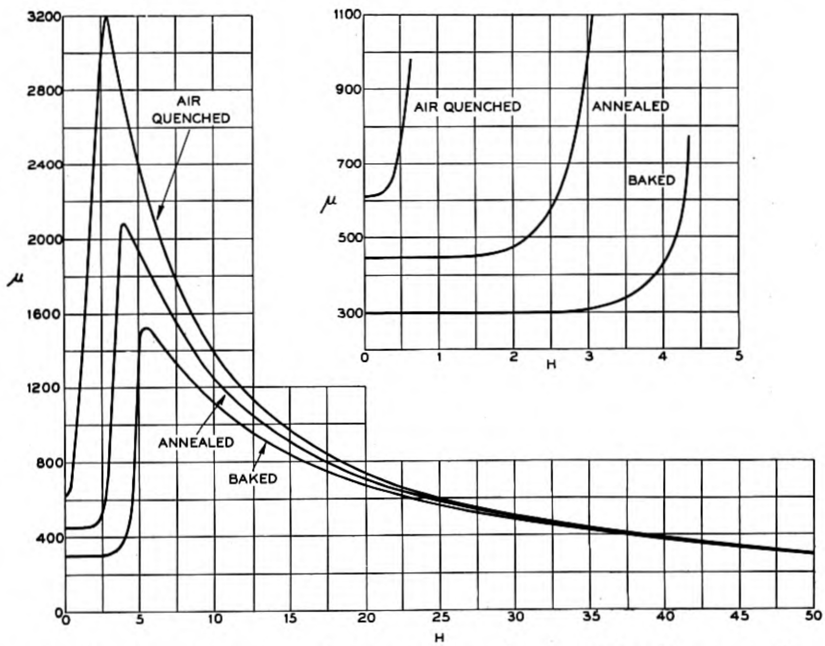

Fig. 11—Permeability curves for a perminvar alloy containing 45 per cent Ni, 25 per cent Co, 30 per cent Fe.

an increase of the magnetizing force from zero to $2\frac{3}{4}$ gauss. The initial permeability for the air-quenched alloy is more than twice that of the baked, but the constancy of permeability is a great deal less. This illustrates the close relation of these two properties. As the magnetizing force approaches 40 gauss the differences in the permeabilities, resulting from different rates of cooling, disappear.

The hysteresis loops for this composition are also of unusual interest. Fig. 12 illustrates the hysteresis characteristics for this alloy, in air-quenched and baked condition, for three maximum flux densities, 750, 1,000 and 5,000 gauss, respectively. For the lowest flux density of the baked sample the ascending and the descending branches of the loop coincide and the loop is represented by a straight line. For the next higher flux density the loop, for the same heat treatment, begins to have a measurable area. At low values of induction, however, the two branches of the loop for the baked alloy approach each other and often come together completely at the origin. The complete loop for a maximum flux density of 5,000 gauss also shows this peculiar shape for the baked alloy. The loop is constricted in the middle, the two branches almost passing through the origin. The air-quenched alloy also shows tendency of constriction but much less than the baked. The areas of the two loops show that for this value of maximum flux

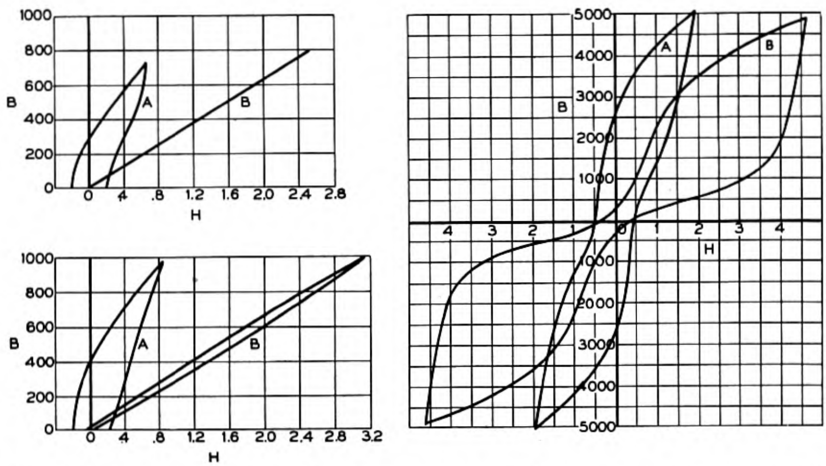

Fig. 12—Hysteresis characteristics for a perminvar alloy containing 45 per cent Ni, 25 per cent Co, 30 per cent Fe. A = air quenched; B = baked.

density the hysteresis loss for the baked sample is greater than for the air-quenched. This condition is the reverse of that for lower flux densities.

The last group of alloys of special interest are the permalloys. In Fig. 13 I have taken the curves for initial permeabilities of the iron-nickel series from the solid diagrams for the air-quenched and the annealed conditions and plotted them on the same scale of coordinates. A curve of initial permeabilities for a series of baked alloys is also plotted in this figure. The baking process for these alloys differed from the one we usually employed in that each alloy was baked until no decrease in the permeability resulted from further baking. For some alloys several weeks were required before this condition obtained. The time was shortest for compositions between 60 per cent and 80 per cent nickel. On both sides of this range the time necessary for stabilization increased both with increasing and decreasing nickel content. With nickel content of less than 42 per cent and more than 88 per cent, approximately, no difference sufficiently large to be attributed to the baking could be observed, even after the alloys had been baked for several weeks.

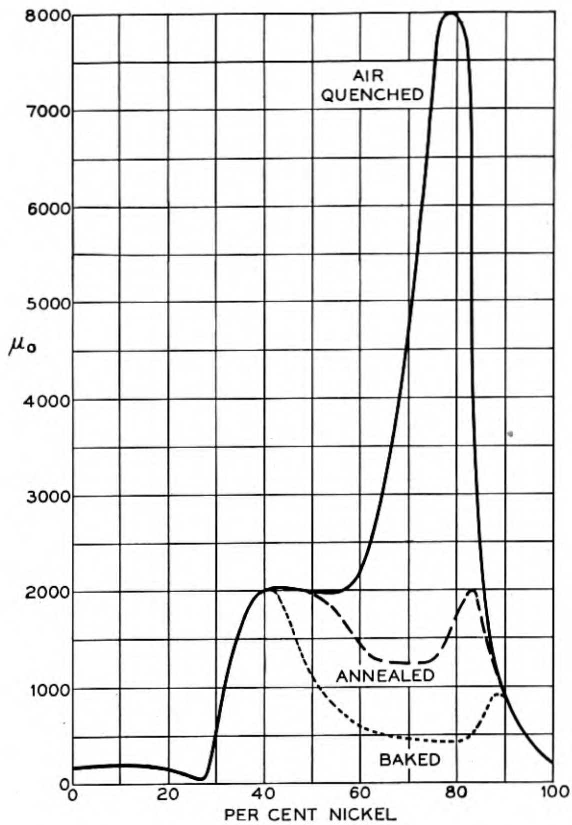

Fig. 13—Initial permeabilities for the Fe-Ni series.

The 78.5 permalloy composition in this series is of special interest because this alloy when air quenched gives the highest initial and maximum permeabilities. The magnetization curves for this composition are plotted in Fig. 14 for annealed and air-quenched samples, and for a sample of annealed iron. The lower part of this graph is shown in the insert on a larger scale. The curves are plotted for magnetizing forces between 0 and 10 gauss only. In these curves the induction for the annealed sample remains lower than for the air-quenched sample, but as the force increases there is a tendency for the two curves to approach each other. This continues with still further increase in the magnetizing force and beyond 50 gauss the two curves coincide.

The permeability curves for these samples are plotted in Fig. 15, illustrating the great difference in their maximum permeabilities. For the annealed and the air-quenched samples, the initial perme-

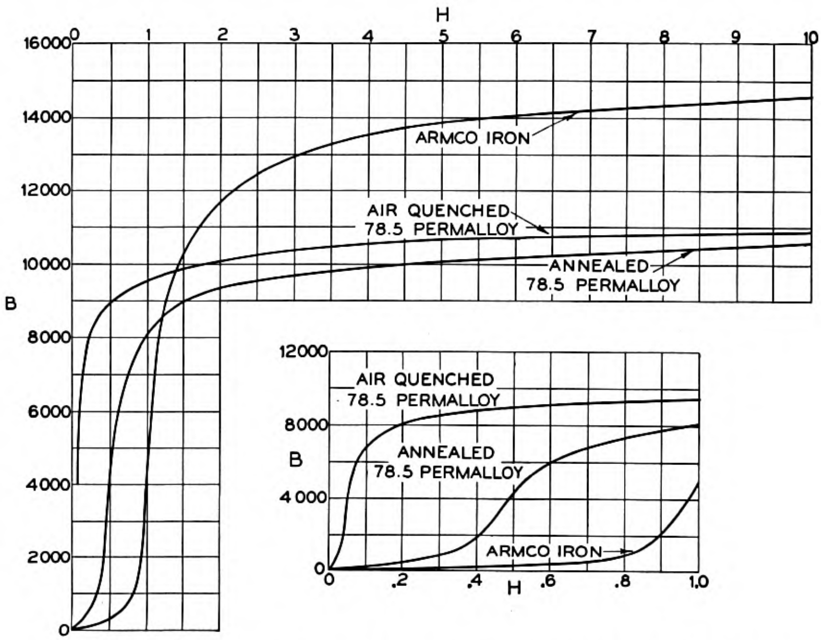

Fig. 14—Magnetization curves for 78.5 permalloy and for Armco iron.

abilities are 2,000 and 9,000, and the maximum permeabilities 10,000 and 87,000, respectively. The initial and the maximum permeabilities for the iron sample are 250 and 7,000, respectively.

The effect of air quenching on the energy loss is illustrated in Fig. 16 in which hysteresis loops for a maximum flux density of 5,000 gauss are plotted for the air-quenched and the annealed samples. The energy loss for the rapidly cooled sample is only 35 per cent of that for the annealed.

In deciding on a rate for air quenching we selected the rate which gave the highest initial permeability for the 78.5 permalloy. In Fig. 17 I wish to illustrate how small changes in this rate affect the initial and the maximum permeabilities for this composition. The scale for maximum permeability is on the left and for initial permeability on the right. The cooling rate is in degrees centigrade per second. It is interesting to note that the highest initial permeability was obtained

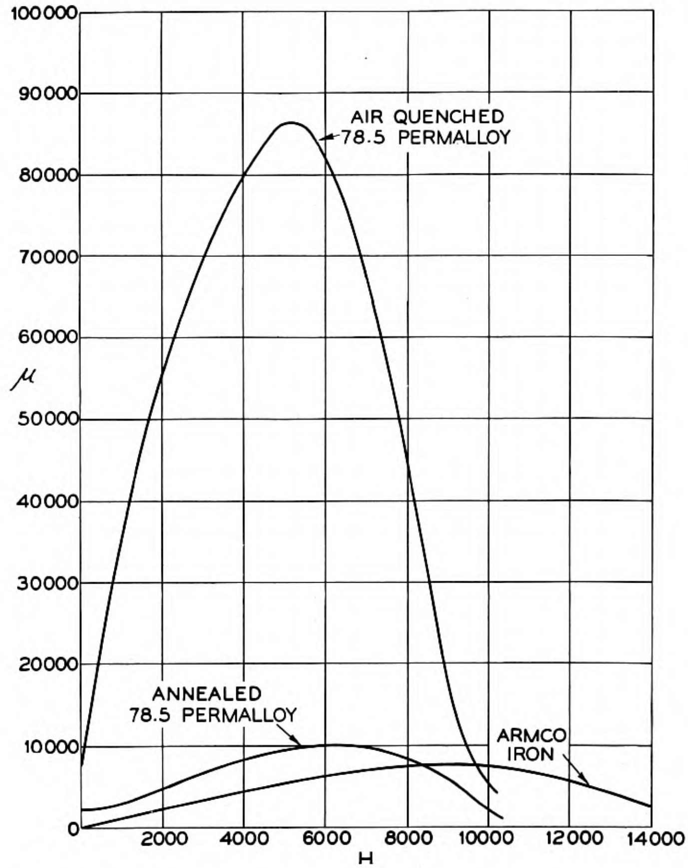

Fig. 15—Permeability curves for 78.5 permalloy and for Armco iron.

when the cooling rate was approximately 20° C. per second, while a rate four times as rapid gave the highest maximum permeability. Ten thousand and 120,000 were the highest initial and maximum permeabilities, respectively, for these particular samples. These values are not the highest we have obtained for this composition. Test samples from other castings have given as high as 13,000 for initial permeability and upwards of 400,000 for maximum.

Fig. 18 illustrates the manner in which the permeability at a low magnetizing force for a rapidly cooled 78.5 permalloy composition is affected by passing it through a temperature cycle between room temperature and 650° C. The permeability was measured for a constant magnetizing force of .003 gauss as the temperature was passed through this cycle. The rate at which the sample was heated and

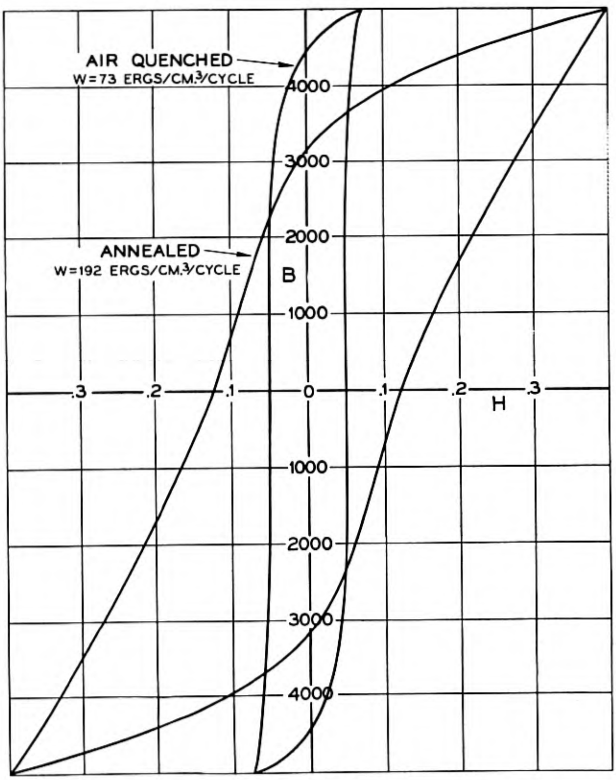

Fig. 16—Hysteresis loops for 78.5 permalloy.

cooled was rather slow, requiring upwards of two hours to complete the heat run.

The permeability of the air-quenched sample was 7,000 at the start, increasing rapidly up to about 315° C. With further increase in temperature there is a rapid drop in permeability until 500° C. is reached. With further increase in temperature the permeability rises very rapidly to a sharp peak at about 530° C. and then decreases, the alloy becoming non-magnetic at 590° C. With decreasing temperature the alloy again becomes magnetic at about the same temperature, at which the magnetism disappeared and the curve for decreasing temperature is the same as for increasing temperature over a short range. At 500° C. the curve for decreasing temperature does not follow its original path but continues to drop until the temperature reaches about 425° C. From that point on until room temperature is reached the return curve is nearly horizontal.

At room temperature the permeability is only 2,000, a drop of 5,000 from its value at the beginning of the run. With the alloy in this condition, if a second cycle is run, the permeability both for increasing

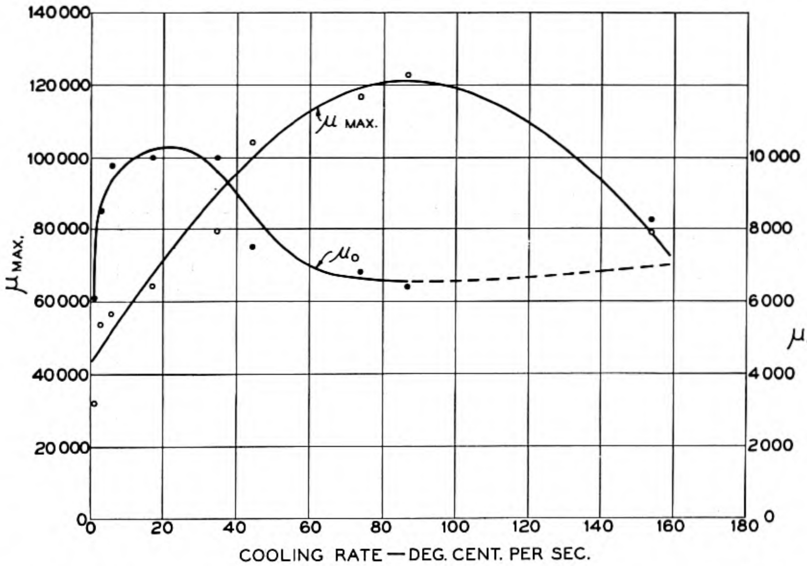

Fig. 17—Initial (μ_0) and maximum (μ_{max}) permeabilities for 78.5 permalloy for different rates of air quenching from 600° C.

and decreasing temperature will be substantially the same as the one in the figure for decreasing temperature. By heating the sample to 600° C. and air quenching, the magnetic properties at the beginning of the test are restored.

The connection between the permeability of this composition and the heat treatment in the temperature range below 600° C. is also illustrated by a series of tests in which annealed rings were air quenched from temperatures below 600° C. The rings were placed in a furnace and heated at 600° for 15 minutes. The temperature was then decreased slowly to 550° C. and held until the alloys had reached a constant condition. One of the samples was then taken out of the furnace and air quenched. The temperature of the furnace was then dropped another step and the process of stabilization and air quenching repeated for the next ring. This was repeated for a number of temperatures until there was substantially no change between two rings quenched from successive temperatures. Another series of annealed rings was slowly heated in successive steps to the same temperatures, stabilized, and then air quenched.

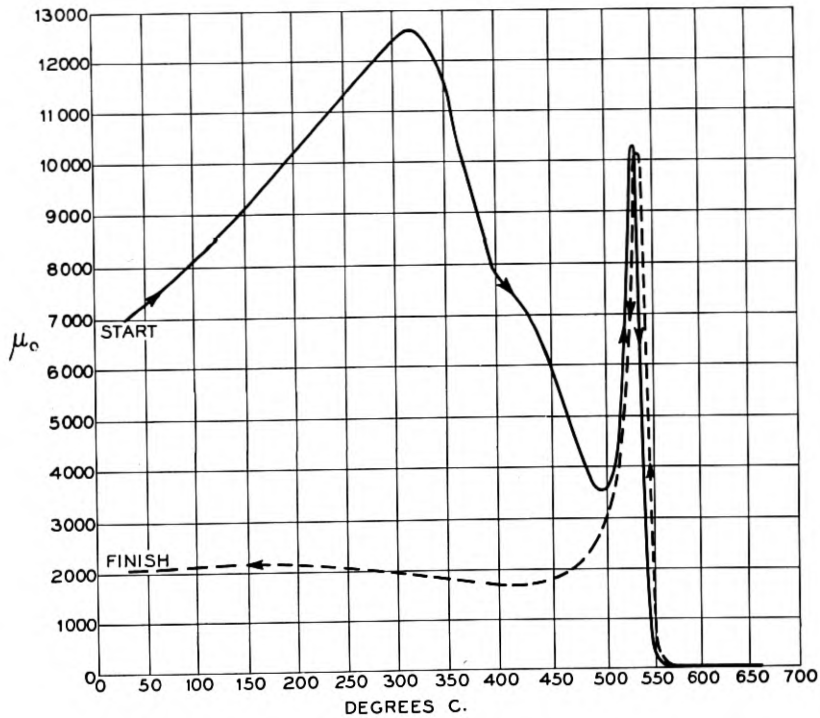

Fig. 18—Temperature-permeability curve for 78.5 permalloy: magnetizing force .003 gauss.

A comparison of the initial permeabilities of these rings showed that each ring attained a definite permeability, characteristic of the temperature from which it was air quenched whether it reached that point from a lower or a higher temperature, provided it was stabilized before air quenching. The air quenched rings stabilized between 500° and 400° C. showed the greatest change in permeability. The time required for stabilization at the higher temperatures was very short, only a few minutes being required in the neighborhood of 500° C., but it increased progressively as the temperature was lowered, and in the lower end of the range several days were required for the alloy to reach a constant condition.

Tests on other compositions showed that those alloys in which the magnetic properties depended on the rate of cooling below 600° C. gave results similar to those for the 78.5 permalloy. The temperature range was also found to be substantially the same as for the 78.5 permalloy, although in some cases there were indications that small changes occurred above 600° and below 400° C.

This connection between heat treatment and magnetic properties led me to conclude that the differences in these properties in the alloys which had been heat treated differently below 600° C. were caused by constitutional changes in the alloys. Such changes are common in alloys in the solid state, often at low temperatures. The progressive change in the permeability as the temperature of the alloy decreases slowly below 600° C., the gradual increase in the time required for a change to complete itself as the temperature drops, and the prevention of the change by rapid cooling through this temperature range support this conclusion.

It is well known that some alloys are in the state of homogeneous solid solutions at high temperatures, but segregate into two or more phases as the temperature drops. Such segregation ordinarily takes place in a definite temperature range, and is progressive in nature. It is a change of this type which I picture as taking place in these alloys during slow cooling. At the upper end of the critical temperature range for each alloy, the homogeneous solid solution begins to segregate into constituents of different composition. This segregation continues until the temperature has dropped to a point where no further changes take place. Rapid cooling prevents this segregation and the alloys remain after cooling in a metastable condition.

We would suppose that if such a change takes place, confirmatory evidences might be found. I shall refer, briefly, to some of our attempts to obtain evidence to confirm our speculations as to the nature of these magnetic changes.

The resistivity was measured for rapidly cooled and for baked alloys both of permalloy and perminvar compositions. These measurements showed that for both types of alloys, baking reduced the resistivity. For example, the resistivity of a 78.5 permalloy sample was measured after baking and after air quenching. The resistivities for the two conditions were 14.2 and 15.8 microhm-cm., respectively. Upon rebaking the resistivity again dropped to 14.5, about the same as before it was air quenched. This change is in accordance with what would be expected if a segregation took place with annealing. A homogeneous solid solution has the highest resistivity and segregation tends to lower it.

Other interesting evidence is obtained from the study of the hysteresis loops. For the perminvar alloys the constricted loops are very marked and easily produced. In the permalloys containing between 60 and 80 per cent nickel also there is a tendency to constriction in the slowly cooled alloy, not so marked but sufficiently prominent to lead me to believe that the same general changes occur in both groups of alloys, differing only in the nature of the segregates and the ease with which segregation occurs. Now we know that homogeneous magnetic materials have a characteristic type of hysteresis loop. For such materials there is no constriction in the middle, but the widest part of the loop is generally at that point. We also can

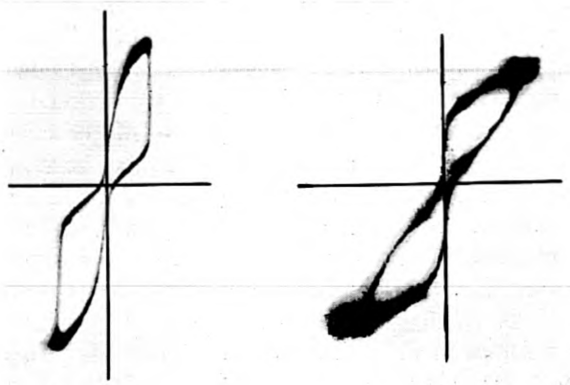

a *b*

Fig. 19—Hysteresis loops: *a*, perminvar (45 per cent Ni, 25 per cent Co, 30 per cent Fe); *b*, bi-metallic rod. Loop traced with cathode ray oscillograph.

construct hysteresis loops which have constrictions by making up cores of several materials in a parallel or parallel-series arrangement.[5] This is illustrated by the hysteresis loop *b* in Fig. 19. This loop is traced by a cathode ray oscillograph for a bi-metallic rod, 15 in. long consisting of a core of .04 in. diameter unannealed piano wire and a .006 in. wall permalloy tube, heat treated to give high permeability and fitting closely to the wire. Curve *a* is a loop similarly traced for a perminvar core. Though the magnetic circuit conditions for the two cores are not the same, the marked similarity of the two loops favors the view that the constricted loop of the perminvar results from segregation.

It is interesting to note in this connection that the examination by X-ray crystal analysis methods of these alloys has not given evidence

[5] E. Gumlich, *Arch. f. Elektrotechnik*, Vol. 9, p. 153, 1920.

of a segregation such as other evidence leads me to think must occur. Perhaps the reason for this is that the different constituent metals are so closely related that small changes in the structure cannot be detected by this means, or perhaps the reason is that the size of the groups of atoms making up the constituents is too small to be detected by X-ray methods.

While the variation in the permeability and in the other magnetic characteristics which could be affected by heat treatment may be explained by the theory of segregation, this theory does not explain why these alloys have such high permeabilities at low magnetizing forces.

Nor does this theory explain the unexpected magnetic characteristics, such as high saturation values of induction, or the low electrical resistance which characterize a large proportion of the alloys in the iron-cobalt series. It has been suggested by Weiss [6] that when the saturation values of an alloy are higher than they are for the constituent metals, it is an indication of the existence of an intermetallic compound. On this ground he has accounted for the high saturation values he found for an iron-cobalt alloy containing 34 per cent cobalt. In our investigation, which was not carried up to the high magnetizing forces used by Weiss, the 50 per cent cobalt alloy gave us as high flux densities as any in the series for magnetizing forces upwards of 1,500 gauss.

It has been found in the study of intermetallic compounds that one indication of their existence is a low resistivity. It is generally believed that if an alloy has lower resistivity than any of its constituent metals, an intermetallic compound exists. In our measurements of the resistivity of the iron-cobalt series we found that the alloys with lowest resistance were those containing between 25 per cent and 60 per cent iron. There is a rather abrupt decrease in the resistivity as the percentage of iron increases beyond 25 per cent. Beyond 50 per cent iron there is a gradual increase with a maximum at about 85 per cent iron. From these measurements we would conclude that if an intermetallic compound exists, it is of a higher cobalt percentage than that suggested by Weiss. From our measurements of the resistivity of the alloys in this series the most probable intermetallic compound would be one containing approximately 66 per cent cobalt of the chemical formula $FeCo_2$.

The data which I have presented are those for the compositions of iron, nickel and cobalt. In addition to these alloys, we have studied the effects of adding non-magnetic elements to numerous alloys of

[6] *Transactions of the Faraday Society*, Vol. 8, p. 149.

particular compositions. I cannot at this time go into a detailed discussion of the results with these, but I shall mention briefly some of them. We found that the addition of some of the non-magnetic metals to both the permalloys and the perminvars made those alloys less sensitive to heat treatment. The resistivity was also generally increased. For some compositions the addition in small percentages

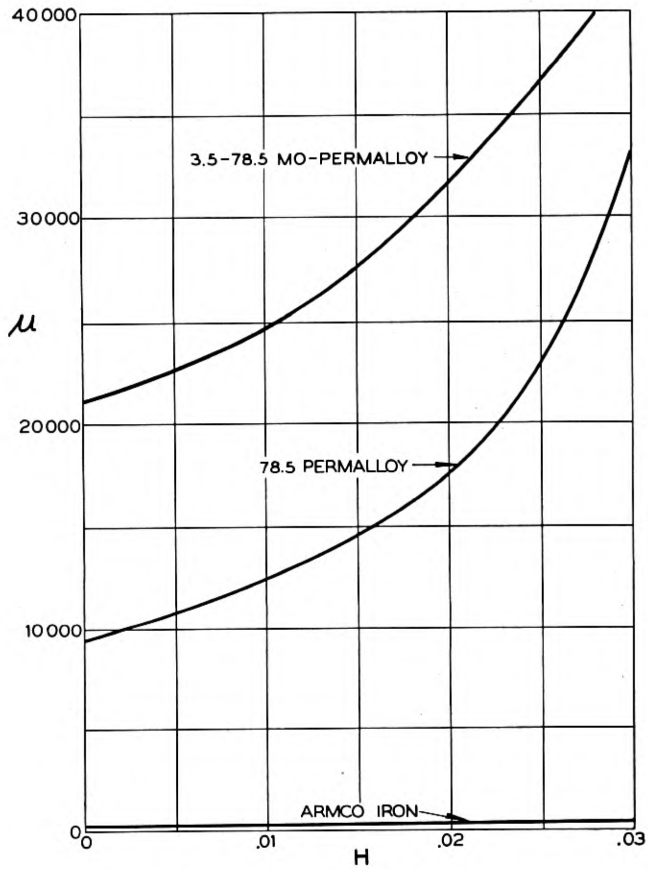

Fig. 20—Permeability curves for permalloys.

of a non-magnetic metal, particularly chromium and molybdenum, increases the permeability at low magnetizing forces. This is illustrated in Fig. 20 where I have plotted the permeability curves for Armco iron, 78.5 permalloy, and a 3.5–78.5 Mo-permalloy. You will note that the initial permeability of the molybdenum-permalloy alloy is 21,000 as compared with 9,000 for the permalloy without molybdenum. As a rule the maximum permeability was generally decreased when a non-magnetic element was added and so were the saturation values of induction.

As our investigation was undertaken primarily for the purpose of searching for magnetic materials which could be used to advantage in the electrical communication field, it may be of interest to describe a few of the principal uses to which some of these alloys have been put.

Of the three groups of alloys which are of special technical interest, the permalloys are now used extensively in electrical communication circuits. Perhaps its most spectacular use is for continuous loading of submarine telegraph cable.

The term loading is used in the electrical communication art to designate a system of adding inductance to a transmission circuit for the purpose of overcoming the unfavorable transmission characteristics resulting from the electrical capacity of the circuit. This system has

Fig. 21—Sample of submarine loaded cable, showing the loaded conductor.

been used in telephone transmission circuits for over a quarter of a century. The standard method used for telephone circuits, in which inductance coils are placed at equally spaced intervals along the transmission line, was not considered practical for deep sea cables. The only suitable method from a mechanical standpoint was a continuous loading in which a magnetic material is distributed uniformly along the whole length of the cable. Before permalloy was developed the best magnetic material available was iron. It could not be used economically for long submarine cables because of its low permeability. With permalloy having between 40 and 50 times the permeability of iron in the range of magnetic field strength encountered in such cables, it was found that beneficial results could be attained and cables of more than five times the carrying capacity of the old type could be built.

The first permalloy loaded submarine telegraph cable was laid in 1924 between New York and the Azores, a distance of approximately 2,300 nautical miles. A sample of the deep sea section of this cable is shown in Fig. 21. Numerous other loaded cables have been laid since 1924; the total mileage of loaded submarine telegraph cables is now upwards of 16,000 nautical miles.

Another purpose for which permalloy is now used extensively is for loading coils for telephone transmission circuits. Before the introduction of permalloy, finely powdered, insulated and compressed iron dust was used for the cores of these coils. Permalloy has now replaced iron for loading coil cores, and upwards of a million cores per year are used by the Bell System.[7] For these cores the permalloy is used in the form of compressed insulated powder. Some of the advantages in using permalloy result from its lower hysteresis losses and higher permeability. Taking advantage of these qualities in the design of the coils, it has been possible to reduce materially their

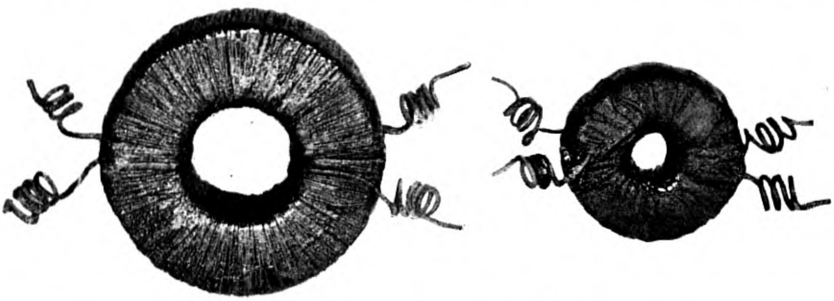

Fig. 22—Compressed powdered core loading coils: left, electrolytic iron core; right, permalloy core.

sizes. This is illustrated in Fig. 22 where two standard loading coils for use in the same circuits are shown. One of these has a permalloy core and the other a core of iron. The former is approximately one-third of the size of the latter.

When these coils are used in service usually a large number are placed in containers which are placed at different points in vaults or on poles along the telephone circuits. In Fig. 23 two such iron cases with their cable connecting stubs are shown; each contains 200 coils. The small case contains the permalloy coils, and the large case the iron core coils. The use of permalloy has reduced the combined weight of the coils and the cases from approximately 1,700 lbs. to about 700 lbs.[8]

[7] The use of permalloy core loading coils is increasing very rapidly. Recent figures show that approximately 2,000,000 of these coils will be required by the Bell System per year during the next few years.

[8] The decreased size of the coils and containers has resulted in a very substantial saving in the cost of loading.

Another use of permalloy in the telephone plant has been found in the case of relay cores. Relays are used to connect and disconnect mechanically the telephone circuits at the central office and at other points. These relays are magnetically operated and their efficiency depends largely on the magnetic quality of the core material. Certain groups of these relays are required to operate under very severe circuit conditions where the operating currents are small and where

Fig. 23—Cast-iron cases each containing 200 loading coils: left, permalloy core coils; right, iron core coils.

the relays are required to distinguish between very small changes in current values. For such circuits, relays with permalloy cores are now used extensively.

The permalloy alloys are also used extensively for cores in high quality audio transformers, in telephone receivers and earphones, and in electrical measuring instruments.

The permalloy series was first developed, and is also the one which was first used, for commercial purposes on a large scale. The other alloys are still in the commercial development stage, but interesting results have been obtained which make us feel confident that both the perminvars and the iron-cobalt alloys will take their places beside permalloy as important magnetic materials in electrical communication.

A Test for Polarization of Electron Waves by Reflection[1]

By C. J. DAVISSON and L. H. GERMER

A homogeneous beam of electrons is directed at 45° incidence against a {111}-face of a nickel crystal. The beam regularly reflected from this face impinges upon a second similar face at the same incidence angle. A Faraday collector is set to receive electrons regularly reflected from the second crystal, but only such electrons are accepted into the collector as have survived the two reflections without appreciable loss of kinetic energy. The collector and second crystal are rigidly joined, and may be rotated about the axis of the beam proceeding from the first to the second crystal. Measurements of the intensity of the twice reflected beam have been made at bombarding potentials from 10 to 160 volts. Within this range selective reflections (intensity maxima) are observed at 20, 55, 77, 103 and 120 volts.

These five selectively reflected beams have been separately tested for polarization by measuring the current received by the collector as a function of the azimuth of the movable system. If electron waves are polarized by reflection the intensity of the twice reflected beam should be greatest when the planes of incidence of the two reflections coincide, and least when they stand normal to one another. No such variation of the current to the collector is observed within the limits of error of the measurements—about one half of one per cent of the total current. *Our observation is that electron waves are not polarized by reflection.*

THE experiment described in this article was undertaken to determine whether or not a beam of electron waves is polarized by reflection from the surface of a nickel crystal. It is similar in certain respects to the experiment with double Nörrenberg mirrors by which one demonstrates the polarization of light by reflection from glass, and in others to the experiment by which Barkla established that X-rays may be polarized. It resembles most closely, however, the variation of the Barkla experiment performed by Mark and Szilard in which the first of the radiators was a crystal and a Bragg reflection beam proceeded to the second radiator. A homogeneous beam of electrons is directed at 45 degrees incidence against a {111}-face of a nickel crystal, and the beam proceeding in the direction of regular reflection from this crystal is then reflected at the same angle of incidence from a second similar crystal. A double Faraday box is placed to receive electrons which have been regularly reflected from the second crystal, but only such electrons are allowed to enter the collector as have retained all or nearly all of their kinetic energy through the two reflections; those which have lost more than a small fraction of their kinetic energy are excluded by a retarding potential of suitable strength.

The second crystal and the collector are joined rigidly together, and may be rotated about an axis which coincides with the axis of the beam proceeding from the first to the second crystal. It is possible, there-

[1] *Phys. Rev.*, Vol. 33, May, 1929, pp. 760-772

fore, to vary the dihedral angle between the plane of incidence of the second reflection and that of the first. There are two positions of the movable system for which these planes coincide. For these "parallel" positions the current entering the collector should be at a maximum provided the electron beam is unpolarized initially and becomes asymmetric at reflection; for the intermediate "transverse" positions the current should be at a minimum. In the analogous experiment in optics the intensity I of the twice reflected beam satisfies the formula

$$I = I_0(1 + p \cos 2\theta),$$

where θ represents the azimuth angle of the movable system measured from either of its parallel positions, and p an amplitude coefficient which serves as a convenient measure of the polarization effect.

In the experiment with electrons our procedure has been to measure the intensity of the twice reflected beam for various values of θ—though chiefly for the values corresponding to the cardinal positions—to assume the same form of relation between intensity and angle as in optics, and to evaluate the coefficient p.

The reflection of electrons from a crystal surface is, like that of X-rays, "selective in wave-length"; the intensity of the reflected beam attains maximum values at various critical wave-lengths or speeds of bombardment. This effect is, of course, accentuated in a beam which has suffered two reflections. In the test for polarization we have made observations in the range of bombarding potentials from 10 to 200 volts, chiefly at five different electron speeds at which there are intensity maxima of the beam twice reflected.

Preliminary observations indicated that at each of these critical speeds the intensity of the reflected beam is, to a first approximation, independent of angle. The acutal values found for p were some of them positive and some negative, and none greater absolutely than 0.02, which was about the order of uncertainty involved in the determinations of the collector currents. These results were described in a letter to the Editor of "Nature." [2]

In the present article the experiment is described more fully, and additional data are adduced from which it is concluded that the value of p, if different at all from zero, cannot be greater than 0.005.

The principal parts of the apparatus are the gun for supplying a homogeneous beam of electrons, the two crystal reflectors, and the collector. These are contained in two metal boxes or enclosures shown in longitudinal sections in Fig. 1. The right hand or gun enclosure contains the electron gun and the first reflector, and is attached rigidly

[2] C. J. Davisson and L. H. Germer, *Nature*, 122, 809 (1928).

to the framework of the apparatus. The left-hand or collector enclosure contains the second reflector and the collector, and is supported from the frame of the apparatus through bearings by which it can be rotated about a horizontal axis. Communication between the enclosures is through the right-hand bearing which is hollow. The sections of the enclosures at right angles to the plane of the drawing are square.

The electron gun is similar in construction to the one described in an earlier paper [3] to which we refer for the details. The apertures are circular and those which define the beam are 2 mm. in diameter.

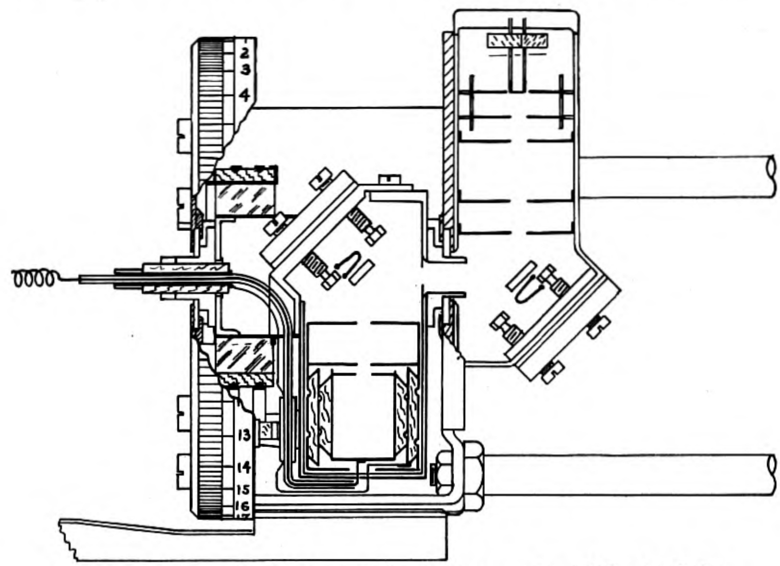

Fig. 1—Cross-section of the experimental apparatus—0.8 actual size.

The reflectors were cut from a single crystal of nickel formed by the slow freezing of pure nickel in vacuum. Their faces, which were polished to fairly good optical flats and then lightly etched by acid, are approximately 4 × 4 mm. in extent. The normals to these faces diverge from one of the {111}-directions of the crystal structure by only about 10 minutes of arc.

The reflectors are so mounted that for each of them the incident beam lies in what we have designated as a {111}-azimuth of the crystal structure, as illustrated in the schematic diagram, Fig. 2. This adjustment may be unimportant, but was made because it has not yet been established that the selectivity of reflection is independent of the azimuth of the incident beam. The {111}-azimuth was chosen rather

[3] C. J. Davisson and L. H. Germer, *Phys. Rev.*, 30, 705 (1927).

than any other because our earlier observations on electron reflection were made with the incident beam in this azimuth, and several of the critical electron speeds for 45 degrees incidence were already known.

Each reflector is attached to a triangular frame which is supported from the diagonal wall of the enclosure through three adjusting screws. Two only of each set are shown in Fig. 1. The frames to which the crystals are attached and other accessory parts have been omitted from the drawing in the interest of clearness.

Small tungsten filaments, mounted one behind each of the reflectors, are supported by stiff wires from quartz plates which are clamped to the outer walls of the enclosures. Electrons emitted by these filaments

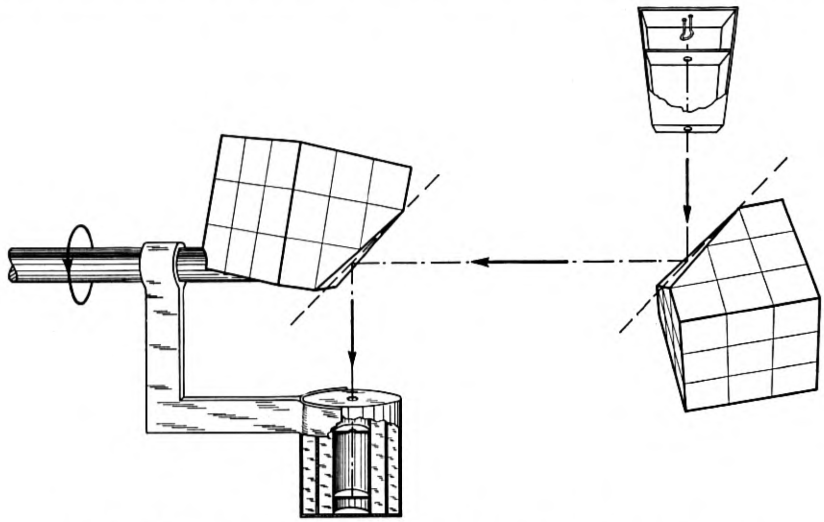

Fig. 2—Schematic diagram illustrating the principle of the experiment.

are used for heating the reflectors by bombardment. The reflectors are not insulated from the enclosures, which in fact contain no insulating material whatever except that incorporated in the gun and the collector.

The metal parts of the collector comprise an inner and an outer box of circular cross-sections and a cylindrical guard electrode of intermediate diameter. These parts are separated by cylinders of pyrex glass, and the assembly constitutes a unit which fits into the end of the collector enclosure. The aperture in the outer box is circular and 2 mm. in diameter; that in the inner box is of the same form but of slightly greater diameter. The guard cylinder is interposed to intercept the leakage current which would flow otherwise from the outer to the inner box. It was anticipated that the electron current entering the collector would be excessively small and that this leakage current, unless guarded against, might prove an intolerable disturbance.

The lead wire from the inner box is guarded from the frame of the apparatus at all points of support within the tube by electrodes connected with the guard cylinder. This lead wire and the wire from the guard electrodes leave the tube through remote seals as indicated in Fig. 3. The isolation of the latter of these seals was a matter of convenience rather than of precaution.

Four electrical connections are required to parts of the movable system—two to the filament and one each to the collector and to the guard electrodes. These are maintained, with the exception of that to the collector, through platinum tipped molybdenum brushes which bear upon platinum rings. The connection to the collector is through a flexible spiral of tungsten wire lying in the axis of rotation.

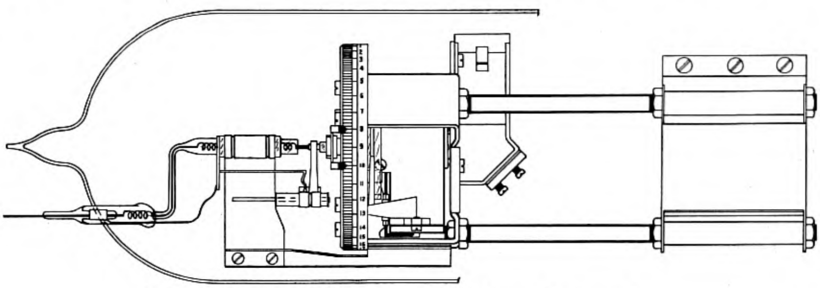

Fig. 3—Outside view of the experimental apparatus.

It may be well to add to this description of the tube a few words in regard to the adjustment of the reflectors to their proper positions and orientations. Each reflector is attached, as has been already mentioned, to a triangular frame which is supported through three adjusting screws from the diagonal wall of the enclosure. By turning these screws the reflector can be rotated through small angles about any axis parallel to the wall, and by the same means its distance from the wall can be varied. These adjustments were sufficient for locating the beam reflected from the first mirror in the axis of rotation, and that reflected from the second in the axis of the collector. They were not sufficient, however, for meeting the further requirement that the incident beam should lie in a {111}-azimuth of the crystal structure. For this adjustment we relied upon orienting the reflector correctly with respect to the triangular frame at the time of its attachment. A mosaic of sharply defined triangular etch pits was visible under the microscope on the surface of the crystal reflector, and it was only necessary to relate these properly to the triangle formed by the frame to insure the desired orientation of the crystal with respect to the incident beam. Short wires attached to the reflector and protruding from it were rested upon the frame, and the reflector was then turned until the triangles on its surface stood in opposition to the triangle formed by the frame, this being the necessary relation. This adjustment was made with the frame and reflector mounted on the movable stage of a tool maker's microscope. One of the wires was then electrically welded to the frame. The adjustment was disturbed slightly by this operation, but the disturbance was corrected for by bending slightly the attached wire before proceeding with the second weld. This alternation of adjustment and welding was continued until all wires were attached. As finally adjusted the orientation of the reflector may have been wrong by one or two degrees, but hardly by more.

In adjusting the first reflector for position two conditions sought were, first that the intersection of the axis of the gun with the axis of the movable system should lie in the surface of the reflector, and second that the normal to the reflector should bisect the angle formed by these axes. These were attained by removing the collector enclosure from the frame of the apparatus and the filament from the gun, and collimating the collector enclosure bearings with the images of the gun apertures formed by the reflector. For making the similar adjustment of the second reflector an aperture was formed in the center of the rear wall of the collector so that a view of the reflector might be had along the collector axis. The gun enclosure which had been detached from the frame of the apparatus during the adjustment of the second reflector was then replaced, and the adjustment of the two reflectors was checked by directing a beam of light along the axis of the gun and finding that the twice reflected beam proceeded accurately along the axis of the collector.

The preparation of the tube—the preheating of the metal parts, the baking, the exhausting, and the sealing off—was the same essentially as described in an earlier paper to which the reader is referred for particulars. (*Phys. Rev.*, loc. cit.)

In operation, the tube is mounted in a cradle with its axis inclined 30 degrees from the horizontal, so that an auxiliary tube lying in the axis and containing charcoal may be kept submerged in liquid air. The movable system swings to the lowest part of its arc, and its angular position with respect to the frame of the apparatus is read against the circular scale shown in Fig. 3. To alter this azimuth angle θ the tube is rotated about its axis; actually the "movable system" remains at rest relative to the earth, and all other parts are rotated.

No means were provided for measuring the current of electrons incident upon the first crystal. We had found, however, from a preliminary investigation of the characteristics of the gun, that currents of the order 2×10^{-4} amperes could be obtained from it. It was known also from these tests that the electrons ejected from the gun are very nearly homogeneous in speed. Given this value for the current in the primary beam, it was possible from our previous observations on the regular reflection of electrons at 45 degrees incidence to estimate the order of magnitude of the current of full speed electrons which might reach the collector after two such reflections. The estimated magnitudes were from 10^{-12} to 10^{-11} amp, and the currents of selectively reflected electrons actually observed have had values within this range.

In measuring these small currents we have had the use of a direct current vacuum tube amplifier designed and built by Dr. J. M. Eglin. It is the type of amplifier described recently by Wynn-Williams,[4] but embodies certain improvements described by Dr. Eglin at a recent meeting of the American Physical Society.[5] Conditions for observing were best when the amplification factor was about 2,000, so that the currents actually measured were of the order of 10^{-8} amp.

A few preliminary observations were made before heating the crystals to free their surfaces from adsorbed gas. The relation between the current entering the collector and the bombarding potential for a fixed angle θ was quite different in these first tests from that observed after the crystals had been heated. The principal feature of this initial current-voltage relation is a strong maximum at 20 volts. Tests were made for polarization with the crystals in this condition but no evidence of such a phenomenon was obtained.

The current-voltage curve characteristic of reflection from the crystals in a thoroughly cleaned condition is shown as Curve A in Fig. 4. The data from which this curve has been plotted were obtained with the faces of the reflectors parallel to one another as illustrated in Figs. 1 and 2. It will be convenient to designate this position of the movable system as the position $\theta = 0°$. The "parallel" positions are then the positions $\theta = 0°$ and $\theta = 180°$ and the "transverse" positions are those for which $\theta = 90°$ and $\theta = 270°$. A curve similar to Curve A is obtained whatever value is chosen for θ. In this and in all other tests the inner box of the collector was maintained at a potential 2 volts above that of the midpoint of the filament.

Curve B of Fig. 4 exhibits, on a different scale of ordinates, the relation between current and voltage observed for angle of incidence 45

[4] C. E. Wynn-Williams, *Proc. Camb. Phil. Soc.*, 23, 811 (1927).
[5] J. M. Eglin, *Phys. Rev.*, 33, 113 (1929).

degrees in our earlier experiments on the single reflection of electrons incident in the {111}-azimuth. The locations of the maxima of this curve are indicated in a diagram which forms a part of a report of these experiments.[6]

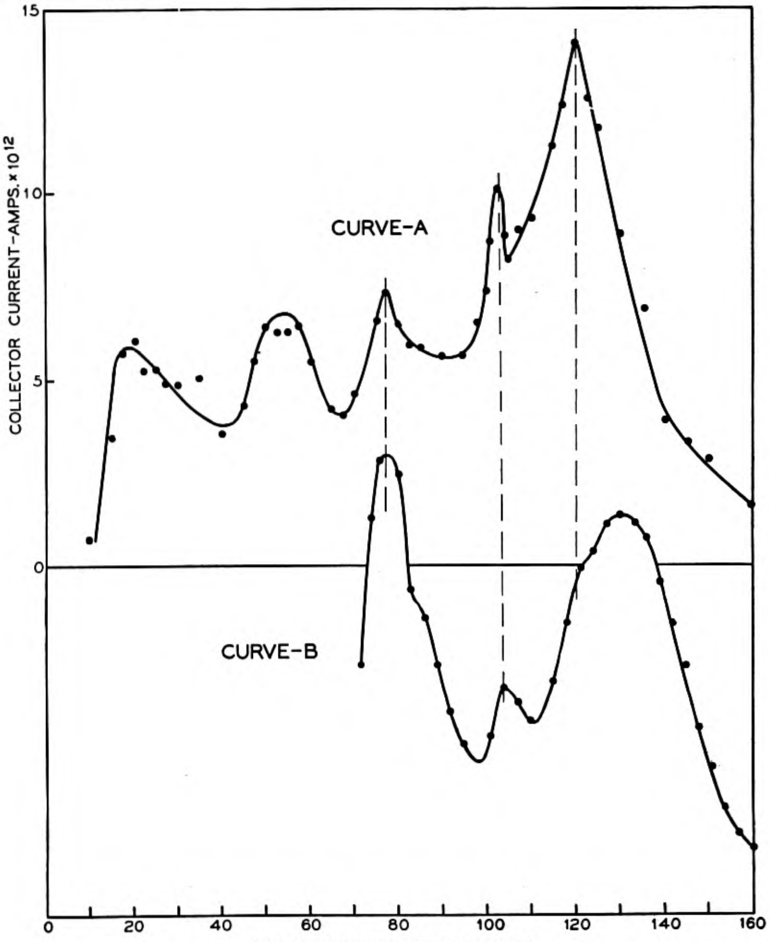

Fig. 4—Variation with bombarding potential of the intensity of beams reflected at 45°. Curve A is the doubly reflected beam of this experiment. Curve B is the singly reflected beam previously reported. (*Proc. Nat. Acad.*, loc. cit.)

The agreement between the curves of Fig. 4 is on the whole satisfactory; each displays three maxima in the voltage range common to both, two of which occur at the same voltages in Curve *A* as in Curve *B*. The voltages at which the third maxima occur—those on the ex-

[6] C. J. Davisson and L. H. Germer, *Proc. Nat. Acad. Sci.*, 14, 619 (1928), Fig. 3.

treme right—differ by about 10 volts. We believe that the position of this maximum is given correctly by Curve A, and that in Curve B it is shifted to the right owing to an eccentricity of the tube used in the earlier experiments. It will be noted that the position of the maximum in Curve A is marked in Curve B by a shoulder which protrudes from the side of the peak. It is with respect to the positions of the maxima only that the curves of Fig. 4 may be legitimately compared, the ordinates in the two cases being proportional to different quantities. Those of Curve A are proportional to the current of full speed electrons entering the collector, while those of Curve B are roughly proportional as has been explained (loc. cit.), to the ratio of full speed electrons, entering the collector to the corresponding current of electrons of all lower speeds.

There is some doubt in our minds as to whether the maximum in Curve A which occurs at 20 volts truly indicates a maximum in the reflecting power of the crystals for electrons of corresponding speed. The current to the collector is determined primarily by the product of the primary current by the square of the coefficient of reflection, so that a maximum in the collector current must correspond to a maximum in the reflecting power if the current in the primary beam is almost or quite independent of voltage, but not otherwise. This condition is known to be reasonably well satisfied in the range of bombarding potentials above 30 or 40 volts. Below this range, however, the current from the gun is limited partly by space charge, and its variation with voltage is rapid. A maximum in the current to the collector in this region must therefore be regarded with a certain suspicion; it may be due to a maximum in the reflecting power of the crystal with which, however, it will fail to coincide in voltage, or it may signify only that the reflecting power has a trend opposite to that of the primary current. We are not, however, greatly concerned in this investigation with the interpretation of this maximum, nor even of the other maxima of Curve A.

Measurements have been made of the intensity of the twice reflected beam as a function of the angle θ for bombarding potentials corresponding to the five maxima of Curve A. In some cases intensities have been measured at intervals of 5 or 10 degrees around the entire circle; but for the most part measurements have been made only at the cardinal positions $\theta = 0$, 90, 180 and 270 degrees. The total number of measurements of this kind is about 500. The complete data for bombarding potential 77 volts, corresponding to the third maximum of Curve A, and for $\theta = 270$ degrees are given in Table I.

TABLE I

Bombarding Potential 77 volts, Azimuth angle $\theta = 270$ degrees. R_0 = zero reading of galvanometer, R = galvanometer reading. $(R - R_0) = D$ = deflection, $\bar{D}$ = arithmetic mean of deflections. $|D - \bar{D}| = S$ = deviation from mean, $\bar{S}$ = mean deviation.

R_0	R	D	S
33.0 mm.			
(33.6)	36.6	3.0	.10
34.2			
(34.55)	37.4	2.85	.25
34.9			
(35.4)	38.6	3.2	.10
35.9			
28.0			
(27.9)	30.5	2.6	.50
27.8			
26.6			
(26.75)	29.7	2.95	.15
26.9			
(27.2)	30.3	3.1	.00
27.5			
36.5			
(36.75)	39.9	3.15	.05
37.0			
(36.5)	40.0	3.5	.40
36.0			
(36.2)	39.4	3.2	.10
36.4			
(36.8)	40.0	3.2	.10
37.2			
(37.3)	40.3	3.0	.10
37.4			
33.6			
(33.85)	37.2	3.35	.25
34.1			
(34.35)	37.1	2.75	.35
34.6			
(35.15)	37.9	2.75	.35
35.7			
(36.15)	39.5	3.35	.25
36.6			
(36.75)	40.0	3.25	.15
36.9			
37.4			
(37.8)	40.9	3.1	.00
38.2			
(38.5)	41.6	3.1	.00
38.8			

R_0	R	D	S
38.8 mm.			
(39.15)	42.1	2.95	.15
39.5			
(39.9)	43.2	3.3	.20
40.3			
40.5			
(40.55)	43.9	3.35	.25
40.6			
34.4			
(34.7)	37.8	3.1	.00
35.0			
(35.4)	38.5	3.1	.00
35.8			
(36.6)	39.8	3.2	.10
37.4			
(37.8)	40.7	2.9	.20
38.2			
(38.4)	41.9	3.5	.40
38.6			
25.5			
(26.0)	28.9	2.9	.20
26.5			
(27.1)	30.1	3.0	.10
27.7			
(28.2)	31.5	3.0	.20
28.7			
(29.3)	32.5	3.2	.10
29.9			
29.4			
(29.8)	33.0	3.2	.10
30.2			
(31.0)	34.1	3.1	.00
31.8			
(31.85)	34.8	2.95	.15
31.9			
(32.45)	35.5	3.05	.05
33.0			
33.8			
(34.4)	37.6	3.2	.10
35.0			
(35.45)	38.5	3.05	.05
35.9			

Number of observations, $N = 36$; $\bar{D} = 3.104$; $\bar{S} = 0.154$

$$\text{Probable error, } \Delta = 0.845 \frac{\bar{S}}{N^{1/2}} = .022 \text{ approx.}$$

$$\therefore \text{ Deflection, } D = 3.104 \pm .022.$$

That the deviations from the mean value of the deflections are distributed in this, and in other cases, in close accordance with the normal error function is illustrated by diagrams displayed in Fig. 5.

The value obtained in Table I for the deflection at $\theta = 270°$ is shown again in Table II, together with the values similarly obtained for the same bombarding potential at the other cardinal positions.

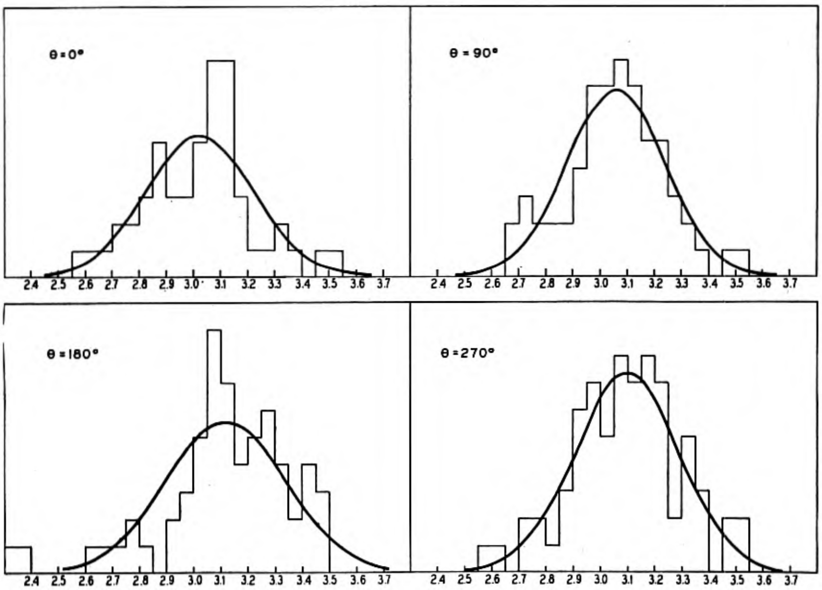

Fig. 5—Plots of all data taken at 77 volts for the four cardinal positions—$\theta = 0°, 90°, 180°, 270°$. The solid curves represent calculated normal error function curves. The data plotted here are summarized in Table II.

TABLE II

Bombarding Potential 77 volts. Wave-length 1.39 A.

Angle θ	No. of Obs.	Deflection
0 deg.	26	3.023 ± .026
90	31	3.057 ± .022
180	31	3.116 ± .027
270	36	3.104 ± .022

The values of these deflections and their probable errors have the characteristics of four measurements of one and the same quantity. There are certain values of deflection common to two of the error ranges but none common to three. This is the situation most likely to be met with if we are measuring the same quantity in each case; the maximum number of overlapping ranges should be one half the total number of ranges. It is of some interest, however, to pretend that the different values found for the deflections correspond to actual differences in the current to the collector, and to attempt to evaluate the amplitude coefficient of the polarization effect. We shall find actually that observations at four positions only are insufficient to determine this constant precisely.

It will be appreciated that differences in the collector current at different angles may arise from mechanical defects in the apparatus—improper alignments, etc.—as well as from polarization, and that in general we shall require for the expression of D as a function of θ a complete Fourier series such as

$$D = D_0 \left[1 + \sum_1^\infty a_n \cos (n\theta + \alpha_n) \right].$$

The data available for evaluating the constants of this series consist of four values of D, corresponding to the four values of $\theta - 0°$, 90°, 180° and 270°. We designate these four values respectively by D_1, D_2, D_3 and D_4. From the four simultaneous equations formed by writing these pairs of values of θ and D into the series we obtain the following relations:

$$D_1 + D_2 + D_3 + D_4 = 4D_0 \left[1 + \sum_1^\infty a_{4n} \cos \alpha_{4n} \right],$$

$$D_1 - D_3 = 2D_0 \sum_0^\infty a_{2n+1} \cos \alpha_{2n+1},$$

$$D_4 - D_2 = 2D_0 \sum_0^\infty (-1)^n a_{2n+1} \sin \alpha_{2n+1},$$

$$D_1 - D_2 + D_3 - D_4 = 4D_0 \sum_0^\infty a_{4n+2} \cos \alpha_{4n+2}.$$

If we make the definite assumption that all periodic terms of orders greater than the second may be neglected, these reduce to the relations

$$D_1 + D_2 + D_3 + D_4 = 4D_0,$$

$$D_1 - D_3 = 2D_0 a_1 \cos \alpha_1,$$

$$D_4 - D_2 = 2D_0 a_1 \sin \alpha_1,$$

$$D_1 - D_2 + D_3 - D_4 = 4D_0 a_2 \cos \alpha_2,$$

from which we may obtain expressions for a_1, α_1 and $a_2 \cos \alpha_2$, but not, unfortunately, for a_2 and α_2 separately; the fourth observation is used up in fixing D_0 in which we have no interest. Observations at one additional angle would have been sufficient to resolve a_2 and α_2, but this was not appreciated at the time the measurements were made.

If we write Δ_1, Δ_2, etc. for the probable errors involved in the measurements of D_1, D_2, etc. we find on solving for amplitudes and phases, and compounding errors [7] that

$$a_1 = \frac{[(D_1 - D_3)^2 + (D_4 - D_2)^2]^{1/2}}{2D_0} \pm \delta(2 + a_1^2)^{1/2},$$

$$\tan \alpha_1 = \frac{D_4 - D_2}{D_1 - D_3} \pm \frac{(\Delta_1^2 + \Delta_3^2)^{1/2}}{D_1 - D_2}(1 + \tan^2 \alpha_1)^{1/2},$$

$$a_2 \cos \alpha_2 = \frac{D_1 - D_2 + D_3 - D_4}{4D_0} \pm \delta(1 + a_2^2 \cos^2 \alpha_2)^{1/2},$$

where

$$\delta = (\Delta_1^2 + \Delta_2^2 + \Delta_3^2 + \Delta_4^2)^{1/2}/4D_0.$$

Substituting into these formulas the values of D and Δ contained in Table II, we find

$$a_1 = 0.0169 \pm .0080,$$

$$\tan \alpha_1 = -0.50 \pm .45$$

$$(136° < \alpha_1 < 177°),$$

$$a_2 \cos \alpha_2 = -0.0018 \pm .0040.$$

The last of these quantities includes the amplitude of the polarization effect as one of its components. To make this explicit we may restrict a_2 and α_2 to represent the amplitude and phase angle of variations of twice the fundamental frequency due to mechanical imperfections only, and use p to represent the amplitude of the polarization effect. We may then write, since the phase angle associated with p is zero,

$$p + a_2 \cos \alpha_2 = -0.0018 \pm .0040,$$

and from this we wish to infer that p is itself a small quantity, the same in order of magnitude as $(p + a_2 \cos \alpha_2)$.

It may be urged, of course, that nothing in regard to the value of p is to be inferred from the value of $(p + a_2 \cos \alpha_2)$, and this in a strictly mathematical sense is true enough; the individual terms may both be large, and the small value of their sum may be entirely fortuitous. While one must recognize this as a possibility, he must recognize also that the likelihood of the occurrence of chance compensations of such perfection in the case not only of this beam, but in the cases of the others as well, is extremely small. The values found for $(p + a_2 \cos \alpha_2)$ for all five beams have been set down in Table III. It will be seen that,

[7] In calculating the probable errors of these functions we have disregarded the small differences in precision involved in the measurements of the various deflections.

with the possible exception of the value for the 103 volt beam, all are equal sensibly to zero.

TABLE III

Beam No.	Bombarding Potential	No. of Obs.	a_1	α_1	$p + a_2 \cos \alpha_2$
1	20 volts	111	0.013 ± .012	133° to 194°	0.0089 ± .0058
2	55	108	0.015 ± .013	107° to 264°	−0.0025 ± .0065
3	77	124	0.017 ± .008	136° to 177°	−0.0018 ± .0040
4	103	30	0.065 ± .011	113° to 127°	0.0230 ± .0057
5	120	146	0.021 ± .004	102° to 121°	0.0053 ± .0020

The large values found for both $(p + a_2 \cos \alpha_2)$ and a_1 in the case of the 103 volt beam are due, we believe, to some departure from the usual conditions of the experiment which occurred while observations on this beam were being made. Fewer measurements were made on this beam than on any of the others, and the discordant values found for its constants are traceable to an exceptionally low value—based on eight readings only—which was obtained for $D_2(\theta = 90 \text{ degrees})$. The discordance of this value with those obtained for the other deflections is evident from the figures set down in the last column of Table IV. These are the differences between the various deflections and the mean of the deflections D_1, D_3 and D_4. It will be noted that the departure of the value obtained for D_2 from this mean is three times as great as that for any of the others. The fact that this single unusual departure is responsible for the exceptionally large value not only of $(p + a_2 \cos \alpha_2)$ but of a_1 as well, is reason, we think, for regarding it as accidental. We believe, therefore, that we are justified in disregarding the result obtained in this case, and in concluding from the values found for $(p + a_2 \cos \alpha_2)$ for the other beams that the amplitude of the polarization effect is zero within the limits of uncertainty of our measurements—that is, within about one half of one per cent.

TABLE VI

103 Volt Beam

θ	No. of Readings	Deflections	$D - \frac{D_1 + D_3 + D_4}{3}$
0 deg.	7	$D_1 = 4.829 \pm .070$	−0.17
90.	8	$D_2 = 4.481 \pm .052$	−0.52
180.	9	$D_3 = 5.133 \pm .031$	+0.13
270.	6	$D_4 = 5.033 \pm .061$	+0.03

. . . .

Experiments designed to test for the polarization of electrons by reflection have been made also by Cox, McIlwraith and Kurrelmeyer, by Joffé, and by Wolf. The experiment by the first-named three [8] is similar in principle and arrangement to our own; the intensity of a beam of electrons which has been twice reflected through 90 degrees is measured while the second reflector and collector are revolved about the direction of incidence of the second reflection. But in other respects the experiments differ. The electrons constituting the primary beam are β-rays from a sample of radium, the reflectors are plates of polycrystalline gold, and the collector is a point-discharge electron counter. The authors report that the shielding between the electron source and the counter was inadequate to suppress entirely an effect due to the gamma radiation, and further that rapid changes in the characteristics of the discharge point made it difficult to obtain consistent data. The results which they publish are ratios of the current received by the collector in one of the "parallel" positions to that received in one or the other of the "transverse" positions, and the ratios of the currents received in the two "transverse" positions. The values found for the first of these ratios depart from unity by much more than the probable error, and show a bias in favor of polarization. The authors do not point this out, however, but lay emphasis instead upon a rather slight departure from unity of the values obtained for the second ratio—that of the currents in the two transverse directions.

The experiment by Joffé is mentioned by Darwin [9] in a short article on the Sixth Congress of Russian Physicists which was held last summer. Darwin remarks that at one of the meetings Joffé reported that he had looked for a polarization of electrons by reflection, but had failed to detect such an effect. So far as we are aware no report of this work has been published.[10]

In the experiment by Wolf [11] a beam of low speed electrons (accelerating potentials of about 10 volts) is deflected in a magnetic field and caused, while still in the field, to impinge at 45 degrees incidence upon a target which in various tests was a plate of brass, a cleft crystal of galena and a crystal of copper. The currents to the target and to an enclosing electrode are measured as the target is revolved about the direction of incidence, and are found to be independent of azimuth. This result is susceptible of two interpretations at least; it may mean that the incident beam is not polarized by the magnetic field, or it may mean that none of the targets serves as an analyser. The latter interpretation, which leaves unanswered the question of polarization in a magnetic field, is consistent with the result which we have obtained.

[8] Cox, McIlwraith & Kurrelmeyer, *Proc. Nat. Acad. Sci.*, 14, 544 (1928).

[9] Darwin, *Nature*, 122, 630 (1928).

[10] A brief account of these experiments has appeared recently in the Comptes Rendus; Joffé and Arsenieva, C. R. *188*, 152 (1929).

[11] Wolf, *Zeit. f. Phys.*, 52, 314 (1928).

The question of the result to be expected from the wave theory of the electron in experiments of the kind here described has recently been considered by Darwin.[12] The conclusion which Darwin reaches is that a beam of electrons initially unpolarized will remain unpolarized after diffraction by a grating provided the forces in the grating responsible for the scattering are electric rather than magnetic, and that therefore any experiment designed to detect polarization by successive reflections from crystals can lead only to a negative result. The result of our experiment is in accord with this prediction.

It is a pleasure to express our best thanks to Mr. G. E. Reitter for the great care with which he constructed the special apparatus used in this experiment, and to Mr. C. J. Calbick for valuable assistance in collecting and reducing the data.

[12] Darwin, *Proc. Roy. Soc.*, 120, 631 (1928).

A Generalization of Heaviside's Expansion Theorem

By W. O. PENNELL

The expansion theorem is one of the most frequently used methods of evaluating operational forms arising from the operational calculus developed by Heaviside. The original theorem, however, is applicable, in general, only to expressions containing integral powers of the operator d/dt. This paper describes an extension to, or a generalization of the original expansion theorem whereby, in general, operational forms with either fractional or integral powers of the operator can be evaluated. A number of operational equivalents are given to be used with the theorem, one of which is the equivalent used by Heaviside. Examples of the application of the theorem to electric circuit problems are shown.

THE well known expansion theorem given by Heaviside in Vol. II of his "Electromagnetic Theory" may be stated as follows:

An operational equation of the form $h = Y(p)/Z(p)$, may under certain well known restrictions on the functions Y and Z, have as its solution

$$h = \frac{Y(0)}{Z(0)} + \sum_n \frac{Y(p_n)}{p_n Z'(p_n)} e^{p_n t}, \qquad n = 1, 2, 3 \cdots. \tag{1}$$

p is the differential operator d/dt, and p_1, p_2 $\cdots$ are the roots of $Z(p) = 0$. $Z'(p_n)$ is the result of substituting p_n for p in $d(Z(p))/dp$. The theorem is true only when no root is zero and all roots are unequal. $Y(p)$ and $Z(p)$ must contain p to positive integral powers only. Various proofs of this theorem have been given and perhaps the simplest depends upon the expansion of $Y(p)/Z(p)$ by partial fractions.

The expansion theorem is valuable in the solution by operational methods, of problems in mathematical physics, and especially electric circuit theory problems.

Generalization of the Expansion Theorem

The generalization of this theorem may be stated as follows: Under certain circumstances it may be possible to write the operational equation

$$h = \frac{Y(p)}{Z(p)} \qquad \text{as} \qquad h = \frac{N(q)}{D(q)},$$

where q is a function of the operator p. With suitable restrictions on the functional forms of N and D the solution of the operational equation is given by

$$h = \frac{N(0)}{D(0)} + \sum_n \frac{N(q_n)}{q_n D'(q_n)} \psi(t, q_n), \tag{2}$$

where $\psi(t, q_n)$ is the equivalent of the operational expression $q/(q - q_n)$

and $q_1, q_2, \cdots$ represent the roots of $D(q) = 0$. If q is the differential operator, that is if

$$q = p = \frac{d}{dt},$$

then as is well known

$$\frac{q}{q - q_n} = \frac{p}{p - p_n} = e^{p_n t}$$

and (2) becomes the Heaviside expression (1).

A proof of the generalized theorem equation (2), is as follows:

By a theorem of partial fractions:

$$\frac{N(q)}{D(q)} = \frac{N(q_1)}{(q - q_1)D'(q_1)} + \frac{N(q_2)}{(q - q_2)D'(q_2)} + \cdots + \frac{N(q_n)}{(q - q_n)D'(q_n)} \quad (3)$$

where $q_1, q_2, \cdots q_n$ are the roots of $D(q) = 0$. The above theorem is true when $D(q)$ and $N(q)$ are rational polynomials and $N(q)$ is of a lower degree than $D(q)$. Further limitations are that no root can be zero and all roots must be unequal.

In writing the above identity in terms of operators it is tacitly assumed that the operators obey the three fundamental laws of algebra, the associative, commutative and distributive laws.

Now

$$\frac{1}{q - q_n} = -\frac{1}{q_n} + \frac{q}{q_n(q - q_n)} \cdot \quad (4)$$

Substituting (4) in (3)

$$\frac{N(q)}{D(q)} = \frac{N(q_1)}{(-q_1)D'(q_1)} + \frac{N(q_2)}{(-q_2)D'(q_2)} + \cdots + \frac{N(q_n)}{(-q_n)D'(q_n)} + \sum_n \frac{N(q_n)}{q_n D'(q_n)}\left(\frac{q}{q - q_n}\right) \quad (5)$$

$$= \frac{N(0)}{D(0)} + \sum_n \frac{N(q_n)}{q_n D'(q_n)} \psi(t, q_n), \quad (6)$$

where

$$\frac{q}{q - q_n} = \psi(t, q_n).$$

The expression fails where $N(0)/D(0)$ is infinite. When the operator

$$q = p = \frac{d}{dt}$$

then

$$\frac{p}{p - p_n} = e^{p_n t}$$

and (6) becomes the Heaviside Expansion theorem.

Although the above proof of (6) is for cases where $D(q)$ is a polynomial, if $D(q)$ is a transcendental function which can be expanded by the process shown, the equation will still hold. It is shown in treatises on trigonometry that tan at, cot at, 1/sin at, 1/cos at, 1/sinh at, 1/cosh at, tanh at, and coth at, all can be expanded in an infinite series of partial fractions which are identical [1] with the expansions obtained by applying the process of equation (3).

Equivalents to be Used in Generalized Theorem

In applying this theorem the following operational equivalents are useful:

Equivalent No. 1:

Let

$$q = p = \frac{d}{dt}.$$

Then

$$\frac{q}{q-a} = \frac{p}{p-a} = e^{at}. \tag{7}$$

This is the equivalent used in the expansion theorem by Heaviside.

Equivalent No. 2:

Let

$$q = p^{1/2} = \left(\frac{d}{dt}\right)^{1/2}.$$

Then

$$\frac{q}{q-a} = \frac{p^{1/2}}{p^{1/2}-a} = e^{a^2t}[1 + \text{erf}\,(at^{1/2})] \tag{8}$$

where

$$\text{erf}\,(at^{1/2}) = \frac{2}{\sqrt{\pi}}\int_0^{at^{1/2}} e^{-\lambda^2}d\lambda.$$

Equivalent No. 3:

Let

$$q = p^{1/s} = \left(\frac{d}{dt}\right)^{1/s} \qquad s = \text{a positive integer.}$$

Then

$$\frac{q}{q-a} = \frac{p^{1/s}}{p^{1/s}-a} = e^{a^st}[1 + \psi_1(t,a) + \psi_2(t,a) + \cdots + \psi_{s-1}(t,a)], \tag{9}$$

where

$$\psi_1(t,a) = \frac{1}{\Gamma(1/s+1)}\int_0^{at^{1/s}} \epsilon^{-\lambda^s}d\lambda,$$

[1] Except in some cases for the first term $Y(0)/Z(0)$.

$$\psi_2(t, a) = \frac{1}{\Gamma(2/s + 1)} \int_0^{a^2 t^{2/s}} e^{-\lambda^{s/2}} d\lambda,$$

. . . .

$$\psi_{s-1}(t, a) = \frac{1}{\Gamma\left(\frac{s-1}{s} + 1\right)} \int_0^{a^{s-1} t^{(s-1)/s}} \epsilon^{-\lambda^{s/(s-1)}} d\lambda.$$

Equivalent No. 4:
Let

$$q = p^2 = \left(\frac{d}{dt}\right)^2.$$

Then

$$\frac{q}{q-a} = \frac{p^2}{p^2 - a} = \cosh a^{1/2} t. \tag{10}$$

Equivalent No. 5:
Let

$$q = p^3 = \left(\frac{d}{dt}\right)^3.$$

Then

$$\frac{q}{q-a} = \frac{p^3}{p^3 - a} = (1/3) e^{a^{1/3} t} + (2/3) e^{-a^{1/3} t/2} \cos\left(a^{1/3} t \frac{\sqrt{3}}{2}\right). \tag{11}$$

Equivalent No. 6:
Let

$$q = p^4 = \left(\frac{d}{dt}\right)^4.$$

Then

$$\frac{q}{q-a} = \frac{p^4}{p^4 - a} = \tfrac{1}{2} \cosh (a^{1/4} t) + \tfrac{1}{2} \cos (a^{1/4} t). \tag{12}$$

Equivalent No. 7:
Let

$$q = (p + b)^{1/2} = \left(\frac{d}{dt} + b\right)^{1/2}.$$

Then

$$\frac{q}{q-a} = \frac{b}{b - a^2} - \frac{a^2}{b - a^2} e^{(a^2 - b)t} + \frac{a\sqrt{b}}{b - a^2} \operatorname{erf}(\sqrt{bt}) - \frac{a^2}{b - a^2} e^{(a^2 - b)t} \operatorname{erf}(a\sqrt{t}).$$

where $b \neq a^2$

Equivalent No. 8:
Let

$$q = \left(\frac{p}{p + b}\right)^{1/2}.$$

Then

$$\frac{q}{q-a} = \frac{1}{1-a^2}\left[e^{a^2bt/(1-a^2)} + ae^{-(bt/2)} I_0\left(\frac{bt}{2}\right) + \frac{ab}{(1-a^2)^2} e^{a^2bt/(1-a^2)} \int_0^t e^{(a^2+1)bt/2(a^2-1)} I_0\left(\frac{bt}{2}\right) dt \right]$$

where $a^2 \neq 1$

and $I_0\left(\frac{bt}{2}\right) = J_0\left(\frac{ibt}{2}\right) =$ Bessel Function of the first kind.

The above equivalents can be obtained by known operational methods and their derivation will not be given here.

In the application of the generalized theorem to electrical problems, equivalents No. 1, No. 2 and No. 3, especially No. 1 and No. 2, are the ones which will be most frequently used. Equivalents No. 4, No. 5, and No. 6, since they involve only integral powers of p are of use in reducing the labor of applying the original expansion theorem to expressions containing only these powers of the operator p or multiples of these powers. Their use in such cases is illustrated by example No. 3 below.

Equivalent No. 7 enables expressions like the following to be evaluated in closed form.

$$\frac{1}{p + c(p+b)^{1/2} + d}, \qquad \frac{1}{(p+b)^{3/2} + cp + d},$$

$$\frac{(p+b)^{1/2}}{(p+b)^{3/2} + cp + d}, \qquad \frac{1}{\cosh (p+b)^{1/2}}, \quad \text{etc.}$$

In applying equivalents No. 2 and No. 7 some of the following properties of the error function are often conveniently used.

$$\text{erf}\,(-t) = -\,\text{erf}\,(t) \qquad \text{and} \qquad \text{erf}\,(it) = \frac{2i}{\sqrt{\pi}} \int_0^t e^{\lambda^2} d\lambda;$$

also

$$\frac{d}{dt}\text{erf}\,[\psi(t)] = \frac{2}{\sqrt{\pi}} e^{-[\psi(t)]^2} \psi'(t)$$

and

$$\frac{d}{dt}\text{erf}\,(at^{1/2}) = \frac{e^{-a^2t}}{\sqrt{\pi}} at^{-1/2}.$$

The value of erf (t) for different values of t may be obtained from tables of the probability integral as for example Pierce Table of Integrals.

The values of erf (it) for values of t from .01 to 2 are given in a table in London Mathematical Society Vol. 29, 1897–98, page 519. The values of erf $(te^{i\pi/4})$ and erf $(te^{-i\pi/4})$ are given by the following formulæ:

$$\text{erf}\ (te^{i\pi/4}) = \sqrt{2i}[C(t\sqrt{2/\pi}) - iS(t\sqrt{2/\pi})], \tag{14}$$

$$\text{erf}\ (te^{-i\pi/4}) = \sqrt{2i}[- iC(t\sqrt{2/\pi}) + S(t\sqrt{2/\pi})], \tag{15}$$

where

$$C(t\sqrt{2/\pi}) = \int_0^{t\sqrt{2/\pi}} \cos\left(\frac{\pi t^2}{2}\right) dt,$$

and

$$S(t\sqrt{2/\pi}) = \int_0^{t\sqrt{2/\pi}} \sin\left(\frac{\pi t^2}{2}\right) dt,$$

and

$$C(- it\sqrt{2/\pi}) = - iC(t\sqrt{2/\pi})$$

and

$$S(- it\sqrt{2/\pi}) = iS(t\sqrt{2/\pi}).$$

Tables of the values of these two integrals known as the Fresnel Integrals are given in various handbooks such as Jahnke and Emde.

Examples of Application of Theorem

A few applications of the theorem will be given.

Example 1:

The operational solution for the current entering an infinitely long ideal cable with a given impressed voltage of the form Ee^{-at} is

$$K\frac{p^{3/2}}{p+a},$$

K being a constant and

$$p = \frac{d}{dt}.$$

To evaluate $p^{3/2}/(p + a)$ in closed form call $p^{1/2} = q$ then

$$\frac{p^{3/2}}{p+a} = \frac{q^3}{q^2+a}.$$

Since the theorem applies in general only when the degree of the numerator is less than that of the denominator we will write

$$\frac{q^3}{q^2+a} = q - \frac{aq}{q^2+a}$$

and

$$\frac{q}{q^2+a}=\frac{Y(q)}{Z(q)}=\frac{Y(0)}{Z(0)}+\sum_n \frac{Y(q_n)}{q_n Z'(q_n)}\psi(q_n, t),$$

$$\frac{Y(0)}{Z(0)}=0. \qquad \frac{Y(q_n)}{q_n Z'(q_n)}=\frac{q_n}{2q_n^2}=\frac{1}{2q_n},$$

$$Z(q) = q^2 + a \text{ and the roots of } Z(q) = 0 \text{ are } q_n = \pm ia^{1/2},$$

$$\psi(q_n, t) = e^{q_n^2 t}[1 + \text{erf } q_n t^{1/2}] \qquad \text{(see equivalent No. 2).}$$

So

$$\frac{q}{q^2+a}=\frac{1}{2ia^{1/2}}e^{-at}[1+\text{erf }(ia^{1/2}t^{1/2})]-\frac{1}{2ia^{1/2}}e^{-at}[1+\text{erf }(-ia^{1/2}t^{1/2})]$$

$$=\frac{1}{ia^{1/2}}e^{-at}\text{ erf }(ia^{1/2}t^{1/2}).$$

Hence

$$\frac{q^3}{q^2+a}=q-\frac{aq}{q^2+a}=\frac{t^{-1/2}}{\Gamma(\frac{1}{2})}-\frac{a^{1/2}}{i}e^{-at}\text{ erf }(ia^{1/2}t^{1/2}),$$

since

$$q=p^{1/2}=\left(\frac{d}{dt}\right)^{1/2}=\frac{t^{-1/2}}{\Gamma(\frac{1}{2})}.$$

Example 2:

The operational expression for the current entering at time t in a cable of distributed resistance R and capacity C with an electromotive force $\sin \omega t$ impressed is given by

$$I=\sqrt{C/R}\,\frac{\omega p^{3/2}}{p^2+\omega^2}$$

where

$$p=\frac{d}{dt}.$$

Put $q = p^{1/2}$. Then

$$\frac{p^{3/2}}{p^2+\omega^2}=\frac{q^3}{q^4+\omega^2}.$$

Here

$$\frac{Y(0)}{Z(0)}=0, \qquad \frac{Y(q_n)}{q_n Z'(q_n)}=\frac{q_n^3}{4q_n^4}=\frac{1}{4q_n}.$$

If

$$q^4+\omega^2=0, \quad q_n=\omega^{1/2}e^{i(\pi/4)}, \quad \omega^{1/2}e^{-i(\pi/4)}, \quad -\omega^{1/2}e^{i(\pi/4)}, \quad -\omega^{1/2}e^{-i(\pi/4)}.$$

So

$$\sqrt{C/R}\,\frac{\omega p^{3/2}}{p^2+\omega^2} = \omega\sqrt{C/R}\sum_n \frac{1}{4q_n} e^{q_n^2 t}[1 + \text{erf}\,(q_n t^{1/2})]$$

$$= \omega\sqrt{C/R}\Bigg[\frac{1}{4\omega^{1/2}e^{i(\pi/4)}} e^{i\omega t}\{1 + \text{erf}\,(\omega^{1/2}e^{i(\pi/4)}t^{1/2})\}$$

$$+ \frac{1}{4\omega^{1/2}e^{-i(\pi/4)}} e^{-i\omega t}\{1 + \text{erf}\,(\omega^{1/2}e^{-i(\pi/4)}t^{1/2})\}$$

$$- \frac{1}{4\omega^{1/2}e^{i(\pi/4)}} e^{i\omega t}\{1 + \text{erf}\,(-\,\omega^{1/2}e^{i(\pi/4)}t^{1/2})\}$$

$$- \frac{1}{4\omega^{1/2}e^{-i(\pi/4)}} e^{-i\omega t}\{1 + \text{erf}\,(-\,\omega^{1/2}e^{-i(\pi/4)}t^{1/2})\}\Bigg]$$

$$= \frac{\omega^{1/2}}{2}\sqrt{C/R}[e^{i(\omega t-\pi/4)}\,\text{erf}\,(\omega^{1/2}e^{i(\pi/4)}t^{1/2})$$

$$+ e^{-i(\omega t-\pi/4)}\,\text{erf}\,(\omega^{1/2}e^{-i(\pi/4)}t^{1/2})]$$

$$= \sqrt{\frac{2C\omega}{R}}[\sin\,(\omega t)S(\omega^{1/2}t^{1/2}\sqrt{2/\pi})$$

$$+ \cos\,(\omega t)C(\omega^{1/2}t^{1/2}\sqrt{2/\pi})].$$

The last transformation is obtained by means of formulæ 14 and 15.

Example 3:

Evaluate

$$y = \frac{1}{p^4 - 3p^2 + 2}.$$

This can be solved by the expansion theorem in the usual way. A somewhat shorter method is to use the generalized theorem with the operator $q = p^2$. Then

$$y = \frac{1}{q^2 - 3q + 2} = \tfrac{1}{2} + \sum_n \frac{1}{2q_n{}^2 - 3q_n}\psi(q_n, t)$$

$$q_n = 1, 2;\ \psi(q_n, t) = \cosh p_n{}^{1/2}t.$$

See equivalent No. 4. So

$$y = \tfrac{1}{2} + \tfrac{1}{2}\cosh t\sqrt{2} - \cosh t.$$

Example 4:

Evaluate

$$\frac{\sinh bp^{1/2}}{\sinh ap^{1/2}} = \frac{\sinh bq}{\sinh aq} = \frac{b}{a} + \sum \frac{\sinh bq_n}{aq_n \cosh aq_n} e^{q_n^2 t}[1 + \text{erf}\,(q_n t^{1/2})],$$

$$-\sinh aq = i\sin iaq.$$

The roots[1] of $\sin iaq = 0$ are

$$q_n = \frac{n\pi}{ia}, \qquad n = \pm 1, \pm 2, \qquad \text{etc.}$$

Substituting these values of q_n in above we get

$$\frac{\sinh bq}{\sinh aq} = \frac{b}{a} + \sum_{\substack{n=\pm 1\\ n=\pm 2\\ \text{etc.,}}} \frac{\sinh \dfrac{n\pi b}{ia}}{\dfrac{n\pi}{i} \cosh \dfrac{n\pi}{i}} e^{-(n^2\pi^2/a^2)t} \left[1 + \text{erf}\left(\frac{n\pi}{ia} t^{1/2} \right) \right]$$

$$= \frac{b}{a} + \frac{2}{\pi} \sum_{n=1,2,3,\cdots} \frac{(-1)^n \sin \dfrac{n\pi b}{a}}{n} e^{-(n^2\pi^2/a^2)t}.$$

If $(\sinh bp^{1/2})/(\sinh ap^{1/2})$ is solved by the expansion theorem and the summation is extended over both positive and negative roots, the result is

$$\frac{b}{a} + \frac{4}{\pi} \sum_{n=1,2,3,\cdots} (-1)^n \frac{\sin \dfrac{n\pi b}{a}}{n} e^{-(n^2\pi^2/a^2)t}.$$

In other words the summation quantity is just double what it should be. In order to correct this in practice, those who have used the theorem for such cases have extended the summation only over the positive roots, notwithstanding the fact that in similar cases with integral exponents such as, for example, $1/\cosh ap$ the summation is extended over all the roots. The truth is the original expansion theorem is not applicable if either numerator or denominator contains p to a fractional form. In the above case were the problems to evaluate $(\sinh bp^{2/3}/\sinh ap^{2/3})$ the expansion theorem gives an entirely incorrect answer, while the correct answer is obtained from the extension to the theorem.

Example 5.

$$\frac{p^{1/3}}{p^{2/3} - 1} = \frac{q}{q^2 - 1} \qquad \sum \frac{q_n}{2q_n^2} \psi(t, q_n).$$

Here

$$\psi(t, q_n) = e^{q_n^3 t} \left[1 + \frac{1}{\Gamma(4/3)} \int_0^{q_n t^{1/3}} e^{-\lambda^3} d\lambda + \frac{1}{\Gamma(5/3)} \int_0^{q_n^2 t^{2/3}} e^{-\lambda^{3/2}} d\lambda \right],$$

$$q_n = \pm 1,$$

[1] Excluding the root $q_n = 0$ which is not used in this case.

$$\frac{q}{q^2-1} = \tfrac{1}{2}e^t\left[1+\frac{1}{\Gamma(4/3)}\int_0^{t^{1/3}} e^{-\lambda^3}d\lambda + \frac{1}{\Gamma(5/3)}\int_0^{t^{2/3}} e^{-\lambda^{3/2}}d\lambda\right]$$

$$- \tfrac{1}{2}e^{-t}\left[1+\frac{1}{\Gamma(4/3)}\int_0^{-t^{1/3}} e^{-\lambda^3}d\lambda + \frac{1}{\Gamma(5/3)}\int_0^{t^{2/3}} e^{-\lambda^{3/2}}d\lambda\right]$$

$$= \sinh t + \frac{\sinh t}{\Gamma(5/3)}\int_0^{t^{2/3}} e^{-\lambda^{3/2}}d\lambda + \tfrac{1}{2}\frac{e^t}{\Gamma(4/3)}\int_0^{t^{1/3}} e^{-\lambda^3}d\lambda$$

$$- \tfrac{1}{2}\frac{e^{-t}}{\Gamma(4/3)}\int_0^{-t^{1/3}} e^{-\lambda^3}d\lambda.$$

Example 6:

If the problem is to evaluate

$$\frac{\sinh b(p+c)^{1/2}}{\sinh a\,(p+c)^{1/2}}$$

Equivalent No. 7 is used. The details will not be worked out since they are quite similar to Example No. 4. The answer is

$$\frac{\sinh b(p+c)^{1/2}}{\sinh a(p+c)^{1/2}} = \frac{b}{a}$$

$$+\frac{2}{\pi}\sum_{n=1,\,2,\,3\,\ldots}(-1)^n\frac{\sin\left(\dfrac{n\pi b}{a}\right)}{n}\left[\frac{c}{c+\dfrac{n^2\pi^2}{a^2}} + \frac{n^2\pi^2}{a^2c+n^2\pi^2}e^{-[(n^2\pi^2/a^2)+c]t}\right].$$

If $c = 0$ the above equivalent reduces to the answer of Example No. 4.

Final Remarks

Operational methods were used by Euler and other mathematicians prior to Heaviside. Their use, however, depended in general upon a formal definition of the operator. Heaviside, on the other hand, adopted a different procedure. In the differential equation of the problem he replaced the operator d/dt by p and obtained the solution of the resulting algebraic equation. He then determined the significance of the operator by the condition that it should give the complete solution of the original differential equation subject to equilibrium boundary condition.

While Heaviside developed the operational calculus in a fairly workable and complete form he failed to correlate it or reconcile it with conventional mathematics or to put its theorems on a rigorous basis. The development since Heaviside's day has been due to a considerable extent to the engineer and mathematical physicist rather than to the pure mathematician.

There are now available a number of methods of evaluating operational forms, among which may be mentioned

The original Heaviside expansion theorem,
Operational Division which gives a series solution,
Contour Integration of the Bromwich-Fourier Integral,
Carson's Integral Equation.

It is thought that this extension to the expansion theorem will be of value as another way of evaluating in closed form certain operational expressions, especially those involving fractional exponents.

In preparing this paper, the author wishes to acknowledge his indebtedness to Mr. R. M. Foster for the contribution of Equivalent No. 7 in its present form and for notes regarding the evaluation of the error function. He is also indebted to Mr. J. R. Carson for reading a draft of the manuscript and for a number of helpful suggestions.

A High Precision Standard of Frequency [1]

By W. A. MARRISON

SYNOPSIS: A new standard of frequency is described in which three 100,000 cycle quartz crystal-controlled oscillators of very high constancy are employed. These are interchecked automatically and continuously with a precision of about one part in one hundred million. They are checked daily in terms of radio time signals by the usual method employing a clock controlled by current maintained at a submultiple of the crystal frequency. Specially shaped crystals are used which have been adjusted to have temperature coefficients less than 0.0001 per cent per degree C.

TO meet the demands for increased precision in measurement and greater reliability of operation a new reference standard frequency system has been developed in the Bell Telephone Laboratories having an absolute accuracy that may be relied upon at all times to better than one part in a million. This reference standard is similar in many respects to one described by J. W. Horton and W. A. Marrison a little over a year ago,[2] but a number of important changes have been made which have contributed to increased accuracy and reliability.

The standard is based on the quartz crystal-controlled oscillator, with a synchronous motor-driven clock, used to determine its rate. It differs from others of the same general type in having a number of similar crystal-controlled oscillators which may be interchanged at will and which are intercompared continuously and automatically with a precision of one part in one hundred million. A number of improvements have been made in the crystal and mounting, and in the circuit, which justify this precision of measurement.

By far the most important element in a crystal-controlled oscillator is the crystal itself and great care was taken in selecting the type to be used in the new standard. A crystal was required as nearly independent as possible of ordinary variations in temperature and pressure and which could be mounted so as to vibrate freely. The effect of temperature appeared to be especially serious as the changes in frequency thus obtained with an ordinary crystal, even with the best commercial thermal regulators available, are greater than are caused by any other single factor in the new standard.

It has been known for some time that plates of quartz cut in the plane of the optic and electric axes usually have positive temperature coefficients and that plates cut in the plane of the optic axis but perpendicular to an electric axis have negative coefficients. It has

[1] Presented before Institute of Radio Engineers, April 3, 1929.
[2] "Precision Determination of Frequency," by J. W. Horton and W. A. Marrison, *Proceedings of Institute of Radio Engineers*, Vol. 16, pp. 137–154, Feb. 1928.

also been known that oscillations may be produced in a crystal either parallel to the impressed electric field or perpendicular to it, the so-called longitudinal and transverse effects. There is a certain amount of mechanical coupling between such different modes of vibration within the crystal, more or less close, depending upon the shape, and in particular depending upon the ratio of dimensions in the principal directions of vibration. In view of these facts it was thought probable that crystals could be produced with such coupling between the modes which have inherently positive and negative coefficients that the resultant temperature coefficient would be nil.

Series of crystals of rectangular and circular shape were made to test this fundamental assumption. It was found that the temperature coefficient does vary with the shape of a resonator and, in particular, that crystals may be proportioned so as to have a coefficient that is practically nil. The relations between the temperature coefficient

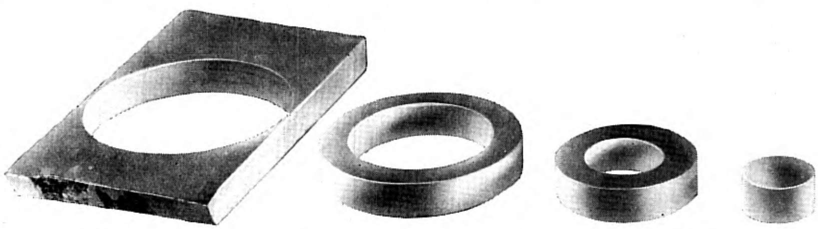

Fig. 1—Crystals used in preliminary temperature coefficient tests.

and the dimensions in the case of rectangular plates have been further studied in detail by F. R. Lack [3] of the Bell Telephone Laboratories.

In the first experiment performed with circular discs for this study a large disc was first cut and smaller ones cut from it, after measurement, to insure constancy of material, thickness and orientation with respect to the crystal axes. The parts remaining after three sizes of discs had been cut in this way, with the remainder of the slab from which they were obtained, are shown in Fig. 1. The slab is shown in the partly assembled original crystal in Fig. 2 to show the manner of cutting. With such circular discs it was found that at least one diameter could be found for which the temperature coefficient is very small throughout the entire room temperature range.

Low temperature coefficient crystals obtained in this way are subject to the usual mounting difficulties, namely that the friction on the mounting considerably increases the decrement, and by an amount

[3] "Observations on Modes of Vibrations and Temperature Coefficients of Quartz Plates," by F. R. Lack, presented before the Institute of Radio Engineers, April 3, 1929.

which may vary with time. A form of crystal is desired which can be mounted so that the parts vibrating at relatively large amplitude do not bear heavily on any portion of the mounting.

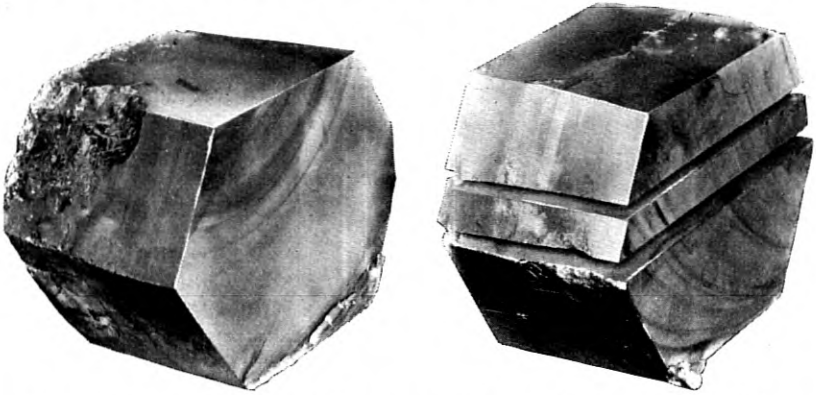

Fig. 2—Partly assembled crystal showing the relation of the slab to the crystal axes.

Further study of temperature coefficients showed that the rings remaining after the small discs had been cut from the larger one,

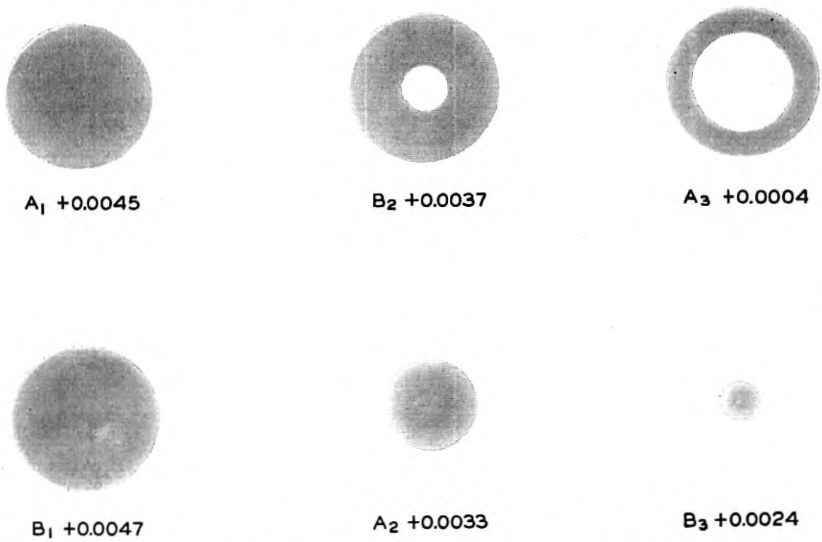

Fig. 3—Temperature coefficients of some discs and rings.

shown in Fig. 1, have a temperature coefficient lower than discs of the same diameter and thickness. This is further illustrated in Fig. 3 which gives the temperature coefficient of two discs and the four parts remaining after holes of different diameters had been trepanned in them.

It is possible to make ring-shaped crystals having negligible temperature coefficients in a considerable range of frequencies, and, since the ring shape permits of an improved method of mounting in which there is very little friction on the holder, they have been adopted for use in the present standard. Such a crystal having a frequency of 100,000

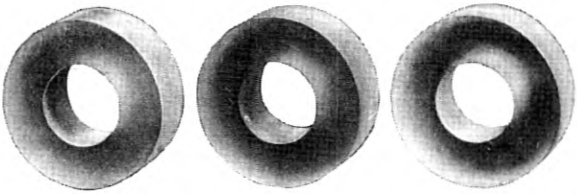

Fig. 4—Three 100,000-cycle low temperature coefficient rings used in frequency standard.

cycles is of substantial size and is reasonably easy to make and adjust. Three of the crystals used in the present standard, adjusted to 100,000 cycles, and having temperature coefficients less than one part in a million per degree C., are shown in Fig. 4.

The variation of frequency with temperature for one of the ring-shaped crystals is given in Fig. 5, showing that it is very small over

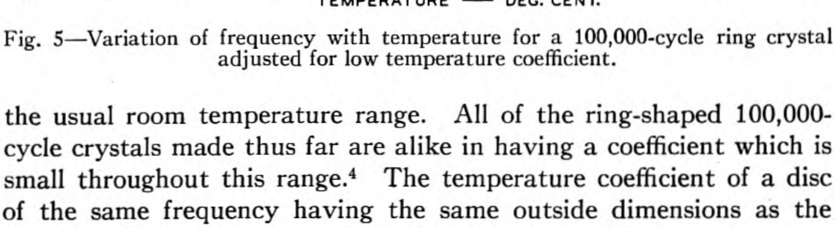

Fig. 5—Variation of frequency with temperature for a 100,000-cycle ring crystal adjusted for low temperature coefficient.

the usual room temperature range. All of the ring-shaped 100,000-cycle crystals made thus far are alike in having a coefficient which is small throughout this range.[4] The temperature coefficient of a disc of the same frequency having the same outside dimensions as the 100,000-cycle rings, is approximately 30 parts in a million per degree C., more than thirty times that of the adjusted crystal.

[4] Where an accuracy of the order of only one part in 100,000 is desired, as in some portable standards, such a crystal could be employed without any form of temperature control.

The manner in which the ring-shaped crystals are mounted in their operating position is shown in Fig. 6. The hole is shaped so that when the crystal hangs on a horizontal cylinder the point of contact is at a theoretical node for mechanical vibration. There is evidence of slight vibration where the central plane intersects the double conical hole but it is small in comparison with that obtained at the outer surface where a crystal is usually supported. The decrement of the crystal when so mounted is considerably less than when it is supported on one of its plane surfaces.

In the mounting the crystal is spaced from the electrodes and is kept approximately central by means of paper spacers on each side. The crystal is free to move laterally in a narrow region but, since it is

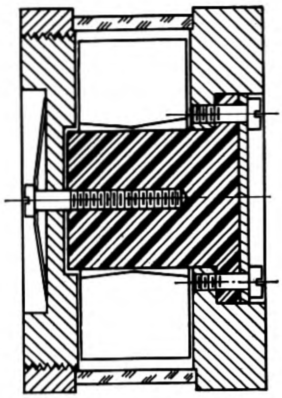

Fig. 6—Section of crystal mounting showing point support.

centrally located, the frequency is at a maximum value and hence a slight motion of the crystal to either side has only a second order effect on the frequency.

The variation of frequency with total electrode spacing is appreciable, but variations due to this factor are avoided by keeping the electrodes accurately spaced by means of a ring of pyrex glass. The temperature coefficient of pyrex is about one quarter of that of crystal quartz perpendicular to the optic axis, so the variation in spacing that is obtained is due almost entirely to the expansion of the crystal. The effect on the frequency due to the differential thermal expansion of the crystal and crystal holder is, however, less than one part in 10^7 per degree C. and so it may be neglected. If it is desired to eliminate this effect entirely a spacer should be used having the same temperature coefficient of expansion as quartz perpendicular to the optic axis, but for practical purposes a material such as pyrex glass or fused quartz is entirely satisfactory.

The crystal holder is constructed so that a slight variation can be made in the total spacing between electrodes. Since the frequency varies with electrode spacing this can be used for making a slight adjustment of frequency. The thread on the adjustable plate is kept tight by spring tension to prevent the spacing from varying irregularly. A crystal holder and a 100,000-cycle crystal are shown in Fig. 7.

Even though the crystal and its mounting have very low temperature coefficients, it is desirable to control their temperature, for which

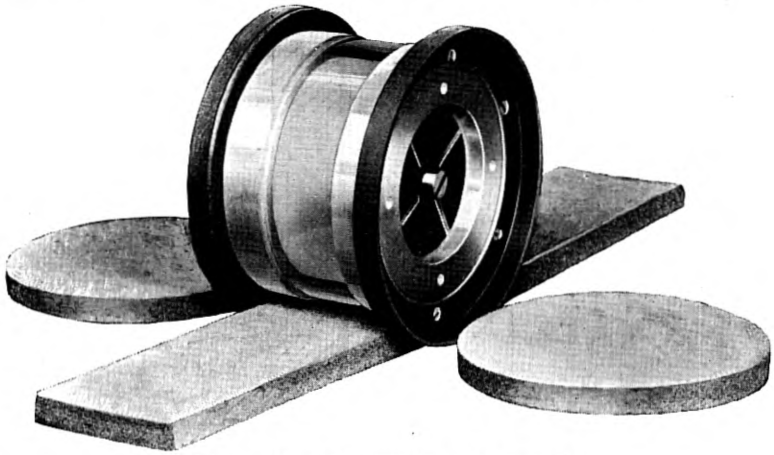

Fig. 7—Crystal mounting with crystal.

purpose the temperature controlling device shown in Fig. 8 has been constructed. It consists of a cylindrical aluminum shell with a wall about one inch thick, with a heater (not shown), and with a temperature responsive element in the wall to control the rate of heating. The aluminum shell has a metal plug that screws into the open end forming a chamber for the crystal which is then completely closed except for a small hole for electrical connections.

Since aluminum is a good thermal conductor the shell equalizes the temperature throughout the chamber and thus avoids the use of a fluid bath. The main heating coil is wound in a single layer over the whole curved surface of the aluminum cylinder, being separated from it only by the necessary electrical insulation. Auxiliary heating coils are wound also on the ends so as to distribute the heating as uniformly as possible. This, in effect, makes the short cylinder behave like a section from an infinite cylinder. To protect the thermostat from the effect of ambient temperature gradients the heating coil has an outside covering consisting of four layers each of thin felt and sheet

Fig. 8—Temperature control chamber with crystal mounting.

copper spirally wound so that alternate layers are of copper and felt, the innermost layer being of felt and the outer one of copper. This is the covering that appears on the complete device shown in Fig. 9.

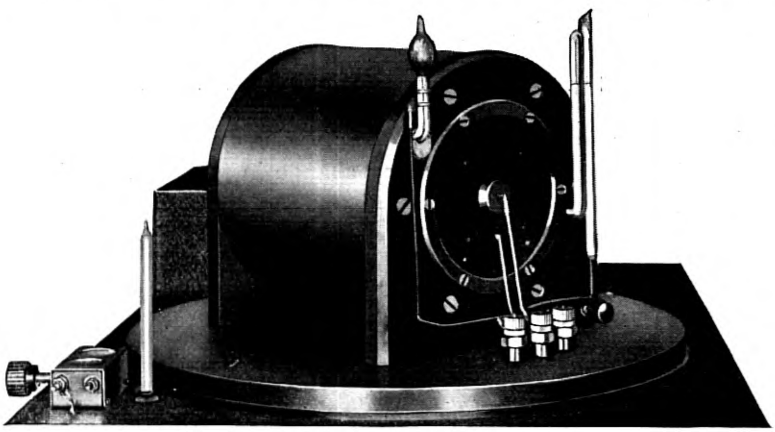

Fig. 9—Complete temperature control unit.

This covering is very effective in reducing surface gradients since the conductivity in directions parallel to, and perpendicular to, the surface differ by a large ratio.

The temperature of the shell rises and falls periodically by about 0.02° C. but even this variation is prevented from reaching the crystal in its mounting by a layer of felt about half a centimeter thick surrounding the crystal holder. At the period of thermostat operation obtained the temperature variations actually reaching the crystal are reduced more than a thousand-fold. The complete temperature controlling device is shown mounted in its operating position in Fig. 9. One of the mounted crystals wrapped in its felt protecting layer is shown in Fig. 10.

To protect the resonator from humidity and pressure variations it is kept under a bell jar at a pressure slightly below atmospheric.

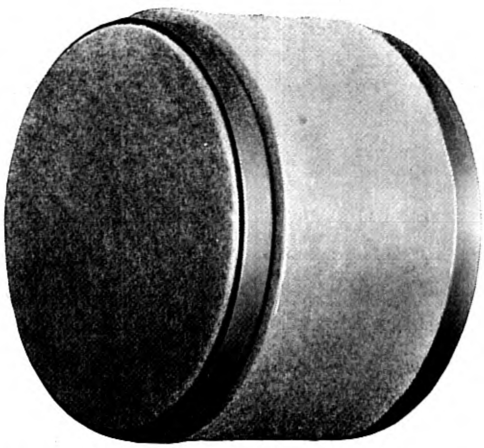

Fig. 10—Crystal mounting with felt insulation.

With the crystals used the frequency varies approximately one part in a million for 10 cm. of mercury change in pressure. It is aimed, therefore, to maintain the pressure constant to about $\pm$ 1 mm. A small mercury gauge within the bell jar indicates the pressure, which may be adjusted by a vacuum pump through a valve in the surface plate. The pressure within the bell jar is affected somewhat by the temperature, and in order to keep it within the required limits it is necessary to maintain a rough control of the temperature within the jar. The pressure gauge does not indicate a change in pressure due to a change in temperature but will indicate any slow leak into the jar that may develop. A thermometer within the bell jar indicates the temperature, from which the change of pressure, and the correction of frequency due to it, may be computed if desired.

Since the frequency varies with the pressure surrounding the crystal an approximate adjustment of the frequency may be made conveniently by an adjustment of pressure.

The circuit of the crystal-controlled oscillator and the first amplifier stages is shown in Fig. 11. The oscillator is of the familiar type in which the crystal electrodes are connected to grid and ground and in which a tuned plate circuit is used. The great advantage in being able to ground one electrode was the major consideration in choosing this circuit. With this circuit, as in the one described a year ago,[2] it has been found possible to choose plate tuning elements such that slight variations in either the inductance or the capacity have little effect upon the frequency. For certain values of inductance and

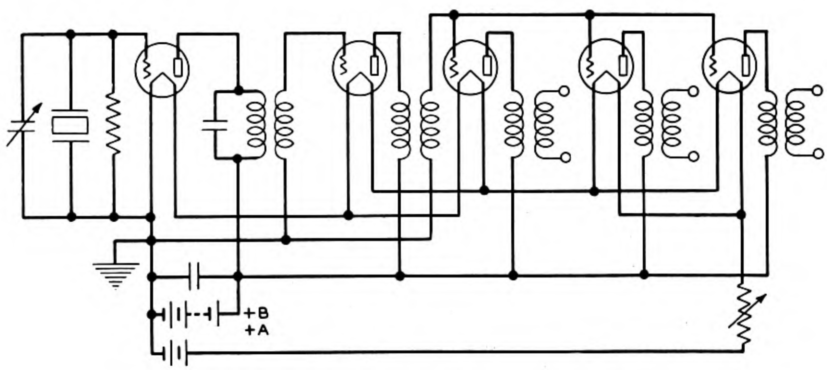

Fig. 11—Circuit of standard frequency oscillator.

capacity the frequency, as a function of their product, takes on a maximum value. The adjustment that gives the maximum value of frequency is used, therefore, so that slight variations, such as those due to temperature coefficient and aging of the tuning elements, will have a negligible effect on the frequency.

The output circuit of the oscillator is very loosely coupled to three independent output amplifiers. This arrangement provides three independent output circuits free from mutual interference and unable to react to an appreciable extent on the crystal oscillator.

The final adjustment of frequency is made with a small cylindrical condenser, having a capacity of about 5 mmf., connected in parallel with the crystal electrodes. The size of this condenser is chosen such that an adjustment of one division on the dial corresponds to a change of frequency of about one part in a hundred million. There are 100 divisions on the dial and a total of 10 turns may be made corresponding to a total possible adjustment of about one part in 100,000. This condenser is shown at C in the circuit drawing.

The oscillator circuit, showing the tubes and transformers, the plate tuning elements, the filament and plate current meters, and the frequency adjusting condenser is shown in Fig. 12. The adjusting condenser is mounted between the meters and is controlled by the large knob and dial.

One complete oscillator unit, consisting of a 100,000-cycle crystal controlled oscillator with three independent 100,000-cycle outputs,

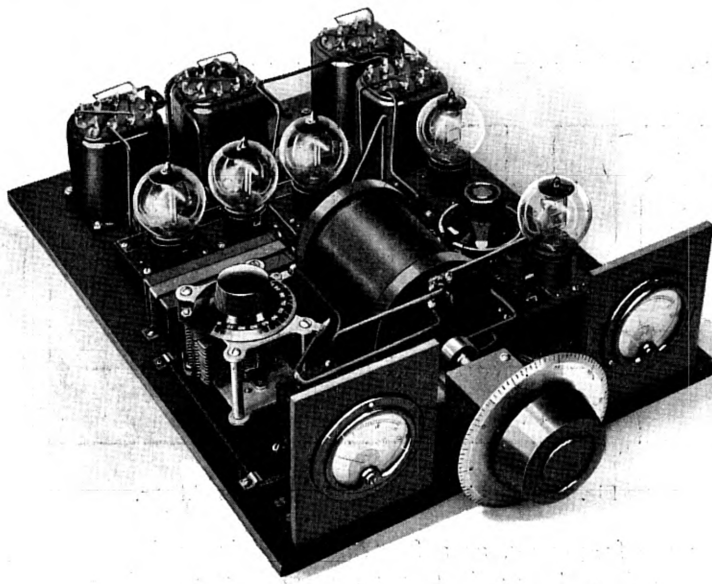

Fig. 12—Standard frequency oscillator without shield.

having a self-contained temperature and pressure controlled crystal, and having a temperature controlled, electrically shielded circuit, is shown in Fig. 13.

The submultiple generator circuit that is used to obtain outputs at 10,000 cycles and 1,000 cycles is shown in Fig. 14. It consists of an inherently unstable vacuum tube oscillator with the tube operating on the curved part of its characteristic. The frequency of this oscillator may be controlled readily by any frequency which is a small multiple or submultiple of it. In this instance the oscillator is controlled by an input having the frequency of its tenth harmonic, the controlling high-frequency input being resistance coupled into the plate circuit of the lower frequency oscillator. The frequency of the controlled oscillator remains indefinitely at an exact submultiple of the controlling frequency.

Two such circuits are used, one to obtain current at 10,000 cycles and one for 1,000 cycles. Of course, additional amplifier circuits are required in order to supply outputs of considerable magnitude at

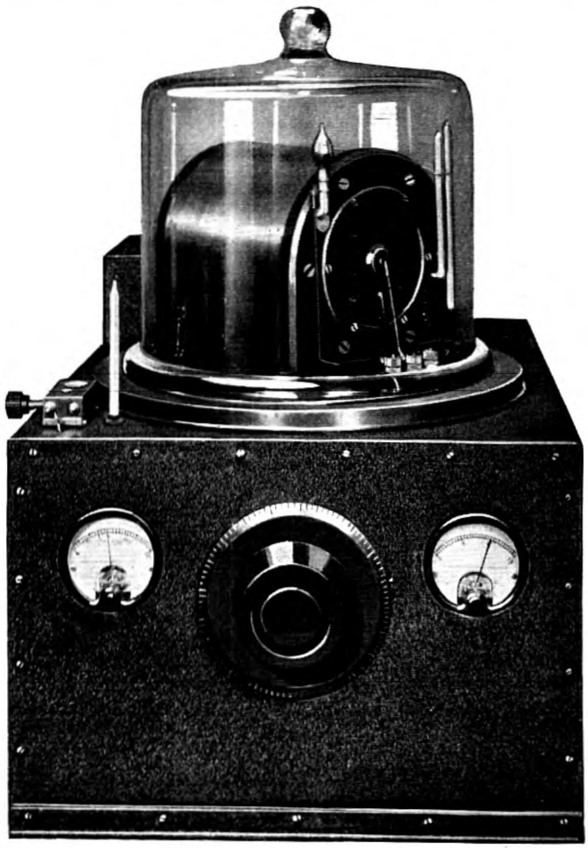

Fig. 13—One complete 100,000-cycle standard frequency unit.

these frequencies, and in such a way that there can be no reaction on the controlling circuits due to load variations or to stray currents at other frequencies fed backward through the output circuits.

A 1,000-cycle motor, operated by current controlled at the 100th submultiple of the standard, drives generators for producing current at 100 cycles and 10 cycles. There are available, therefore, frequencies in decade steps from 100,000 cycles to 10, all controlled by the 100,000-cycle primary oscillator.

The 1,000-cycle motor is geared to a clock in such a way that, when the controlling frequency has its nominal value exactly, the clock keeps accurate time. In order to check the frequency of the system, therefore, it is only necessary to observe changes in rate of the clock so controlled.

An error of 0.864 second per day in the rate of the clock corresponds to an error in the frequency controlling it of one part in 100,000. It is possible to check the rate of the clock visually with an accuracy of about 0.2 second from audible time signals but obviously this is not sufficiently accurate for our purpose, giving an accuracy of only about one part in 400,000 in a day's observation. In order to facilitate the

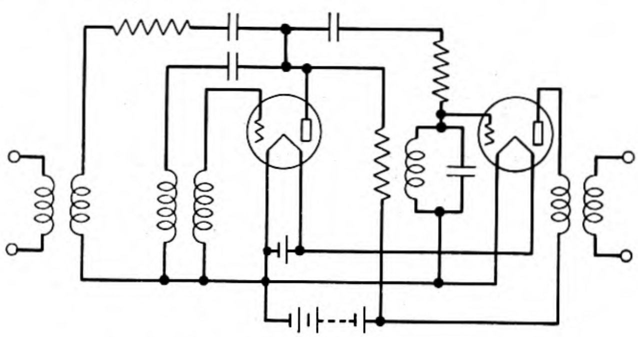

Fig. 14—Circuit of submultiple generator.

comparison with time signals, a contact operated by a cam driven by the 1,000-cycle synchronous motor makes a contact once each second, or to be exact, once for each 100,000 cycles of the primary oscillator. This contact operates one element of a two element recorder while time signals operate the other. Comparisons may thus be made by actual measurements on tape and can be made with greater accuracy than can be judged by eye.

The 1,000-cycle synchronous motor, with its two generators and induction starting motor geared to the clock, is shown in Fig. 15. In this figure the seconds contact mechanism may be seen on the vertical shaft intermediate between the shaft of the motor and the second-hand shaft of the clock.

The assembled rotor of this motor is shown in Fig. 16. The large disc is the 1,000-cycle motor rotor. The disc below it is a hollow steel flywheel filled with mercury used to reduce hunting. The small rotor below the flywheel is the rotor of the unipolar 10-cycle generator. The disc above the motor rotor is the armature of the 100-cycle generator. The squirrel cage armature of an induction motor for starting is immediately above the 100-cycle generator rotor.

A single constant frequency generator is no longer sufficiently reliable as a standard of frequency of high precision and, as has been the practice where accurate time standards are maintained, three

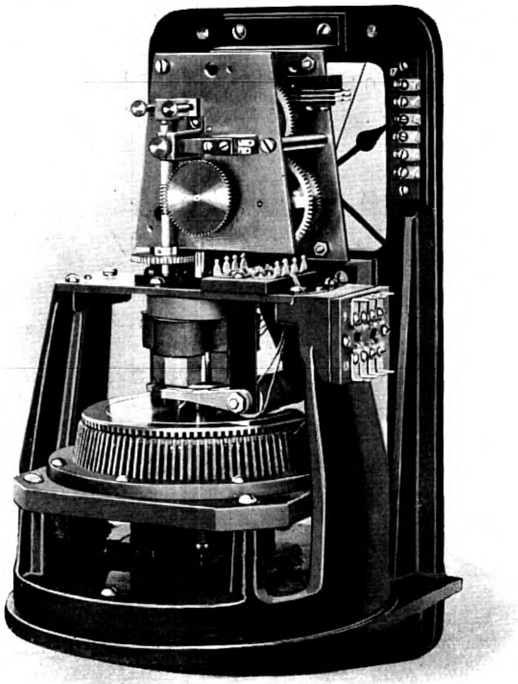

Fig. 15—1,000-cycle synchronous motor, generators, and clock.

similar units have been installed. Means are provided for inter-checking them continuously and automatically with the highest precision justified. The use of three such generators with means for interchecking them makes it possible to determine very quickly if and when one generator fails to operate properly.

Only one submultiple generator, clock, and multiple output amplifier is provided, but a special 3-way switch is used by means of which any one of the three primary oscillators may be selected and used as the controlling unit. The oscillators may be interchanged in any order without interrupting the circuits controlled by them.

In the method used for automatic interchecking a fourth oscillator unit is used, identical with the other three except that the frequency is maintained at a slightly different value. The difference between the frequency of this oscillator and that of the other three is kept at about 1 cycle in 10 seconds. The number of beats between the fourth oscillator and each of the other three oscillators is recorded automatically during each 1,000 second interval. The number of beats thus recorded is approximately 100 during each interval.

In 1,000 seconds each oscillator generates approximately one hundred million waves. The numbers that are recorded are, therefore, the number of parts in one hundred million by which oscillator No. 4

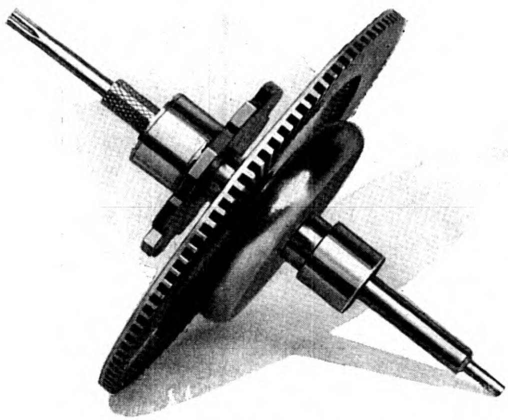

Fig. 16—Rotor of motor-generator.

differs from each of the three primary oscillators during the interval. If the numbers recorded during successive intervals remain the same, the oscillators either did not vary, or they all varied in the same direction by the same number of cycles. If the numbers recorded in successive intervals vary by say 1, 2 or 5, it means that the oscillators have drifted, relative to each other, by so many parts in one hundred million.

Designating the frequencies of the four oscillators by

$$f_1, f_2, f_3, f_4, \tag{1}$$

the three numbers recorded are

$$1{,}000\ (f_4 - f_1),\ 1{,}000\ (f_4 - f_2),\ 1{,}000\ (f_4 - f_3). \tag{2}$$

The mean of these numbers is

$$1{,}000\left(f_4 - \frac{f_1 + f_2 + f_3}{3}\right). \tag{3}$$

If we subtract each of the original three recorded numbers from the mean we obtain

$$1{,}000\left(f_1 - \frac{f_1 + f_2 + f_3}{3}\right) = \delta_1, \tag{4}$$

$$1{,}000\left(f_2 - \frac{f_1 + f_2 + f_3}{3}\right) = \delta_2, \tag{5}$$

$$1{,}000\left(f_3 - \frac{f_1 + f_2 + f_3}{3}\right) = \delta_3. \tag{6}$$

Thus we may compute readily the performance of each of the four oscillators referred to the mean of the three similar primary oscillators. It is obvious that the accuracy of intercomparison of the three similar oscillators does not in any way depend upon the constancy of oscillator No. 4. For convenience in reducing the results, however, it is controlled as carefully as the others.

The records and computed results for approximately ten hours are given in Table 1. During this time the largest relative variation between any two of the four oscillators taken in pairs was 5 parts in 10^8. The random variations between 1,000 second periods appear to be in the order of one or two parts in a hundred million. These random variations are superposed on slow drifts of a quasi-periodic nature probably caused by temperature changes in the circuit and amounting to less than one part in ten million. In addition to these effects a slow, steady drift is expected due to a settling-down of the oscillator circuit and the crystal in its mounting as well as due to aging of the vacuum tubes and even of the crystal itself. The effects of aging can, of course, only be determined after long continued operation.

It is preferable in some cases to refer the performance of each of the four oscillators to the mean performance of all four. This is in the event that all four oscillators are equally reliable in which case the mean of all four makes a better reference standard than the mean of any three. If we designate the numbers

$$1{,}000\ (f_4 - f_1),\ 1{,}000\ (f_4 - f_2),\ \text{and}\ 1{,}000\ (f_4 - f_3)$$

TABLE 1

A TEN-HOUR RECORD OBTAINED BY MEANS OF THE BEAT RECORDER.

The columns δ_1, δ_2 and δ_3 indicate the difference between each oscillator and the mean of the three during each 1,000 second interval expressed in parts in one hundred million.

Serial	Mean	$(f_4 - f_3)$	δ_3	$(f_4 - f_2)$	δ_2	$(f_4 - f_1)$	δ_1
45	86	92	+6	98	+12	69	−17
44	86	92	+6	98	+12	68	−18
43	87	92	+5	99	+12	69	−18
42	87	93	+6	99	+12	70	−17
41	86	92	+6	99	+13	68	−18
40	87	94	+7	98	+11	68	−19
39	86	93	+7	99	+13	67	−19
38	87	94	+7	99	+12	67	−20
37	86	93	+7	99	+13	67	−19
36	87	95	+8	99	+12	66	−21
35	86	93	+7	98	+12	67	−19
34	87	95	+8	100	+13	66	−21
33	87	94	+7	100	+13	66	−21
32	87	95	+8	101	+13	66	−21
31	87	95	+8	101	+14	65	−22
30	87	94	+7	101	+14	66	−21
29	87	94	+7	101	+14	65	−22
28	87	95	+8	101	+14	66	−21
27	87	94	+7	102	+15	65	−22
26	87	95	+8	101	+14	66	−21
25	88	94	+6	103	+15	66	−22
24	88	94	+6	103	+15	68	−20
23	89	96	+7	103	+14	68	−21
22	89	95	+6	103	+14	68	−21
21	89	95	+6	103	+14	68	−21
20	90	95	+5	105	+15	69	−21
19	89	95	+6	103	+14	69	−20
18	89	95	+6	104	+15	68	−21
17	88	94	+6	102	+14	68	−20
16	89	95	+6	104	+15	69	−20
15	89	95	+6	102	+13	69	−20
14	89	95	+6	103	+14	69	−20
13	89	95	+6	102	+13	69	−20
12	89	94	+5	103	+14	70	−19
11	89	95	+6	103	+14	69	−20
10	90	95	+5	103	+13	71	−19
9	89	95	+6	103	+14	70	−19
8	89	95	+6	103	+14	69	−20
7	89	94	+5	103	+14	70	−19

by a, b, and c respectively, it can be shown readily that the numbers

$$a - \frac{a+b+c}{4},\ b - \frac{a+b+c}{4},\ c - \frac{a+b+c}{4} \text{ and } -\frac{a+b+c}{4} \quad (7)$$

represent the difference between each of the oscillators Nos. 1, 2, 3 and 4 respectively and the mean of all four, expressed in parts, in one hundred million. This method treats all four oscillators symmetrically. The symmetry is evident if we substitute in (7) the values (2) assigned to a, b, and c, whence we get:

$$a - \frac{a + b + c}{4} = 1{,}000 \left(\frac{f_1 + f_2 + f_3 + f_4}{4} - f_1 \right), \tag{8}$$

$$b - \frac{a + b + c}{4} = 1{,}000 \left(\frac{f_1 + f_2 + f_3 + f_4}{4} - f_2 \right), \tag{9}$$

$$c - \frac{a + b + c}{4} = 1{,}000 \left(\frac{f_1 + f_2 + f_3 + f_4}{4} - f_3 \right), \tag{10}$$

$$- \frac{a + b + c}{4} = 1{,}000 \left(\frac{f_1 + f_2 + f_3 + f_4}{4} - f_4 \right). \tag{11}$$

Fig. 17—Four 100,000-cycle oscillators with auxiliary equipment.

The four oscillators used in the equipment described are shown in Fig. 17. The panels on which the controlling and measuring circuits are mounted are at the right of the picture. The 1,000-cycle motor-driven clock is at the top of the nearest panel. A schematic of the apparatus showing the general arrangement of parts is given in Fig. 18.

The circuit of one element of the modulator for producing low-frequency beats is shown in Fig. 19. The input circuits *A* and *B* are supplied from oscillator No. 4 and one of the other three, respectively. The plate circuit includes the windings of a balanced relay

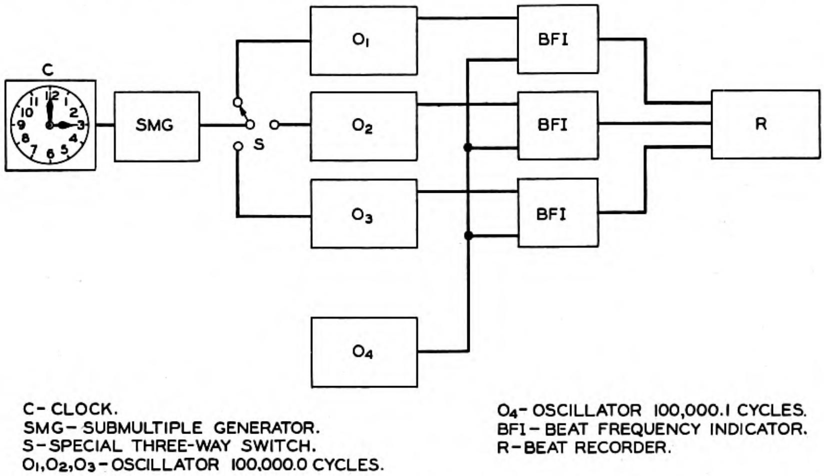

Fig. 18—Schematic of complete frequency standard system.

which makes a contact once for each cycle difference between the input frequencies at *A* and *B* and which operates the recording mechanism accordingly.

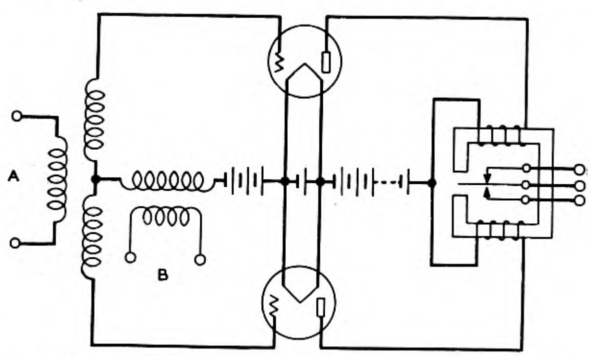

Fig. 19—Balanced modulator of beat frequency indicator.

The beat recorder is a counter arranged to count these relay operations for a definite time interval, in this case for 1,000 seconds, and then to print the total and reset to zero. Five such units are provided which print on a wide strip of paper similar to that used in an adding machine. Three of the counters are used as outlined above. The fourth counter is to be used for recording the mean of these three numbers, computed automatically by an auxiliary device. The remaining one is a serial counter which is used to record the time, either directly, or by numbering the 1,000 second intervals consecutively.

The five element counter is shown in Fig. 20 with the cover removed to show part of the mechanism. The energy for actuating the counting and resetting mechanism is obtained from a small motor running continuously. These elements are operated at the proper times by clutches controlled by electro-magnets which are selected by the relays in the modulator circuits described above. The counting, printing,

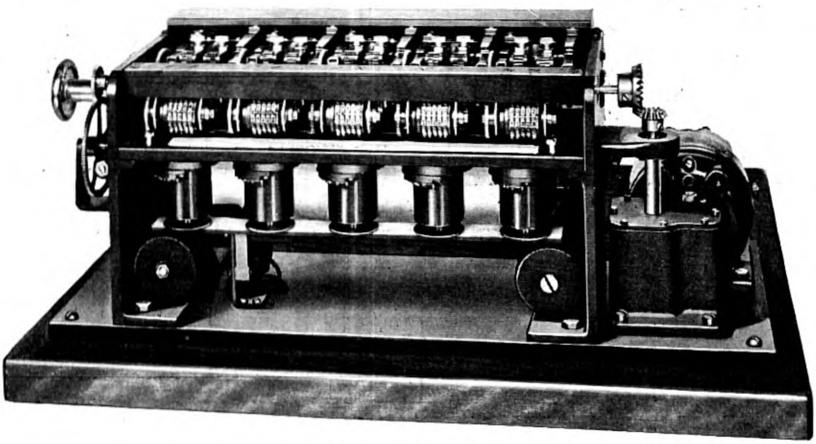

Fig. 20—Automatic beat counter.

and resetting operations are interlocked by means of cams and relays so that no counts may be missed through superposition of operations. The electrical circuit of one unit of the recorder is shown in Fig. 21.

The 1,000 second intervals are determined by a cam operated by the 1,000-cycle synchronous motor. It might be questioned whether one of the crystals being checked should be used to determine the 1,000 second intervals. No serious error arises from this, however, since the percentage variation in the interval due to a change in rate of the crystal is only one millionth of the percentage variation in the recorded beat number. Thus, using one crystal to determine the intervals, used in comparing its rate with other crystals, makes the final measurement subject to an error from this cause of only about 0.0001 per cent.

In order to determine extremely small relative variations in frequency between two oscillators a method of measurement is used in which the duration of individual beats between two oscillators may be measured with an accuracy of about one part in 10,000. This is equivalent to saying that the average beat frequency during each 10 second interval is measured with an accuracy of one part in ten thousand. Since the percentage error in the beat frequency is one million times greater than the percentage error in the primary frequency, to measure the beat frequency with an accuracy of one part

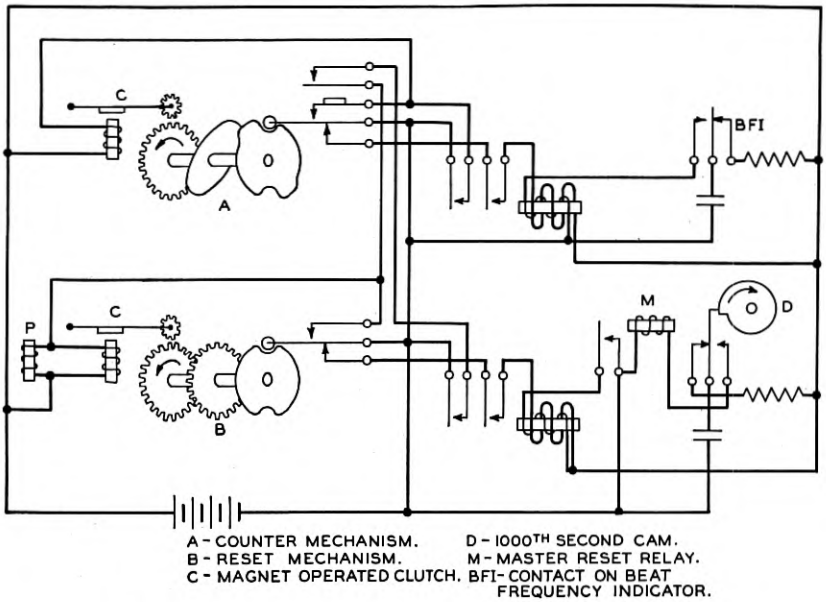

Fig. 21—Electrical circuit of one element of beat counter.

in ten thousand is equivalent to intercomparing the primary frequencies with a precision of one part in ten thousand million. By such a precise method of measurement a great deal can be learned about the nature of the variations that do occur.

The circuit of this device is shown in Fig. 22. Fig. 23 is a photograph of the actual apparatus used in obtaining the data given in Fig. 24. A circular transparent scale *S*, having 100 numbered divisions, is driven at 10 revolutions per second by a 1,000-cycle synchronous motor controlled by one of the crystals. A modulator operates the balanced relay at the difference frequency between the crystal controlled oscillators. This relay discharges condenser C_1

through the primary of an induction coil, which discharge produces a spark across the gap below the circular scale. The portion of the scale illuminated by the spark is photographed on slowly moving

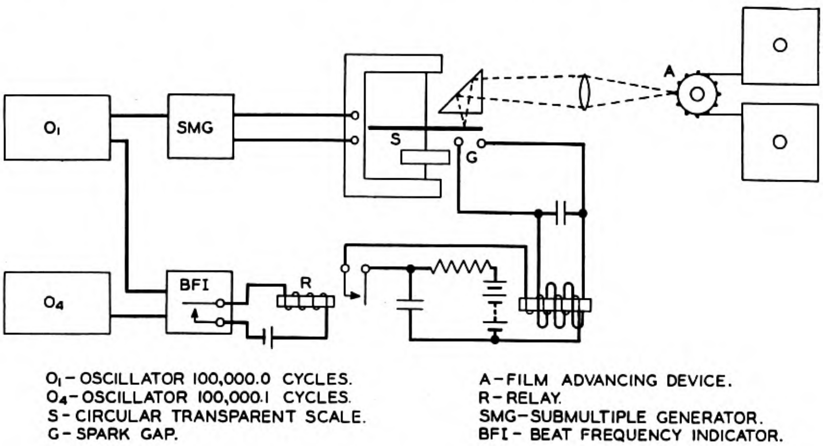

Fig. 22—Circuit of device for determining beat periods accurately.

film at *A*. In this manner, assuming a beat frequency of 0.1 cycle per second, 360 checks per hour may be obtained with practically no supervision.

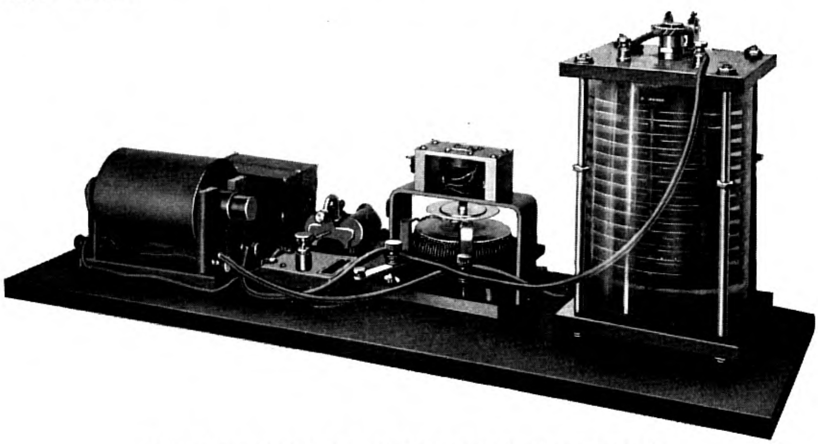

Fig. 23—Apparatus used for measuring beat periods.

If the sparks occur at exactly an even number of revolutions of the motor apart, the same portion of the scale will be photographed by each spark. If the intervals differ from such a value by 0.001 second, the successive photographic images will differ by one scale division.

Thus, the length of the beat periods may be read directly from the photographic records with an accuracy of 0.001 second, which determines the length of the 10 second periods with an accuracy of one part in ten thousand. Thus a variation of one division on the photographic record corresponds to a relative variation of one part in ten billion between the two frequencies, compared during an interval only ten seconds long. The whole number of revolutions of the scale may be determined readily by auxiliary means.

The two graphs in Fig. 24 show typical variations between two crystal oscillators operating under rather unfavorable conditions. One crystal was not in its sealed bell jar and one circuit was only

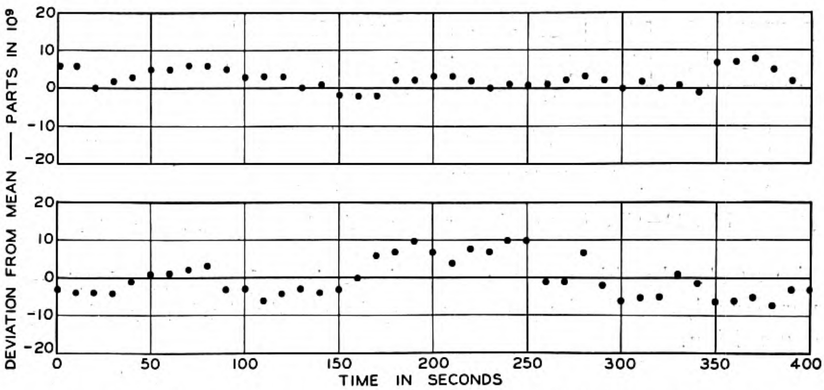

Fig. 24—Relative rates of two pairs of crystal oscillators showing small random variations in frequency.

partially shielded and was exposed to draughts of varying temperature. Even under these conditions, however, the variations from the mean did not exceed one part in 10^8 during the test.

The checking methods just described are intended primarily to indicate more or less rapid changes in frequency. Slow changes, and, of course, the absolute rate, can best be determined in terms of standard time. This is done, as previously indicated, by checking the rate of a clock controlled by one of the crystals against radio time signals. Unfortunately no long checks have been obtained as yet in this way, but several tests made over periods of a few days indicate a constancy of rate in the order of 0.01 second a day.

The measurements made so far indicate that the frequency of a crystal controlled oscillator such as described when suitably controlled, may be expected to be constant to at least one part in 10^7 over periods of seconds or over periods of days. It is hoped that it will be possible in the near future to present accumulated data on the performance of the frequency standard system described.

Observations on Modes of Vibration and Temperature Coefficients of Quartz Crystal Plates [1]

By F. R. LACK

The characteristics of piezo-electric quartz crystal plates of the perpendicular or Curie cut are compared with parallel or 30-degree cut plates with reference to the type of vibration of the most active modes, the frequency of these modes as a function of the dimensions, and the magnitude and sign of the temperature coefficients of these frequencies.

It is pointed out that the two principal modes of the perpendicular cut plate appear to be of the longitudinal type, the high-frequency mode being a function of the thickness while the low-frequency mode is a function of the width (along the electric axis). Both modes have a negative temperature coefficient of frequency. Of the two corresponding modes of the parallel cut plates a shear vibration is responsible for the high frequency. This frequency has a positive temperature coefficient. The low-frequency mode is of the longitudinal type and has a negative temperature coefficient.

Considering only the high-frequency vibration of these plates it is observed that there are characteristic variations of the frequency and temperature coefficient with the ratio of dimensions of the plate and the temperature, which are peculiar to the parallel cut plate. These variations can be attributed to a coupling of the shear and longitudinal modes.

It is then shown that if the parallel cut plate be treated as a group of coupled oscillatory systems with appropriate temperature coefficients the usual coupled system analysis will explain the curves of frequency *vs.* dimensional ratio, frequency *vs.* temperature, and temperature coefficient *vs.* dimensional ratio that are characteristic of this plate. This analysis offers an explanation of the low temperature coefficients which can be produced by a proper choice of the dimensional ratios.

WITH the increasing demands of the radio industry for a high degree of carrier-frequency stability, considerable attention has been focused recently on the piezo-electric quartz crystal as a circuit element in frequency generating systems. The low damping of these mechanical oscillators, combined with their piezo-electric properties makes them particularly suitable for frequency control where a high degree of constancy is required. The frequency stability of the quartz plates prepared in the usual manner, is however, often not sufficient for many of the demands for constant frequency. For instance such a crystal plate does not compare favorably as a substandard of frequency with a good astronomical clock. To meet the demands for frequency substandards as well as many other practical problems concerning frequency generation in the communication art, it becomes necessary to devise methods for improving the frequency stability of these crystal systems. This involves a study of the many factors upon which this stability depends.

A crystal plate constitutes an extremely complex vibration system with a large number of degrees of freedom which are for the most

[1] Presented April 3, 1929, before Institute of Radio Engineers.

34

part combinations of certain fundamental types of vibration. The ultimate frequency stability attained with a given crystal-controlled frequency generator is then a function of the equivalent electrical characteristics of the combination vibration set up in the crystal plate as well as the constants of the rest of the generator circuit. In particular, the frequency change in a crystal oscillator with changes in tube constants or attached load is a function of the equivalent electrical decrement of the vibration which the crystal happens to be executing. Further, the temperature coefficient of frequency of the crystal oscillator depends largely upon the temperature coefficient of frequency of the crystal vibration, which in turn depends upon the change with temperature of the various mechanical elastic constants that are called into play by this vibration.

The general relation between stress and strain, which in an ordinary isotropic medium involves only two constants, in crystal quartz requires six.[2] The choice of a particular constant or constants that enter into a given mode of vibration depends upon the orientation of the plate with respect to the original crystal axes, and the particular type of vibration, whether longitudinal, torsional, etc.

It is to be expected, therefore, that there will be a variation among the characteristics of the modes of vibration of plates cut in a different fashion, as well as between the different modes of a given plate. In practice we have found considerable difference in the magnitude of the electric and electrothermal constants, between the various modes of vibration of a given crystal plate, even when the vibration frequencies are within a few hundred cycles of each other.

To secure uniformity of results with respect to frequency stability it becomes necessary, therefore, to study the various possible modes of vibration of these crystal plates in detail, and set up certain criteria by which it will be possible to produce plates that will vibrate in a definite mode whose characteristics are known.

The theoretical aspects of this problem offer considerable difficulty, for it will be remembered that the classical case of the vibrations of an isotropic plate whose edges are free has as yet only been solved approximately,[3] and with the extension of the theory made necessary by the crystalline nature of quartz, the complexity of the problem is considerably increased, with the possibility of a complete solution very remote.

Using long rods or bars of crystal, instead of plates, other investi-

[2] Voigt's "Kristallphysik," pp. 749–755, or Love's "Mathematical Theory of Elasticity," Chap. VI.

[3] Rayleigh, "Theory of Sound," Chap. X and X_A.

gators [4] have been able to set up the three types of vibration (longitudinal, flexural, and torsional) common to isotropic bars. Moreover, the formulæ for these vibrations in isotropic material can be used to determine the frequency of the quartz rods to a good first approximation.

Returning to the problem of the plate, if the experimentally determined facts concerning plates of certain definite orientations are examined, it will be seen that they suggest the treatment of the plate as a special case of a bar. A résumé of these facts will illustrate this point and at the same time indicate the effect of orientation on the character of the modes of vibration.

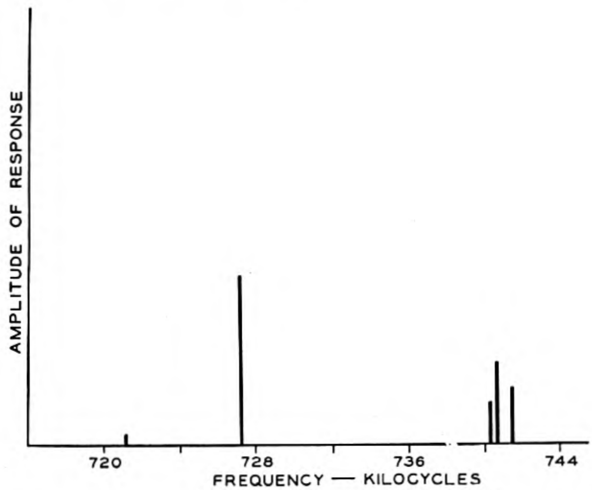

Fig. 1—Response frequencies of 32 x 47 x 2.760 mm. parallel cut crystal plate in the region of the major high frequency.

In general, a quartz crystal plate cut with any orientation with respect to the crystal axes will respond to a large number of frequencies. A plot of these frequencies showing their spacing and the relative magnitudes of response [5] may be termed the frequency spectrum of the plate. Fig. 1 shows part of the high-frequency region of such a spectrum. In these frequency spectra there are usually one or more frequencies at which the crystal will react with sufficient voltage to drive a vacuum tube in the usual crystal oscillator circuit.

[4] Cady, *Proc. I.R.E.* 10, p. 83, 1922. Harrison, *Proc. I.R.E.* 15, p. 1040, 1927 Giebe, *ZS. f. Phys.* 46, p. 607, 1928.

[5] The amplitude of response in this case is the maximum amplitude of current through the crystal at constant voltage, which in turn is a measure of the equivalent series resonant impedance of the crystal system.

The relation between these major response frequencies and the dimensions of the plate for the two principal orientations can be outlined as follows:

Curie or Perpendicular Cut

When the crystal plate is so cut that its major surfaces are parallel to the optic axis and perpendicular to an electric axis (the Curie or perpendicular cut, see Fig. 2) there are two major response frequencies, one high and one low.[6] The high frequency is a function of the

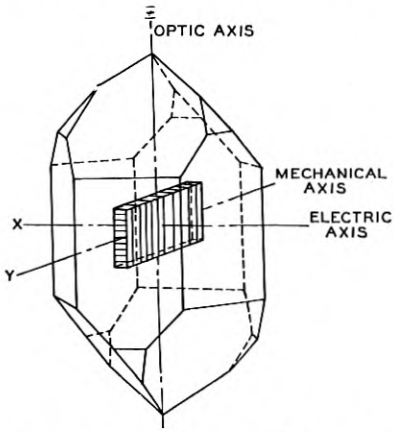

Fig. 2—Orientation of a perpendicular or Curie cut plate with respect to the crystal axes.

thickness of the plate and to a good approximation is given by the expression

$$f = \frac{K}{t}, \tag{1}$$

where t is the thickness in millimeters and $K = 2.860 \times 10^6$. If the plate could be considered as a bar of length t then the frequency of a simple longitudinal vibration would be given by the expression

$$f = \frac{1}{2t}\sqrt{\frac{E_{xy}}{d}}, \tag{2}$$

where E_{xy} is Young's modulus in the X-Y plane and d is the density. If the numerical values[7] of E_{xy} and d are substituted in the above

[6] For this discussion the low-frequency flexural vibration of the type described by Harrison will not be considered.

[7] For numerical values of the elastic constants and the density of quartz, see Sossman, "The Properties of Silica," the American Chemical Society Monograph Series.

expression it is found that the same value for K is obtained as that of equation (1).

The low frequency is a function of the width, the dimension parallel to the Y axis, and is given by the same expression as equation (1) with the same value of K, the width in millimeters being substituted for the thickness.

For this type of crystal plate there are then two possible major modes which appear to be of the longitudinal type and depend upon the same elastic constant. (Young's modulus in the X-Y or equatorial plane has the same magnitude in any direction.)

The temperature coefficient of both these frequencies is negative, which is in agreement with the temperature coefficient of Young's modulus for the equatorial plane.[8]

The Parallel or 30-degree Cut

When the crystal plate is so cut that its major surfaces are parallel to both the optic and electric axes (the parallel or 30-degree cut, see Fig. 3) this 30-degree shift in orientation from the perpendicular

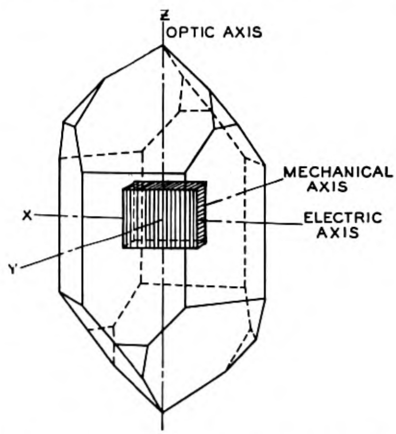

Fig. 3—Orientation of a parallel or 30-degree cut plate with respect to the crystal axes.

changes the characteristics in some important respects. As before there is a high and a low principal frequency, but in this case the high frequency sometimes occurs as a doublet (two response frequencies a kilocycle or so apart).

For thin plates of large area the high frequency is a function of the thickness of the plate and is given by the approximate expression

[8] Perrier & Mandrot, *Mem. Soc. Vaudoise Sci. Nat.* (1923), 1, pp. 333–364.

$$f = \frac{K}{t}, \tag{3}$$

where t is the thickness in millimeters and K is now 1.96×10^6. It will be noted that this constant differs from that found in the case of the perpendicular cut crystal. Moreover the temperature coefficient of this frequency is positive.

These facts lead one to believe that this is not a simple longitudinal vibration. Cady [9] has pointed out that if it be considered as a shear vibration in the X-Y plane the frequency can be calculated using the appropriate shear modulus.[10]

The low frequency is a function of the width, the dimension parallel to the electric or X axis, and is given by the same expression and constant as the frequencies of the perpendicular cut plate. It has the same characteristic negative temperature coefficient.

For these parallel cut plates there are then two possible major modes which, however, differ in type of vibration and sign of temperature coefficient.

Limiting this discussion to the high-frequency region, it is seen that these parallel and perpendicular cut plates have different frequency-thickness constants and temperature coefficients of opposite sign. On closer examination it is found that there is an additional difference which involves the variation of the magnitudes of these frequency-thickness constants and temperature coefficients with the ratio of width to thickness of the plate.

For the perpendicular cut plate the frequency-thickness constant changes but little with the size of the crystal. The same is true for the temperature coefficient, and from recent measurements on a number of sizes of plates the magnitude of this coefficient lies between minus 20 and minus 35 cycles in a million per degree centigrade.

The parallel cut plate, on the other hand, has a frequency-thickness constant which for any but thin plates of large area varies considerably with the width. The temperature coefficient also varies with the width, and is in addition a function of the temperature. This coefficient has a wide range of values whose limits are approximately plus 100 cycles in a million per degree centigrade and minus 20 cycles in some special instances, with all possible intermediate values including zero. Then, as has been mentioned before, these parallel cut

[9] Cady, *Phys. Rev.*, 29, p. 617, 1927.

[10] If it could be shown that the shear modulus of this plane had a positive temperature coefficient it would substantiate this assumption, but there is no information at present available regarding the effect of temperature on the elastic constants other than for the two values of Young's modulus.

crystals frequently have two high-frequency modes of vibration within a kilocycle or so of each other and will start on either of these modes if the circuit constants are changed slightly. These two modes usually have widely different characteristics.

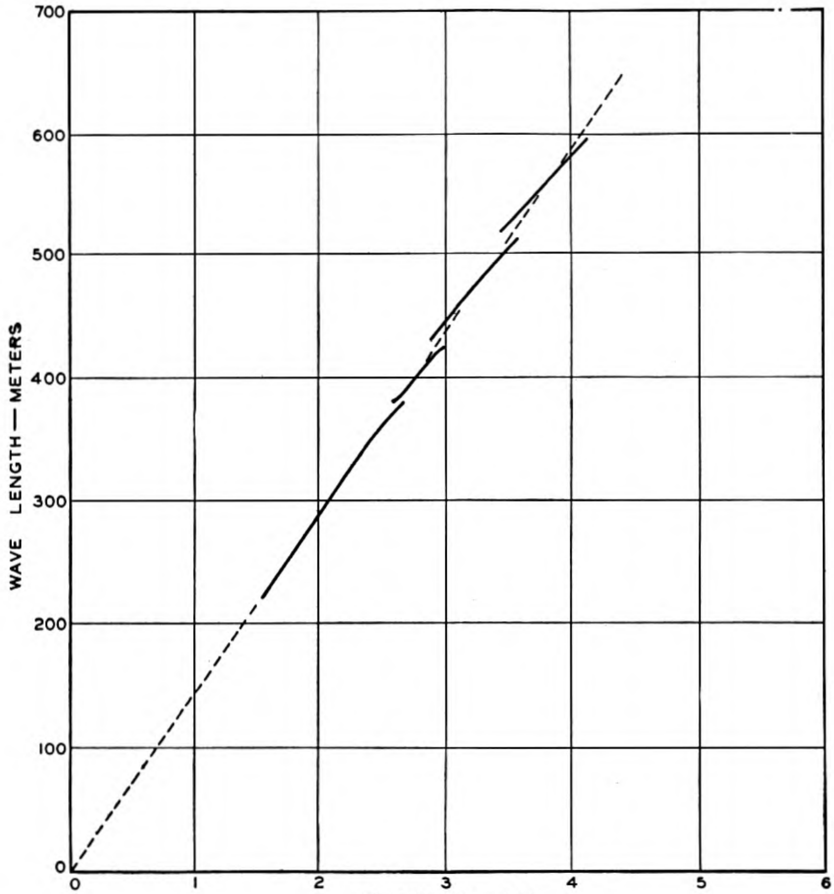

Fig. 4—The wave-length at which a 2.5 cm. square parallel cut crystal plate will operate in an oscillator circuit as its thickness is progressively reduced.

Apart from this seemingly erratic variation it has been the experience of this laboratory that the parallel cut crystal will oscillate more readily in the Pierce type of oscillator circuit. For this reason this type of crystal has been used for a number of purposes and these observed variations have been the object of considerable study.

As a result of this work an explanation has been evolved to account for these variations. This explanation not only suggests reasons for the above mentioned phenomena, but, what is more important, it indicates the procedure by which it is actually possible to produce crystals having negligible temperature coefficients. Before outlining this theory the experimental facts which served as its foundation will be discussed in detail.

Frequency-Thickness Constant as a Function of Dimensions

When work on the production of parallel cut crystals in the broadcast frequency band was first started, it was found that it was very difficult to grind crystals for certain low frequencies using a 2.5 cm. square plate because of discrete jumps in frequency for a small reduction of thickness. Fig. 4 is a typical curve showing the wave-length [11] as a function of the thickness for a 2.5 cm. square crystal. This curve should be a straight line (for from equation (3) it is evident that $\lambda = K't$) but it will be noted that there are certain discontinuities

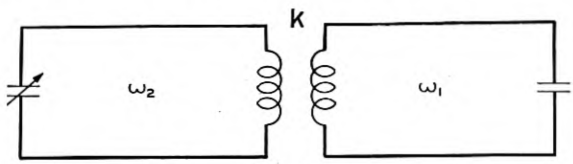

Fig. 5.

at the upper end. It was found that these discontinuities were present at frequencies that could be identified with harmonics of the frequency the crystal would have if it were vibrating in the direction of its length along the electric axis.

This was the first definite indication obtained in the Bell Telephone Laboratories that the longitudinal vibration of the crystal in the direction transverse to the applied field could affect the frequency supposed to depend only on the thickness. It was checked by further work on crystals of other dimensions, and in each case the position of these discontinuities was found to depend on the width of the crystal.

The presence of a resonant system whose frequency depends upon the width is evidently responsible for this phenomena, this system affecting the frequency of the vibration along the thickness through some form of mechanical coupling. At the suggestion of Mr. R. A. Heising of the Bell Telephone Laboratories, an explanation of these experimental facts was developed based on the treatment of the plate

[11] In plotting the change in rate of vibration of a crystal plate as a function of the dimension, it is more convenient to use wave-length instead of frequency because of the direct linear relation between the dimensions and the wave-length.

as a system of coupled circuits.[12] Consider the two coupled oscillatory circuits shown in Fig. 5 having the uncoupled angular frequencies ω_1 and ω_2, then the frequencies of the coupled system in the absence of damping will be given by the usual expression [13]

$$\omega = \frac{\sqrt{\frac{1}{2}(\omega_1^2 + \omega_2^2) \pm \frac{1}{2}\sqrt{(\omega_1^2 - \omega_2^2) + 4k^2\omega_1^2\omega_2^2}}}{\sqrt{1 - k^2}}, \tag{4}$$

k being the coupling.

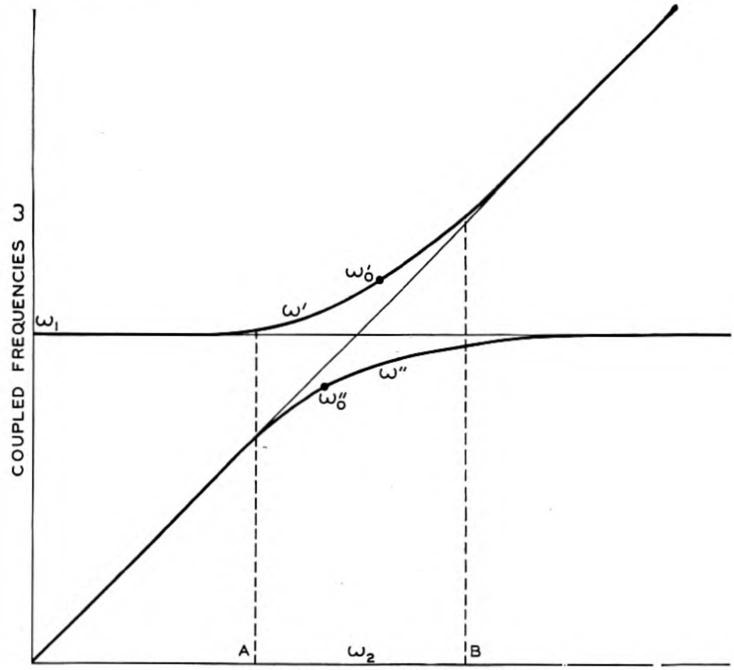

Fig. 6—Angular frequencies of a system of two coupled circuits as a function of the tuning of one circuit, the tuning of the other circuit being fixed.

If these two frequencies be plotted as a function of the tuning of the second circuit, i.e., ω_2, the familiar set of curves shown in Fig. 6 results.

Suppose now other circuits are added to the system as shown in Fig. 7, each additional circuit being fixed at a harmonic of the uncoupled frequency of circuit No. 2, and so linked with this circuit mechanically that the group is tuned as a whole.

[12] The term "circuit" is introduced here to describe a mechanical oscillatory system because many readers are accustomed to think in terms of electrical circuits.
[13] See Pierce, "Elec. Osc. & Waves," Chap. VII.

There are now two possible combinations depending upon which circuit or group of circuits is kept fixed while the other is varied. If the case in which the second group of circuits is kept fixed be examined first, it will be seen that as the frequency of circuit No. 1 is varied it will come into tune successively with each of the circuits of the second group. The result will be a series of coupling curves with the characteristic reaction illustrated by Fig. 6 repeated at each coincident point. If it be assumed that the coupling decreases as the order of the harmonic increases, then the magnitude of the reaction also decreases. This is illustrated by Fig. 8, which shows the coupling curves of such a system plotted in terms of the equivalent electrical wave-length.

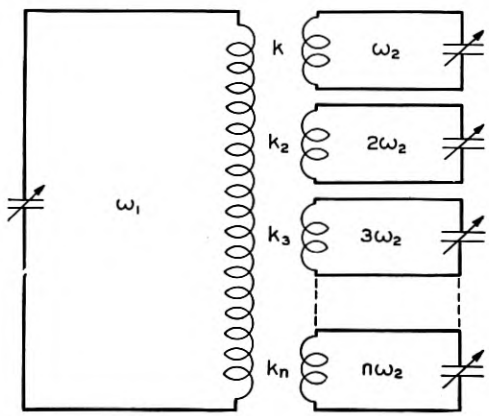

Fig. 7.

Returning to the crystal plate, if the vibration in the direction of the thickness be identified with circuit No. 1 while the width vibration and its harmonics be identified with circuit group No. 2, then Fig. 8 should represent what happens to the crystal wave-length as the thickness is reduced. Comparing Figs. 4 and 8, it is seen that this is true in a restricted region but that the wave-lengths which depend upon the width vibration do not continue much beyond the coupling region in the experimental curves. This is to be expected, for these wave-lengths which depend upon a harmonic of a vibration transverse to the applied field are more difficult to excite than the fundamental in the direction of the field. This particular point is discussed further in connection with temperature coefficients.

If now the case be examined in which the tuning of the second group of circuits is varied, it will be seen that the coupling curves are slightly different in character. The curves for this case are illustrated by Fig. 9 which shows the wave-lengths of this system as a function of the tuning of circuit group No. 2. Fig. 10 shows the wave-lengths at which a parallel cut plate will oscillate plotted as a function of the width. The similarity between this experimentally

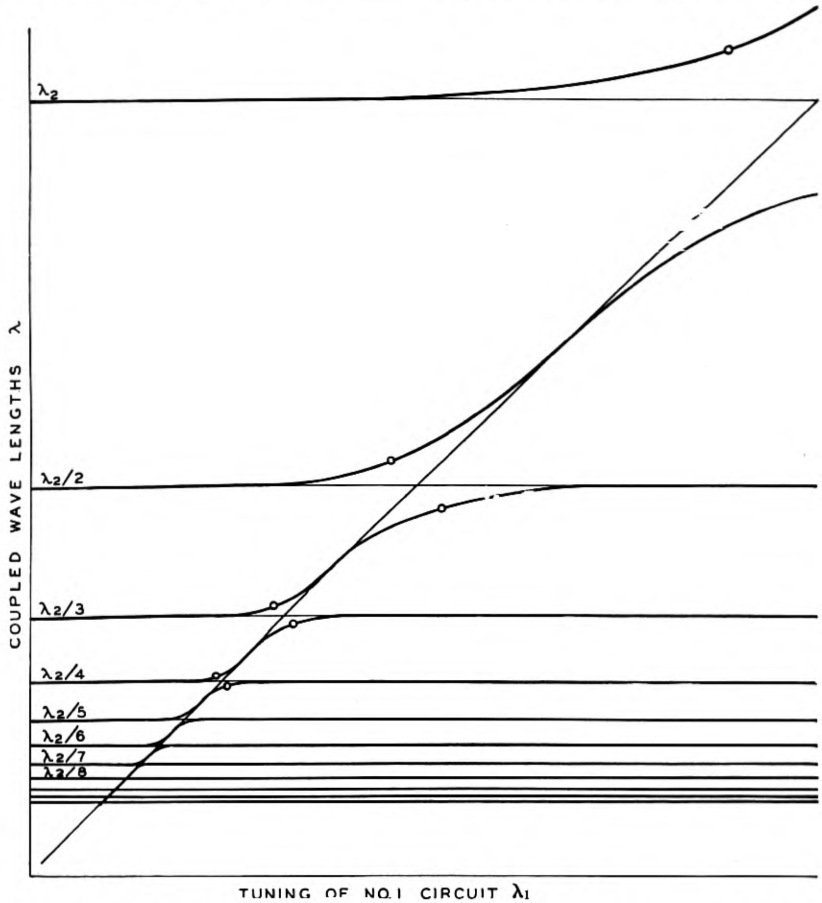

Fig. 8—Wave-lengths of the system of coupled circuits of Fig. 7 as a function of the tuning of circuit No. 1, the tuning of circuit group No. 2 being fixed.

determined curve and Fig. 9 is at once apparent. There is one anomalous segment of a curve between the 7th and 8th harmonics, the line AB; but it is possible that this is caused by the coupling of some third free period which has not been considered, perhaps a high order harmonic of a flexural vibration. In general, however, the curves of wave-length versus thickness for these crystal plates are of such a character as to indicate that the analogy between the two systems of coupled circuits and the crystal modes of vibration is sufficiently good to serve as a useful guide.

If, then, these parallel cut crystal plates are considered as a system of coupled circuits the reason for the variation of the frequency-thickness constant with dimensional ratios and the presence of the frequency doublets is at once apparent. With the coupling at the various harmonics determined, the character of these variations can

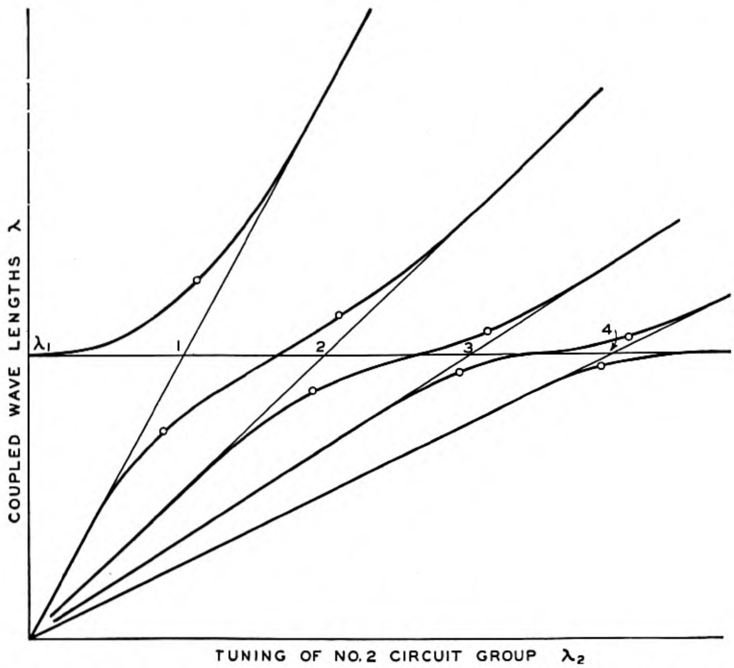

Fig. 9—Wave-lengths of the system of coupled circuits of Fig. 7 as a function of the tuning of circuit group No. 2, the tuning of circuit No. 1 being fixed.

be predicted. Given an experimentally determined series of coupling curves similar to Fig. 10, the coupling at the *n*th harmonic can be determined from the expression

$$k_n = \frac{\left(\frac{\lambda'}{\lambda''}\right)^2 - 1}{\left(\frac{\lambda'}{\lambda''}\right)^2 + 1}, \tag{5}$$

where λ' and λ'' are the wave-lengths of the coupled system at the point where $\lambda_1 = n\lambda_2$.

Temperature Coefficient as Function of Dimensions and Temperature

As mentioned above, when the temperature coefficients of these parallel cut crystals were studied it was found that there was considerable variation between plates having the same thickness but slightly different areas, and the temperature coefficient of a given plate was found to be a function of the temperature. To illustrate this last point a typical frequency-temperature curve for a parallel

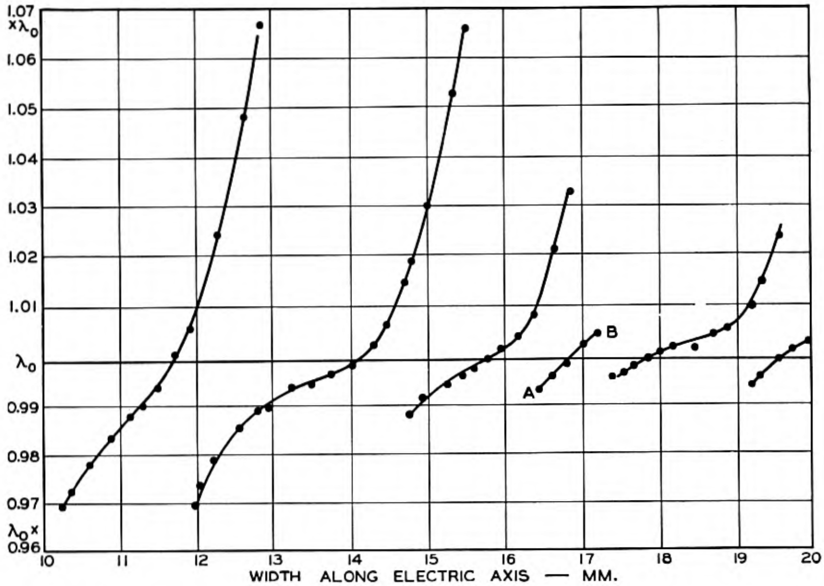

Fig. 10—The wave-lengths at which a parallel cut crystal will operate in an oscillator circuit as its width (the dimension along the electric axis) is progressively reduced, the other dimensions being fixed.
$\lambda_0 = 153 \times$ thickness.
Thickness along mechanical axis = 1.64 mm.
Length along optic axis = 54.8 mm.

cut crystal is shown in Fig. 11. It will be noted that the frequency increase is linear until a given temperature is reached, at which point the curve flattens off and then begins to reverse. Just beyond the point of reversal the frequency jumps to a new value and, if the curve is continued, the frequency increases again at the same rate as originally. This type of frequency-temperature curve is common to a large percentage of parallel cut crystals, the only difference being the width of the flat part of the curve and the temperature at which the discontinuity occurs.

Mr. W. A. Marrison of the Bell Telephone Laboratories first suggested that low temperature coefficients could be obtained with parallel cut crystals by utilizing the coupling of two modes of vibration having individual coefficients of opposite sign. Several of this type of low temperature coefficient crystals were produced by Marrison

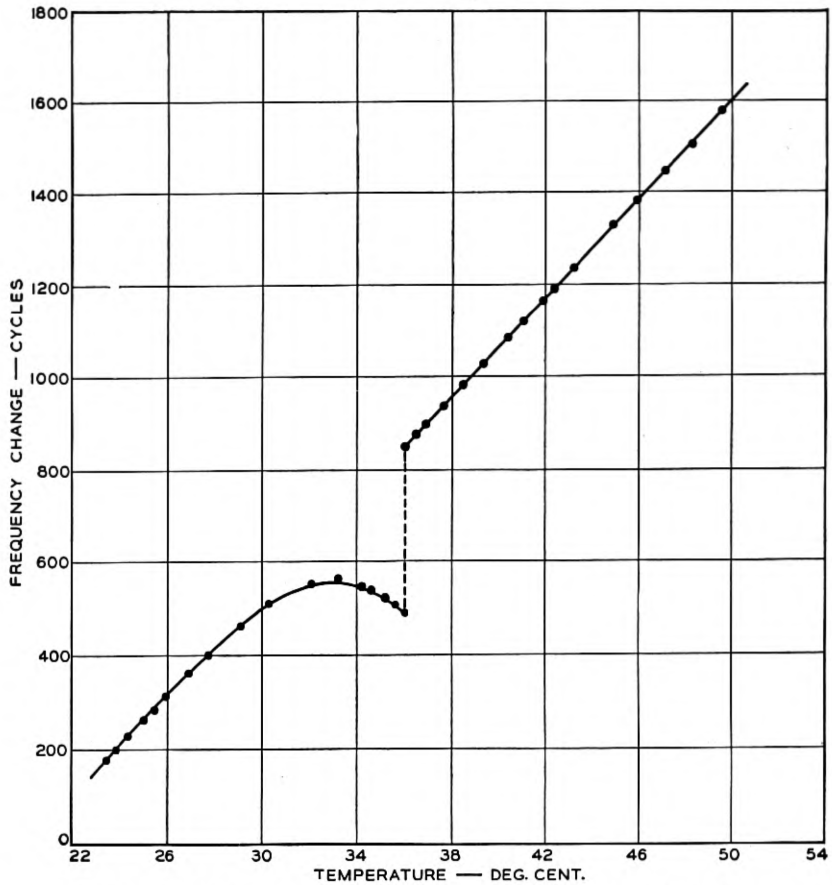

Fig. 11—The frequency change of a 32 x 47 x 2.760 mm. parallel cut crystal with temperature.

and are described in his concurrent paper "A High Precision Standard of Frequency."

If Heising's coupled circuit analysis is extended to include the effect of temperature and the proper temperature coefficients with due regard to relative magnitude and sign are identified with each circuit, the change in temperature coefficient with dimensional ratio and temperature can be explained. In addition, the dimensional ratios or tuning points which yield zero temperature coefficients for a given temperature can be predicted if the coupling is known.

Referring again to Fig. 6, suppose the two coupled circuits have temperature coefficients of opposite sign, circuit No. 1 being positive and circuit No. 2 negative, for ω_2 less than ω_1 say at the point A, ω' has a positive and ω'' a negative temperature coefficient. For a value of ω_2 greater than ω_1 say at B, ω' now has a negative and ω'' a positive temperature coefficient, ω' and ω'' having interchanged rôles. Somewhere between therefore, both ω' and ω'' must have had a zero temperature coefficient. Returning to equation (4), if this expression for ω be differentiated with respect to the temperature, regarding k, the coupling as constant, and the result placed equal to zero, the condition that ω is independent of temperature[15] is obtained as follows:

$$\omega^2 = \frac{\omega_1^2\omega_2^2(m - n)}{(m\omega_1^2 - n\omega_2^2)}, \tag{6}$$

where

$$m = \frac{1}{\omega_1}\frac{d\omega_1}{dT} = \text{temperature coefficient of circuit No. 1,}$$

$$n = -\frac{1}{\omega_2}\frac{d\omega_2}{dT} = \text{temperature coefficient of circuit No. 2;}$$

now let $Q = n/m$ then equation (6) becomes

$$\omega^2 = \omega_2^2 \frac{1 - Q}{1 - Q\left(\dfrac{\omega_2}{\omega_1}\right)^2}, \tag{7}$$

solving equation (7) for ω_2/ω_1 replacing ω^2 by its value from equation (4)

$$\left(\frac{\omega_2}{\omega_1}\right)^2 = \frac{k^2(1 - Q)^2}{2Q} + 1 \pm \sqrt{\left[\frac{k^2(1 - Q)^2}{2Q}\right]^2 + \frac{k^2(1 - Q)^2}{Q}},$$

which when k is small becomes

$$\left(\frac{\omega_2}{\omega_1}\right)^2 = 1 \pm \frac{k(1 - Q)}{\sqrt{Q}}. \tag{8}$$

This equation gives the tuning points, or the values of ω_2 at which the angular frequencies of the coupled system, ω' and ω'', will have

[15] Dr. F. B. Llewellyn of the Bell Telephone Laboratories is responsible for this analysis.

zero temperature coefficients, in terms of the ratios of the uncoupled temperature coefficients and the coupling.

Referring again to Fig. 6, ω_0' and ω_0'' represent the values of ω' and ω'' which would have zero temperature coefficient provided m is greater than n, that is, the temperature coefficient of ω_1 is greater in magnitude than that of ω_2. Carrying this idea over to the case of the group of circuits for which the curves of Figs. 8 and 9 are drawn,

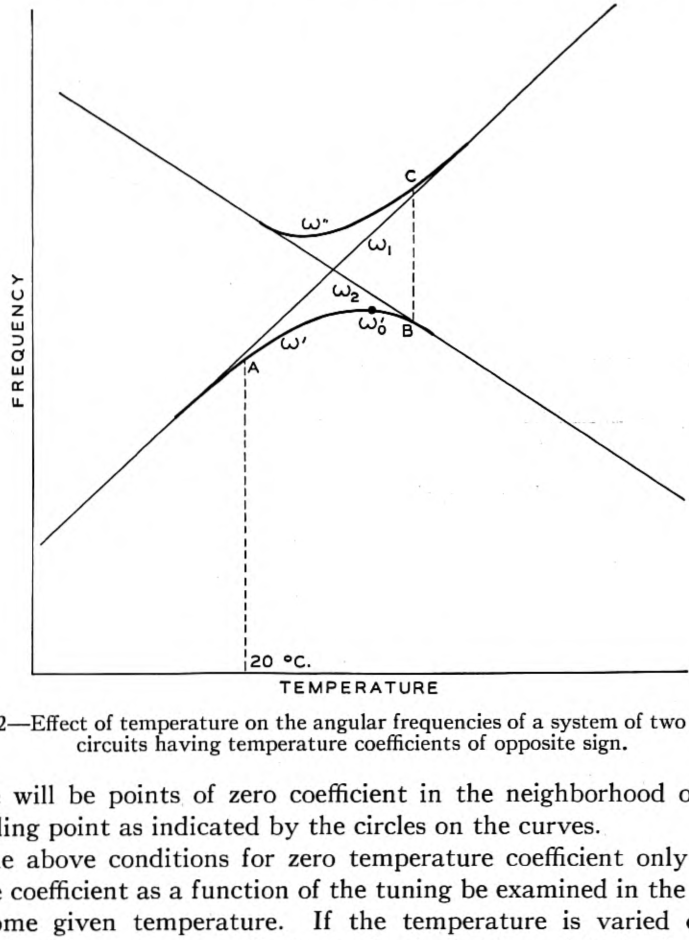

Fig. 12—Effect of temperature on the angular frequencies of a system of two coupled circuits having temperature coefficients of opposite sign.

there will be points of zero coefficient in the neighborhood of each coupling point as indicated by the circles on the curves.

The above conditions for zero temperature coefficient only apply if the coefficient as a function of the tuning be examined in the region of some given temperature. If the temperature is varied over a considerable range a small change in the tuning of both circuits is effected, one having its frequency raised, the other lowered. The result of this tuning on the frequencies of the coupled system can be illustrated by Fig. 12, which shows the tuning with temperature on a magnified scale. In this figure, the lines ω_1 and ω_2 represent the change in frequency of these circuits with temperature if there were no coupling between them. The change of the frequencies of the coupled system with temperature is shown by the curves ω' and ω''. It will be seen that both these frequencies pass through regions of zero temperature coefficient.

Such frequency-temperature curves can be derived graphically by a construction similar to that shown in Fig. 13. This figure illustrates what happens when the tuning of both circuits No. 1 and No. 2 is varied, and consists of a series of the usual coupling curves (the

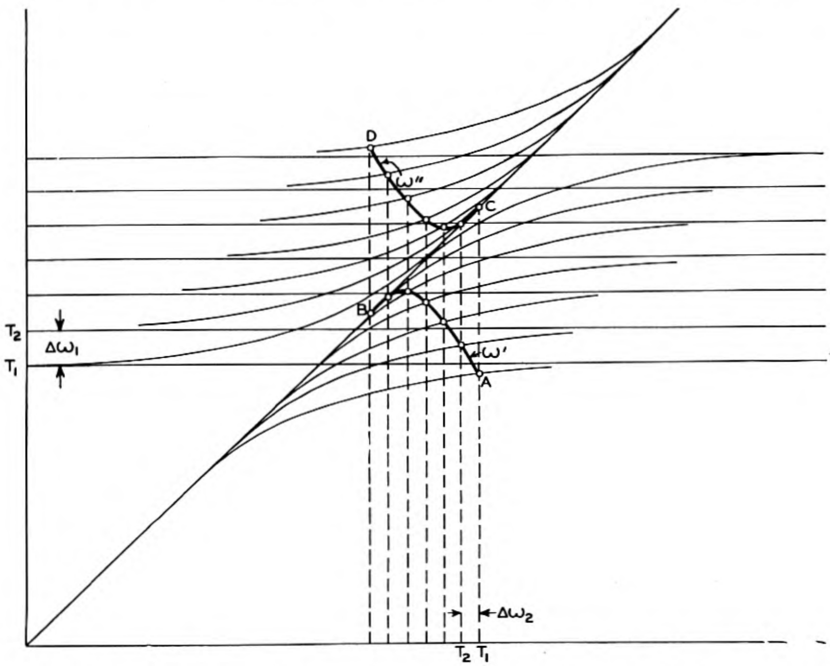

Fig. 13—Effect on the angular frequencies of a system of two coupled circuits as the individual circuits are tuned simultaneously in opposite directions.

coupled frequencies plotted as a function of ω_2), each set of curves of the series being drawn for a different value of ω_1. When the temperature is increased from T_1 to T_2, the uncoupled frequency of circuit No. 2 is reduced by an amount $\Delta\omega_2$ and the uncoupled frequency of circuit No. 1 is increased by an amount $\Delta\omega_1$. The result is the frequencies ω' and ω'' move from curve to curve in the direction shown by the lines AB and CD.

Now if the variation of the temperature coefficient of a crystal plate when used in an oscillator circuit be examined at a given temperature as the width is changed (which amounts to a change in the tuning of the transverse vibration), it will be seen that the experimental results are in accord with the above treatment. Fig. 14 shows the temperature coefficient of the two frequencies of a crystal plate at 58° C. as its width is progressively reduced in the neighborhood of the 5th harmonic of the transverse vibration. These curves show how the temperature coefficients change sign in this region. The dotted sections of the curves are extrapolated, for owing to the rapid reduction in activity once a coupled frequency acquires a negative coefficient,

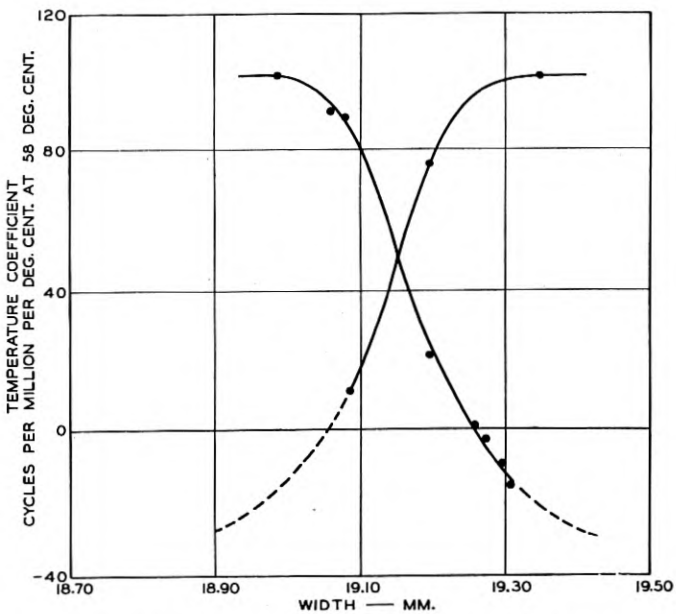

Fig. 14—The change of temperature coefficient of a parallel cut crystal at 58° C. as the width is progressively reduced in the region where the fifth harmonic of the vibration in the direction of the width coincides with the frequency of the vibration in the direction of the thickness.

data on the crystal plate used as an oscillator are difficult to obtain in this region.

Returning to the experimentally determined curve of frequency versus temperature for a parallel cut crystal plate shown in Fig. 11, this can also be explained with the aid of the above analysis. Referring to Fig. 12, if it be assumed that at 20° C. the crystal is oscillating with a frequency A, this is in the region where this particular frequency has a positive temperature coefficient. As the temperature increases the frequency increases in the direction of B, passing through a maximum at the point ω_0' where it has zero coefficient, and then decreases. As the frequency decreases the activity of this particular mode decreases rapidly and finally the crystal "hops" frequency to point C on the ω'' curve. From this point on the frequency with

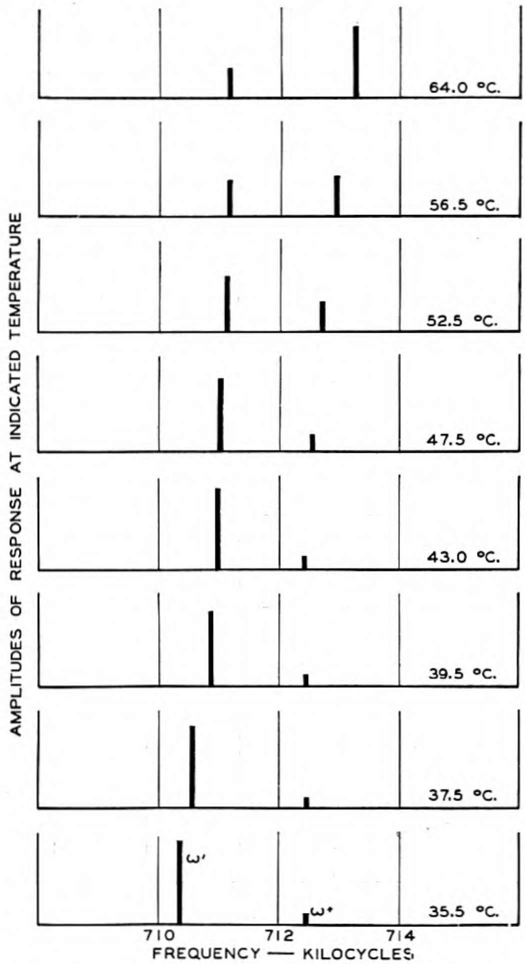

Fig. 15—The response-frequency spectra of a parallel cut crystal plate at different temperatures illustrating the interchange of activity between the two frequencies as the frequencies of the two modes of vibration pass through a coincident value.
Length of plate along optic (Z) axis = 47 mm.
Width along electric (X) axis = 19.35 mm.
Thickness along mechanical (Y) axis = 2.75 mm.

temperature increases, for this frequency has a positive temperature coefficient in this region.

If it were not for the decrease in activity of the period with the negative temperature coefficient it is to be expected that the crystal frequency, instead of "hopping," would continue to decrease with increase in temperature. In some instances (for low order of harmonics) the crystal frequency will decrease for a few degrees, and it

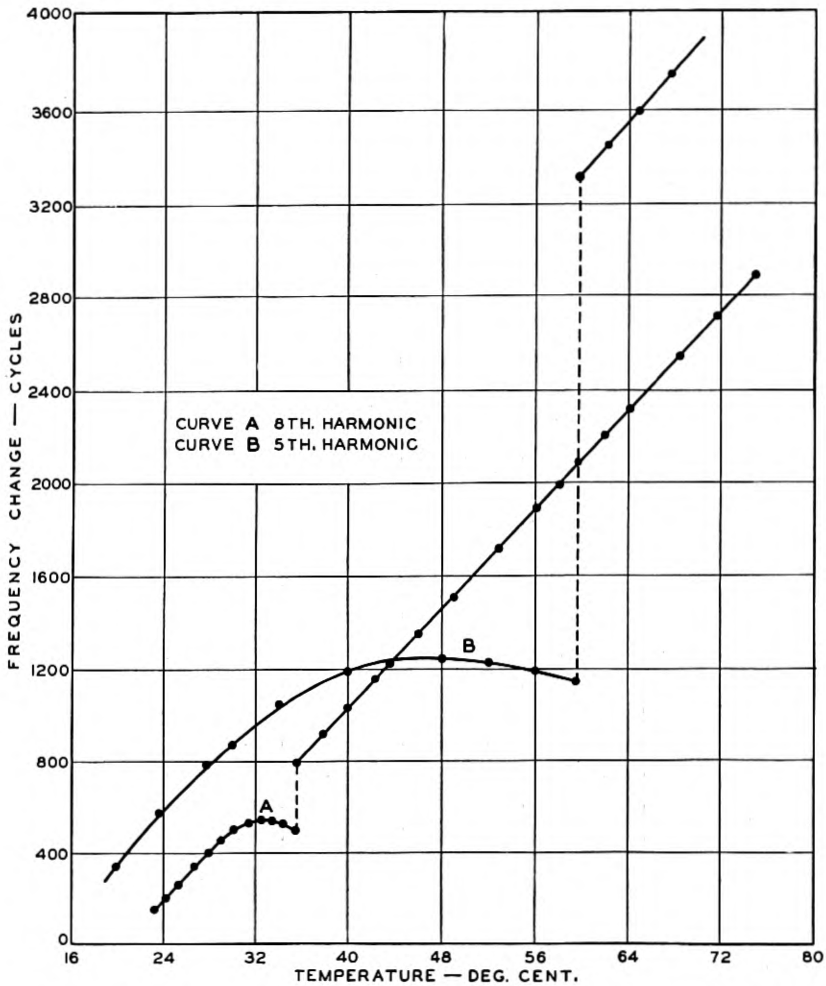

Fig. 16—The frequency change with temperature of two parallel cut crystals of different width.

Curve *A* region of eighth harmonic
(width = 32.0 mm.)
Curve *B* region of fifth harmonic
(width = 19.35 mm.)

The other dimensions of the plates are identical.

is found that the magnitude of the negative coefficient for this region approximates that to be expected for the transverse vibration alone. In general, however, a frequency jump occurs just after the zero temperature coefficient region is passed.

This interchange of activity of these two periods as they interchange temperature coefficients can be studied in detail by examining the changes in the spectrum of a crystal at different temperature levels. Fig. 15 shows a series of spectra of a crystal taken for different temperatures in the region of zero temperature coefficient, the dimensions of the crystal being unchanged. These spectra illustrate the rapid decrease in activity of the frequency ω' after it passes through zero temperature coefficient while at the same time ω'' increases and assumes the place of major activity vacated by ω'.

The assumption that the coupling increases with the decrease in the order of the harmonic finds confirmation in the experimentally determined facts as computed from curves of the type shown by Fig. 10. As the coupling increases the temperature range for which there is no frequency change with temperature increases, that is the region of zero temperature coefficient becomes extended. To illustrate this, Fig. 16 shows two curves of frequency versus temperature, one for the coupling of a fifth harmonic, the other for an eighth.

It would, of course, be desirable to extend the zero temperature coefficient range over the limits of temperature to be expected in normal operation. This necessitates tight coupling of the two modes which in turn demands a dimensional ratio in the neighborhood of unity. The cross sectional area of such a plate in the direction of its thickness and width approaches a square in shape which, for high-frequency crystals, is of very small dimensions.

Before concluding it should be noticed that since both modes of the perpendicular cut crystals have a negative temperature coefficient, it is to be expected that it would be impossible to obtain zero temperature coefficient crystals with this orientation. This seems to be true as far as our experience with those crystals is concerned.

Master Reference System for Telephone Transmission [1]

By W. H. MARTIN and C. H. G. GRAY

The telephone transmission system described here is the Master Reference System of the Bell System for the expression of transmission standards and the ratings of the transmission performance of telephone circuits. The transmitter and receiver elements of this system are reference standards for the ratings of the transmitting and receiving performance of terminal station sets.

A replica of this reference system, installed in Paris, has been adopted as the Master Reference System of the International Advisory Committee on Long Distance Telephone Communication in Europe. The establishment of these two master systems provides a common reference for the telephone transmission work of the Bell System and the telephone administrations which are members of this International Advisory Committee.

THE Master Reference System for Telephone Transmission, as its name indicates, is to serve as the fundamental circuit in the ratings of the transmission performance of telephone circuits. In describing this system, therefore, it will be advantageous to outline first the general considerations underlying the methods of determining and specifying these ratings and their applications.

The conversions and transfers of energy which constitute the process of telephone transmission result in general in a difference between the speech sounds at the sending end of the telephone circuit and the sounds reproduced at the other end in the ear of the listener. These reproduced sounds may differ from the original in three important respects; their loudness, their distortion or degree to which their wave shape departs from facsimile reproduction, and the amount of extraneous sound or noise which accompanies them. From the standpoint of telephony, the major importance of a difference between the original and reproduced sounds is determined by its effect on "intelligibility," that is, the degree to which the latter sounds can be recognized and understood by the listener when carrying on a telephone conversation. The tolerable departure of the reproduced from the original sounds is limited also by certain effects which are noticeable to the listener before they materially affect intelligibility, such as loss of naturalness.

Measurements of intelligibility are of utmost importance in rating the performance of telephone circuits, but they are unduly cumbersome for direct use in the detailed development and design of telephone circuits and their many parts, particularly where small effects are concerned. It has been desirable, therefore, to handle telephone

[1] Presented before A. I. E. E. Summer Convention, June 24–28, 1929.

transmission work in two steps. One natural division is suggested by the statement that intelligibility is a function of the relation between the output and input speech sounds, and of the psychological reaction of the listener to these output sounds. Because of the complex nature of the speech sound waves, however, it has been found more practicable to treat the transmission performance of telephone circuits in the following two parts: (1) the physical performance of the circuit, and (2) the relation between physical performance and intelligibility. The physical performance of a circuit is taken here to cover the transmission characteristics which can be specified in terms of the performance for single frequencies, a number of frequencies being taken to cover the range which is important for the reproduction of speech sounds. These measurements of physical performance cover such things as the response-frequency characteristic of the circuit over the range of speech frequencies, the distortion due to non-linear elements, phase distortion and the extraneous currents which cause noise. These determinations of physical performance do not include measurements of the speech sounds themselves, nor of the functioning of the talker and listener. This differentiation is advantageous in segregating the studies of speech sounds and of the psychological phases of the work, and permits the design of the operating plant and a large portion of the development work to be carried out on a physical basis.

The determination of the relation between intelligibility and the physical performance of a telephone circuit is a laborious process, because persons play the parts of generators and meters and a number of people must be used in both parts to take into account the normal ranges of their performance. The goal of this portion of the work has been, therefore, to establish suitable relations which will permit the determination of the intelligibility of a circuit by computations which start with the physical characteristics of the circuit. This work [2] has involved determinations of the capabilities of circuits having various kinds of physical characteristics to reproduce intelligible speech, investigations of the nature of speech sounds and hearing, and of people's customs in using the telephone.

Prior to the time when suitable means were available for measuring the physical performance of telephone circuits, and when the kinds of circuits in commercial use were quite similar in their distortion characteristics, the practice was adopted of rating the performance of a circuit by comparing it on a loudness basis with a reference circuit which was adjustable in attenuation, and whose distortion was closely similar to that of the commercial circuits. In such a comparison, a

[2] "Speech and Hearing," by H. Fletcher, published by D. Van Nostrand Co.

determination is made of the equivalence of loudness or volume of these two circuits by talking alternately over them and adjusting the reference circuit until the sounds coming out of the two receivers are judged to be equal. For the conditions where volume is the important controllable characteristic of telephone circuits, these loudness comparisons constitute a practicable and effective means of indicating the performance of these circuits.

The reference circuit adopted about twenty-five years ago for these loudness comparisons consisted of transmitters, receivers, station sets, cord circuits and a line, of types which were then used commercially. In this reference circuit the line was an adjustable artificial line simulating a 19 AWG. cable circuit having a capacity per loop mile of 0.054 mf. The amount of cable in this line to give a loudness

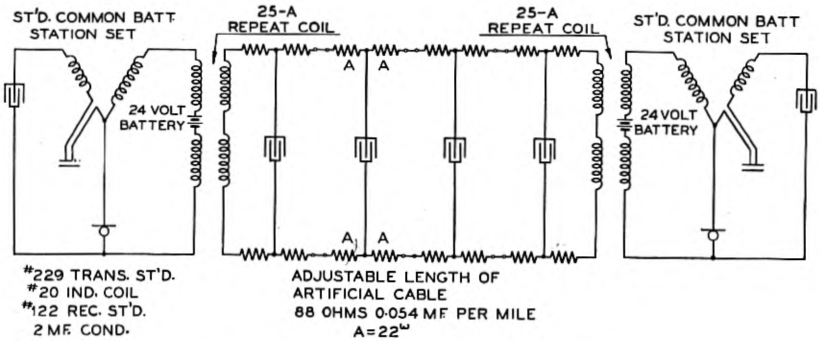

Fig. 1—Standard cable reference system.

balance was taken as the rating of the circuit under comparison. This reference system, shown schematically in Fig. 1, has been called the Standard Cable Reference System.

In addition to this rating of the performance of a telephone circuit, this standard cable reference system has had other applications. Certain settings of this reference system were selected as specifying the standards of transmission which were to be provided in the design and operation of commercial circuits for the several kinds of service, such as local and toll. The effect of introducing or changing any part in a commercial circuit was rated in terms of the amount of cable by which it was necessary to change the line of the reference system to produce the same effect on the loudness of the reproduced speech sounds. Likewise, the transmitters and receivers of this reference system were used as reference instruments for the comparison and rating of other transmitters and receivers.

This cable reference system has played a very important and necessary part in the development of telephone transmission, in that it has provided a ready means of rating the performance of the various parts of the system and of any changes, and made it possible to design commercial circuits to provide a predetermined grade of service. The performance of this system was specified by stating the kinds of apparatus and circuits used. The performance of the elements of the electrical portion of the system could be checked by voltage, current and impedance measurements, but for the transmitters and receivers reliance for constancy of performance was placed primarily upon the careful maintenance and frequent cross comparisons of a group of transmitters and receivers which were specially constructed to reduce some of the sources of variation in the regular product instruments. In this way, reasonable assurance of the performance of the reference system was secured. This system has been widely used both in this country and in other parts of the world, and the performances of the various systems have been kept in accord by frequent circulation of calibrated transmitters and receivers.

As the telephone art has developed, modifications have been found to be desirable in this reference system to make it more suitable for its purpose. Telephone instruments and circuits have been designed and used which have less distortion than existed in the corresponding parts of the cable reference system. For this reason it is desirable to have as a new reference system one with which the transmission over the most perfect telephone circuit or over some less perfect one may be simulated at will. The change of the unit of transmission from the mile of standard cable to the decibel[3] has brought about the need for a change in the line of the reference system.

In selecting a new reference system, it is obviously desirable to eliminate as far as possible the factors which are not subject to exact measurement, or which may possibly vary with time. For this reason, the elements of the new system have been chosen so that their performance may be definitely measurable at any time, and may remain as far as possible invariable. This applies also to those elements which are provided for insertion in the system when it is wished to produce some distortion which will make more easily possible a loudness balance between the reference system and the circuit under investigation.

A reference system such as that described here, in which the essential elements are so constructed as to reproduce speech with a high degree

[3] "Decibel" (db) is the name for the Transmission Unit which has superseded the "mile of standard cable." W. H. Martin, *Bell System Technical Journal*, January, 1929, and *A. I. E. E. Journal*, March, 1929.

of perfection, and with which provision may be made for modifying the speech in definite and reproducible ways, affords a convenient means for studying the capabilities of telephone circuits of different physical performances. These investigations, however, are outside the purpose of this paper, which is to describe the new reference system and its application in making volume ratings.

General Requirements

The outstanding conception of the new reference system is that its performance should be suitable to serve as a reference base line for indicating the performance of all telephone circuits and that the transmitter and receiver elements of the new system should provide similar base lines for the performance of electroacoustic converters. To meet these needs properly the performance of the system and its parts should be capable of being measured and definitely specified in terms of physical quantities. In this connection, there arises a matter which has been the subject of much discussion, namely, as to whether or not the specified performances of the reference transmitter and receiver should be those which are realized when used as telephone instruments. In regard to the transmitter, the difficulty comes in specifying the input when it is placed in front of the mouth of the talker. This is due to the non-uniformity of the sound field from the speaker's mouth, the nature of the waves of speech sounds and the reflections of these waves from the transmitter. In regard to the receiver, the difficulty is due to determining the output when the receiver is held to the ear. To obviate these, it has been decided to specify the performance of the transmitter in terms of the electrical output for a given pressure on the diaphragm of the transmitter and of the receiver in terms of pressure set up in a simple closed chamber for a given electrical input to the receiver. These conditions are definite and reproducible.

The most important requirement, then, for the reference system is that the physical performance of the system and of its component parts should be capable of being measured and definitely specified in terms of physical quantities. If this requirement is realized, a system providing the specified performance can be set up wherever desired. This has been the main criterion in the design of the master reference system for telephone transmission which is described here.

The second main requirement is that specifiable and predeterminable changes can be made with respect to the performance which is selected as the reference. These changes must be capable of varying the relation between the loudness of the reproduced sounds with respect to the initial sounds, the distortion of the wave shape of these reproduced sounds, and also the amount of noise accompanying these reproduced sounds.

For convenience in specifying these requirements, it has been found desirable to impose another requirement, namely, that the system be capable of giving a performance which is as free as possible from distortion and noise. It should be noted that two kinds of distortion must be taken into account: that due to unequal efficiency for sounds of different frequencies and that due to non-linearity causing unequal efficiency for sounds of different magnitudes. This requirement is also of advantage in insuring that the reference system and its parts will have less distortion than any circuit or instrument with which it may be compared. This will permit the simulation of the distortion of such instruments or circuits by the insertion of distortion in the reference system.

For convenience in use, it is highly desirable that the performance of the reference system and its parts be constant for a reasonable time under normal operating conditions.

General Features

The master reference system [4] employs a transmitter and receiver which are capable of a high degree of freedom from distortion. The transmitter is of the condenser type and the receiver is of the moving coil type. Both these instruments are materially lower in efficiency than commercial types of apparatus, but this condition is compensated for by the use of multi-stage vacuum tube amplifiers. These instruments, together with their associated amplifiers, constitute reference standards for converters between acoustic and electrical energy. The third necessary element of a telephone transmission system, namely the line, is provided by a network of resistance elements. Such a line can be made to provide uniform attenuation over a wide frequency range, and can be made to control the magnitude of this attenuation over a large range. This line is taken as giving a reference performance for lines.

The specification of the performance of such a system is based on the principle of the thermophone, which is a converter of electrical energy into acoustic waves by means of the heat generated by the passage of an electrical current through a resistance. From a knowledge of the form and physical constants of this resistance element, of the medium in which it is used, and of the electrical input to the element, the acoustic pressure generated in a chamber of known size

[4] A discussion of a preliminary model of this system was given in "A Telephone Transmission Reference System," by L. J. Sivian, *Electrical Communication*, October, 1924.

can be determined by theoretical considerations.[5] The performance of the condenser transmitter is determined by making its diaphragm a wall of a simple closed chamber in which the thermophone is placed. By this means a known pressure wave of any frequency over the range desired can be impressed upon the diaphragm of the transmitter. The voltage output of the transmitter for a specified circuit condition is then measured. From this measurement the ratio of the voltage output to the acoustic pressure on the diaphragm is established for that instrument and circuit condition. With the performance of the transmitter thus established, the performance of the receiver element of the reference system is measured by acoustically coupling the receiver to the condenser transmitter, so that the receiver actuates the transmitter, and then determining the relation of the pressure generated by the receiver in the coupler to the voltage input to the receiver. The performance of the line element is determined by well-known means. The performance of the whole system can then be expressed in terms of the pressure produced by the receiver with respect to the pressure on the diaphragm of the transmitter.

The performance of this system is practically free from distortion for the energies which it is required to handle, and probably materially excels in this respect that of any previous system. With this system, volume relations between output and input sounds can be varied over a wide range with practically no accompanying distortion. In comparing such a system, however, with commercial systems, it is advantageous also to be able to control distortion. This is particularly the case when using the instruments of the master system for rating the volume efficiency of commercial types of transmitters and receivers. To facilitate this, arrangements are made for the introduction into the amplifiers associated with the transmitter and receiver, of networks which may be designed to give a variation of efficiency with frequency which corresponds to that obtained with commercial apparatus. These networks and their distortion effect can, of course, be definitely specified. The line element of this master system can be replaced by a line or network giving any type of distortion desired. Also, known amounts of extraneous currents to produce noise can be introduced into this circuit without otherwise appreciably affecting its performance. This is accomplished by connecting a relatively high impedance source of voltage of the desired wave shape across a circuit element of relatively low resistance.

This system provides a performance which is definitely known, and

[5] The theory of the thermophone as a precision source of sound is outlined in papers by H. D. Arnold and I. B. Crandall, *Physical Review*, July, 1917, and by E. C. Wente in the *Physical Review*, April, 1922.

which can be varied over a range of volume and distortion. It well meets the requirements and represents a material advance over the standard cable reference system which it now replaces. In order to tie together ratings established in terms of the old system with those of the new system, comparisons of the two have been made to determine the adjustments of the new system which make its loudness performance correspond with that of the old.

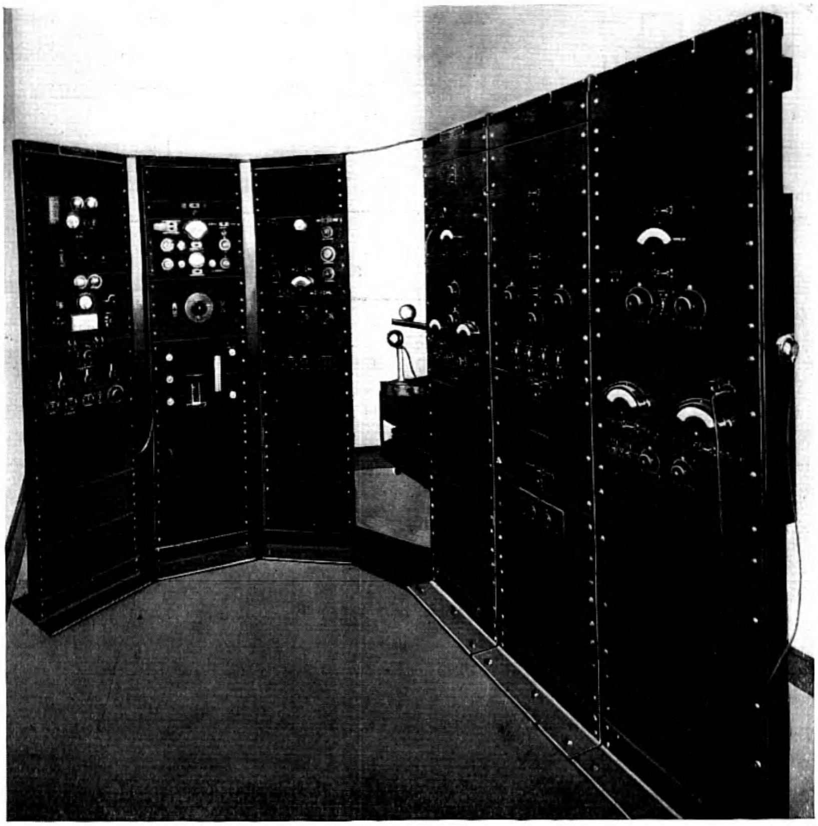

Fig. 2—Master reference system for telephone transmission with associated calibration apparatus.

Description of Master Reference System

The master reference system with associated calibration apparatus is shown in Fig. 2. This equipment, mounted on steel panels and racks, and arranged as shown, is installed in a room, shielded from acoustical and electrical disturbances, at the Bell Telephone Laboratories in New York City. In Fig. 2 the transmitter, line, and receiver of the reference system are shown on the three racks at the right. The calibration apparatus, consisting of an oscillator, thermophone, vacuum tube voltmeter and volume indicator are shown on the other three racks. A schematic diagram of the master reference system is shown in Fig. 3.

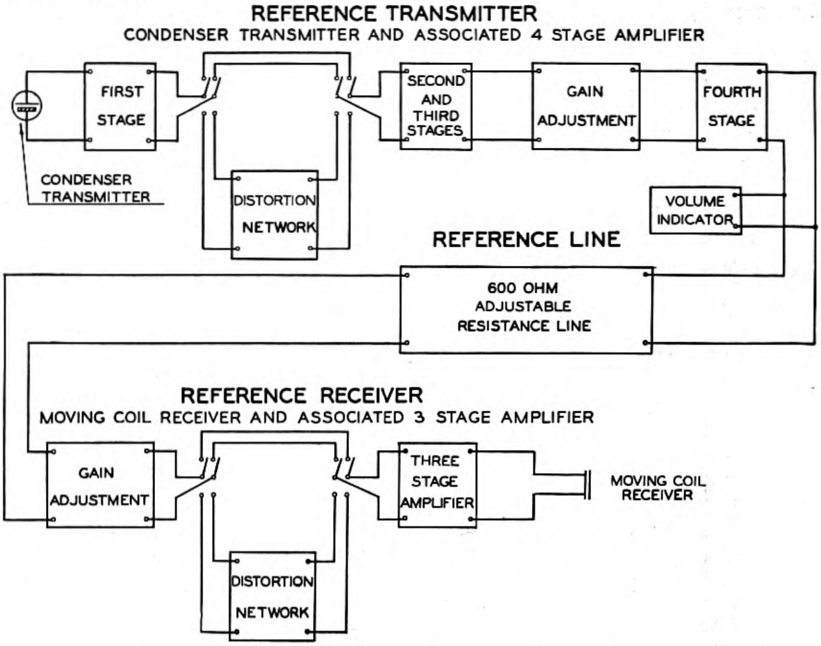

Fig. 3—Schematic diagram of master reference system.

The reference transmitter consists of a condenser transmitter and associated four-stage amplifier. The condenser transmitter is simple and rugged in construction. It has been available for work of this nature for several years during which time considerable experience has been obtained with it. In this system the condenser transmitter is held in an adjustable mounting and is equipped with a guard by means of which the speaker can keep his lips at a fixed distance from the diaphragm. This guard consists of a wire ring 4.7 cms. in diameter, held parallel to and at a distance of 4.1 cms. from the diaphragm of the transmitter by three wire supports. A volume indicator with meter visible to the speaker enables him to maintain an approximately constant talking intensity. In the condenser transmitter,[6] shown in

[6] The theory and operation of this transmitter are discussed in papers by I. B. Crandall, *Physical Review*, June, 1918, and E. C. Wente, *Physical Review*, July, 1917, and *Physical Review*, May, 1922.

Fig. 4 and in cross-section in Fig. 5, a thin highly stretched duralumin diaphragm is mounted close and parallel to a steel plate grooved and

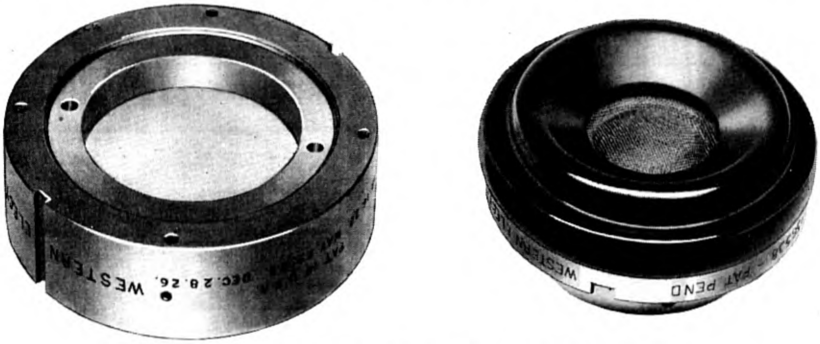

Fig. 4—Condenser transmitter and moving coil receiver.

perforated for air damping. This diaphragm and plate form the electrodes of a condenser polarized by a battery through a high

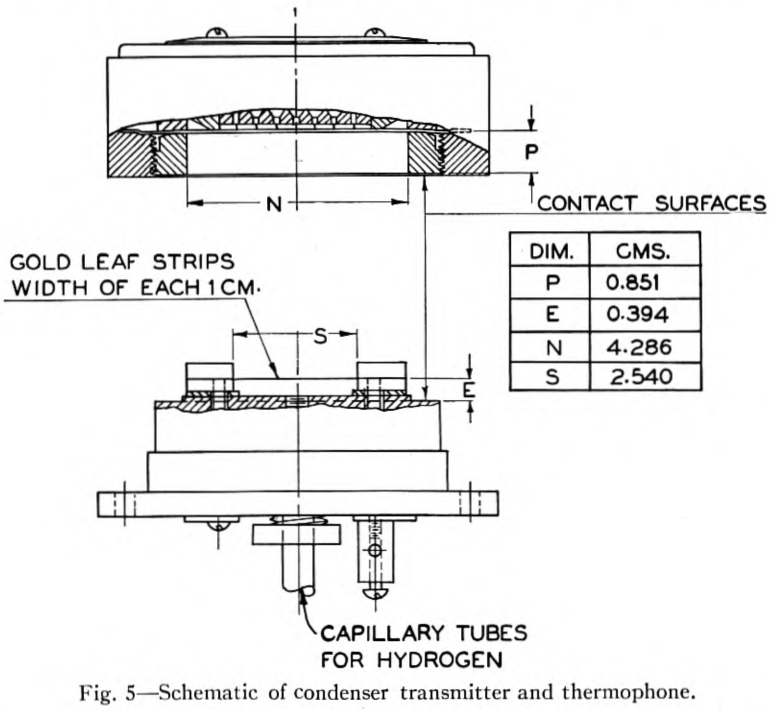

DIM.	CMS.
P	0.851
E	0.394
N	4.286
S	2.540

Fig. 5—Schematic of condenser transmitter and thermophone.

resistance. Sound vibrations impinging on the diaphragm actuate it and produce variations in the capacity of this instrument. The resulting alternating potentials, faithfully representing the sound pressure waves, are amplified by the associated amplifier. Between the first and second stages of this amplifier, provision has been made for the introduction of distortion networks to simulate the distortion of any transmitting system. Between the last two stages are attenuating networks permitting adjustment of the relation between transmitter input and transmitter output over a range of 22 db in steps of

Fig. 6—Thermophone in chamber for calibrating transmitter.

0.1 db. The output impedance of the amplifier is 600 ohms with negligible phase angle.

The reference line consists of a series of balanced resistance networks. This line has a characteristic impedance of 600 ohms matching the output impedance of the reference transmitter and the input impedance of the reference receiver, thereby eliminating any reflection effects at these junctions. By means of suitable controls the attenuation may be varied over a range of 101 db in steps of 0.2 db.

The reference receiver consists of a moving coil receiver and associated three-stage amplifier. Means are provided for adjusting the relation between the input to the receiver and its output over a range of 22 db in steps of 0.1 db. As in the case of the reference transmitter, provision has been made for the introduction of distortion networks to simulate the distortion of any receiving system. In the moving coil receiver[7] shown in Fig. 4 and in cross-section in Fig. 7, a coil of aluminum ribbon, by vibrating relatively to a fixed permanent magnet, actuates a clamped, unstretched, thin duralumin diaphragm to which

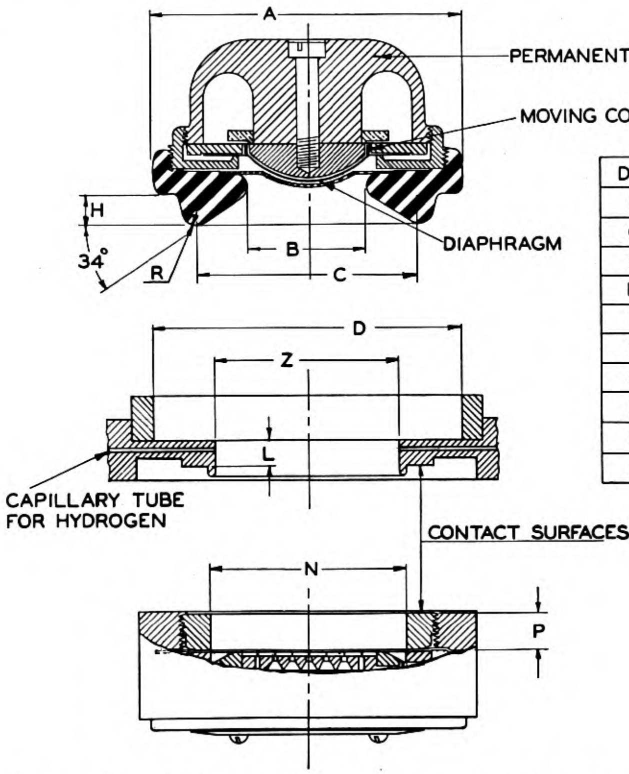

DIM.	CMS.
B	2.54
C	4.76
L	0.49
N	4.286
P	0.851
Z	3.97
A	6.67
D	6.68
H	0.64
R	0.36

Fig. 7—Schematic of moving coil receiver, coupler and condenser transmitter.

it is attached. Air damping in this receiver is secured by an arrangement somewhat similar to that employed in the condenser transmitter. The structure is simple, rugged, and, from the standpoint of freedom from distortion, its performance is comparable to that of the condenser transmitter. The central surface of the diaphragm is protected by a meshed wire screen instead of by the more usual type of receiver cap. This construction avoids resonance effects which

[7] This instrument, which is similar in many respects to one described by E. C. Wente and A. L. Thuras in the *Bell System Technical Journal*, January, 1928, will be discussed in a future paper by the same authors.

would otherwise occur in the confined air space between diaphragm and cap. The contour of the ear piece, resembling that of the familiar telephone receiver, permits the listener to readily center the receiver on his ear.

In order that an individual part of any telephone circuit may be compared with the corresponding element of the master reference system, the system is arranged so that the reference transmitter, reference line or reference receiver, may be replaced by the corresponding part to be rated.

Calibration of Master Reference System

To specify adequately the performance of the master reference system, in terms of definite physical quantities, apparatus is associated with the system for making electroacoustic calibrations of the reference transmitter and reference receiver, and electrical calibrations of the circuits. In general, the method employed in these calibrations is to adjust the setting of an attenuator to obtain a deflection on the galvanometer of a vacuum tube voltmeter, equal to the deflection produced when measuring the output of the element under calibration. This avoids the necessity for an absolute calibration of the measuring device.

The source of alternating currents, used for calibrating purposes, is an oscillator, capable of producing currents with a harmonic output usually less than 3 per cent of the fundamental.

The measuring equipment used for making the above calibrations consists of a two-stage vacuum tube voltmeter in conjunction with a tuned circuit connected across its input. By means of this tuned circuit, harmonics of the fundamental frequency to be measured are attenuated by at least 20 db.

The calibration of the condenser transmitter is made with a thermophone, the gold leaf thermal elements being shown in Fig. 6. In Fig. 5 is shown a cross-section of a condenser transmitter and a thermophone. Petrolatum is used to form a seal between the instrument and the thermophone block. The air in this small enclosed chamber, formed by the walls and diaphragm of the condenser transmitter and the thermophone block, is replaced by hydrogen. Since the velocity of sound in hydrogen is approximately four times that in air, the frequency range over which measurements may be made before standing wave effects are experienced is extended by the use of this gas. In addition, the efficiency of the thermophone is increased, the constant of diffusivity for hydrogen being greater than that for air. Both alternating and direct currents are passed through the gold leaf thermal elements, the direct current being sufficiently large to make negligible the double-frequency effect resulting when alternating current is supplied to the thermophone. The alternating current passing through the thermal-elements (gold leaf being selected because of its low heat capacity) causes variations in their temperature. Periodic expansions and contractions of the surrounding gas, resulting from the varying heat transfer occasioned by the periodic temperature changes of the thermal elements, constitute sound waves of precisely determinable pressure. These sound waves actuate the transmitter and the ratio of the voltage output to the sound pressure gives the transmitter calibration. The process involved is as follows: Referring to Fig. 8.

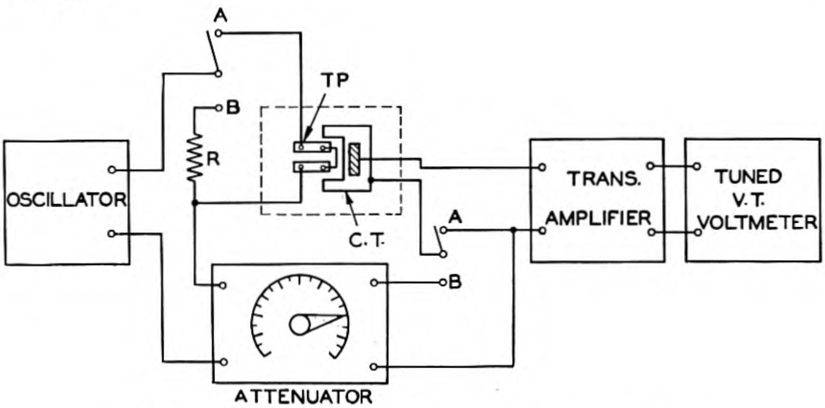

Fig. 8—Circuit for calibrating condenser transmitter.

E_T = Voltage generated by condenser transmitter per bar (one dyne/cm.^{2}).

I_1 = Alternating current through thermophone and attenuator.

P = Pressure developed by thermophone per volt alternating current across it.

V_{VM} = Voltage across voltmeter.

A = Ratio of voltage delivered to 600-ohm load by the transmitter amplifier to voltage impressed in series with condenser transmitter.

V_0 = Voltage across attenuator input.

R_1 = Input impedance of attenuator.

R = Thermophone resistance.

N = Attenuator setting in db.

TP = Thermophone.

CT = Condenser transmitter.

With the switches in Fig. 8 in position "*A*," the alternating current input to the thermophone and the amplifier gain are adjusted to obtain a convenient voltmeter deflection (V_{VM}). Then:

$$V_{VM} = I_1 R P E_T A.$$

Operating the switches to position "*B*" and manipulating the attenuator to attain the same voltmeter deflection as before we obtain

$$V_{VM} = V_0 A \times 10^{(-0.05N)} = I_1 R_1 A \times 10^{(-0.05N)}.$$

Then:

$$E_T = \frac{R_1 \times 10^{(-0.05N)}}{RP}.$$

The moving coil receivers are also calibrated in a sealed chamber in an atmosphere of hydrogen by an arrangement shown in cross-section

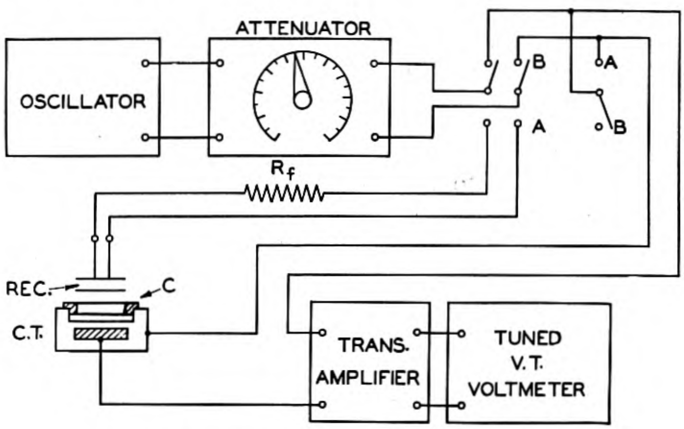

Fig. 9—Circuit for calibrating receiver.

in Fig. 7. A condenser transmitter, calibrated in the above manner, is actuated by the sound output of the receiver under test driven by the oscillator. The process involved is as follows: Referring to Fig. 9.

V_{VM} = Voltage across voltmeter.
V_0 = Voltage across attenuator input.
V_R = Voltage across receiver terminals

$$= \frac{V_0 R_R}{R_R + R_f} \times 10^{(-0.05N_a)}.$$

R_R = Impedance of receiver plus cord.
R_f = Fixed resistance.
P_R = Pressure developed by receiver per volt across receiver terminals.
E_T = Voltage developed by condenser transmitter per bar (one dyne/cm².).
A = Ratio of voltage delivered to 600-ohm load by the transmitter amplifier to voltage impressed in series with condenser transmitter.
N_a = Attenuator reading with switches on "A."
N_b = Attenuator reading with switches on "B."
C = Coupler (Fig. 7).
CT = Condenser transmitter.

With the switches indicated in Fig. 9 in position "A" the attenuator is adjusted to position N_a to produce a convenient deflection on the voltmeter (V_{VM}). Then:

$$V_{VM} = V_0 \frac{R_R}{R_R + R_f} P_R E_T A \times 10^{(-0.05N_a)}.$$

Operating the switches to position "B" and adjusting the attenuator to some position N_b to reproduce the above voltmeter deflection V_{VM} we obtain:

$$V_{VM} = V_0 A \times 10^{(-0.05N_b)}.$$

Then:

$$P_R = \frac{(R_R + R_f) \times 10^{0.05(N_a - N_b)}}{R_R E_T}.$$

The calibrations of the purely electrical elements of the circuit are made by measurements of input, output, and impedance.

Fig. 10 shows, for particular amplifier adjustments which are discussed below, the frequency response characteristics of the reference transmitter, reference receiver and the complete reference system with 0 db in the line. The characteristic of the reference transmitter and also of the reference receiver, in each instance, is that of the instrument and associated amplifier combined. However, as the frequency response of each of the amplifiers is uniform within 2 db from about 50 to 10,000 cycles per second, the curves shown are essentially the calibrations of the instruments determined as described above. The primary purpose of these characteristics is to show the performance of these elements for definitely specified physical conditions. Consequently, no corrections are included in these curves for the effect on the sound field of the speaker when talking into the condenser transmitter. Neither have corrections been applied for the effect of leakage between the listener's ear and the earpiece of the receiver nor

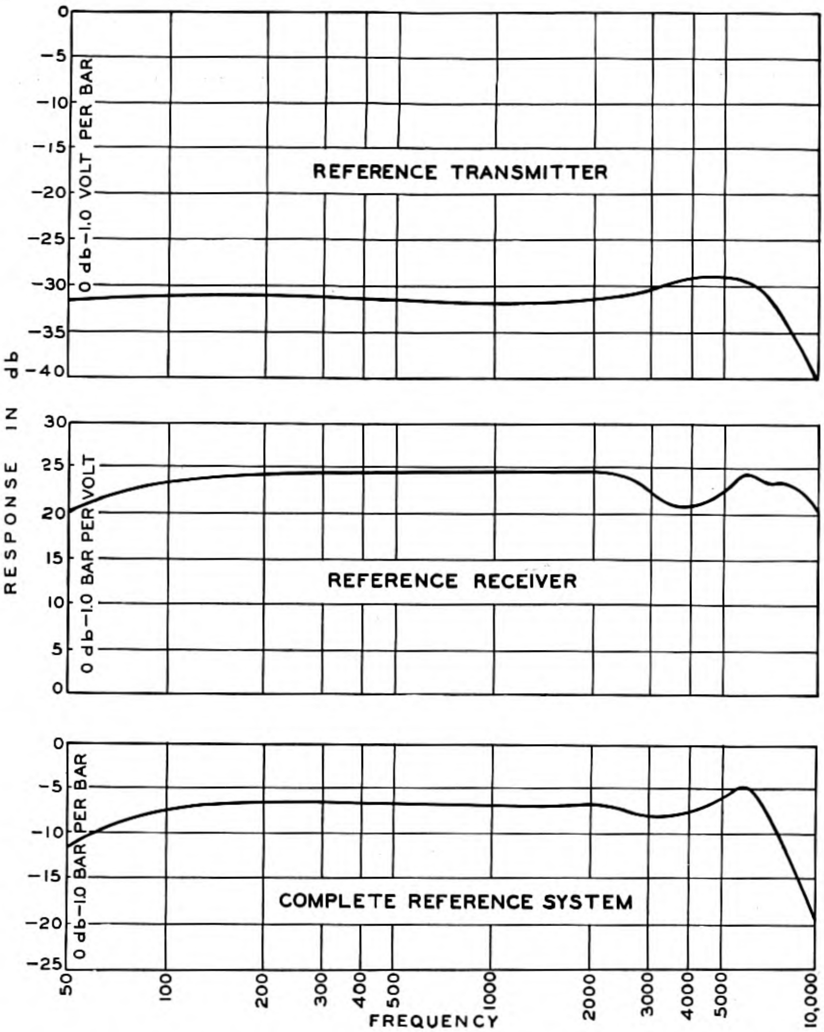

Fig. 10—Response characteristics of reference transmitter, reference receiver and complete reference system with 0 db in the line.

for the difference between the volume enclosed in the sealed chamber when making the calibration as compared with the volume enclosed in the ear canal when the receiver is held to the ear. The reference line, consisting of balanced resistance networks, has a uniform frequency response characteristic. The characteristic of the complete system, therefore, except as its level is affected by the attenuation in the reference line, is that of the reference transmitter and reference receiver combined, there being no reflection effects at the junctions of the reference line with either the reference transmitter or receiver.

Fig. 11 shows the effect of introducing distortion networks in both the reference transmitter and reference receiver. The distortion net-

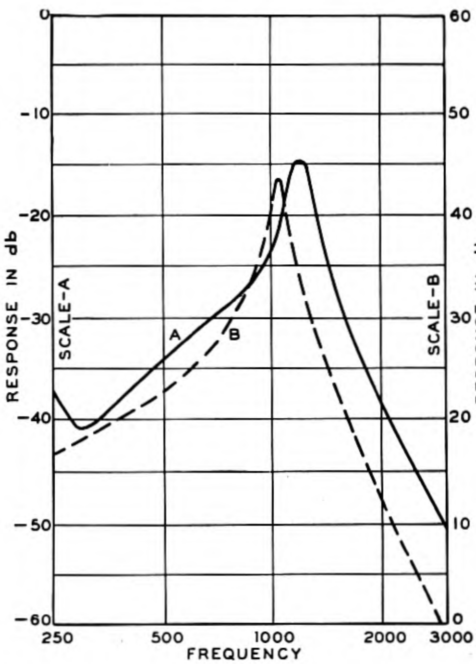

Fig. 11—Response characteristics of reference transmitter and receiver with distortion networks.
A = Reference transmitter—0 db—1.0 volt per bar.
B = Reference receiver—0 db—1.0 bar per volt.

work introduced in the reference transmitter simulates the distortion in the transmitter, station set and cord circuit, of the standard cable reference system. Similarly, the distortion network introduced in the reference receiver simulates the distortion of the receiver, station set and cord circuit, of the standard cable reference system. These two networks are designated, respectively, Transmitter Distortion Network No. 1 and Receiver Distortion Network No. 1. The distortion of any transmitter, receiver, or station set may be similarly simulated by the design and introduction in the master reference system of a proper network. The advantage of such a procedure will be evident to those familiar with the difficulties of making voice volume balances between instruments of widely different frequency characteristics. The volume efficiency of any instrument can also be reproduced by adjustment of the controls in the amplifiers of the reference transmitter or receiver as the case may be. The results of voice volume balances made with the distorted reference system can be referred to the undistorted master reference system by applying a correction for the volume effect of the distortion network in the master reference system, this effect being determined independently as a rating of the distortion network.

Experience has shown that amplifiers properly designed and constructed remain essentially constant with time. Such changes in gain as may occur because of replacement of vacuum tubes or other apparatus may be readily compensated for by adjustments of potentiometers provided for this purpose. Condenser transmitters are affected to some extent by variations in temperature and barometric pressure. The magnitude of variation at any frequency between 50 and 10,000 cycles per second from these causes may be as much as 2.5 db, although under normal operating conditions such as those experienced in buildings in this climate, the variation is usually not more than 1 db. Since changes of this character are gradual in nature, their magnitude can be readily determined by a thermophone calibration. Corrections for any change in sensitivity of the instrument may then be made by adjustment of the controls in the amplifier associated with the condenser transmitter to maintain the proper gain in the reference transmitter. Similarly, any variations in the response of the moving coil receiver may be compensated for by adjustment of the gain controls in the amplifier associated with this receiver. The magnitude of the variations, at any frequency between 50 and 10,000 cycles per second, in the moving coil receiver may be as much as 3 db although usually variations of less than 1.5 db are observed. The calibration of the condenser transmitters, and indirectly of the moving coil receivers, is dependent upon the gold leaf thermophone, whose pressure characteristic is computed from physical measurements. Results obtained with thermophones can be held within about 0.5 db of the average obtained by using a group.

Comparison of Master Reference System and Standard Cable Reference System

Since the master reference system is to replace the standard cable reference system for volume ratings, the two systems have been compared by means of voice volume balances so that data obtained in the future may be directly comparable in this respect with those obtained in the past. The respective elements of the two systems, as well as the systems as a whole have been compared. The station set and cord circuit at the sending end of the standard cable system are taken as comprising the transmitting element of that system and, likewise, the corresponding apparatus at the listening end as the receiving element. In these measurements the reflection gain at the junction of the standard cable line and the output terminals of the transmitting element of the standard cable reference system has been taken as part of the transmitting efficiency of that element. Similarly, the reflection gain at the junction of the standard cable line and the input terminals of the receiving element of the standard cable reference system has been taken as part of the receiving efficiency of this element.

In the voice calibration of the master reference system to determine the adjustments which make this system equivalent on a volume basis to the standard cable reference system, eight series of voice tests were made. The purpose of the first five series of these tests was to determine the adjustments which make the master reference system with transmitter distortion network No. 1 and receiver distortion network No. 1 inserted in their respective elements, equivalent on a volume basis to the standard cable reference system. The purpose of the sixth and seventh series of tests was to determine the volume effects of the insertion of these distortion networks in the reference transmitter and receiver. The eighth series of tests was a direct comparison of the master system without distortion networks and the standard cable system, and so serves as an overall check on the determinations of the preceding tests.

In the first series of tests a comparison was made of the reference receiver with its distortion network and the receiving element of the standard cable system by interchanging the two in the standard cable system, with 24 miles of artificial cable in the line. The receiving element of the master system was adjusted so that its sound output was judged to be equal for this condition to that of the receiving element of the standard cable system. In the second series of tests a similar comparison was made of the reference transmitter with its distortion network and the transmitting element of the standard cable reference system. These transmitting elements were connected in turn to a 24-mile standard cable line terminated by the reference receiver with its distortion network, the receiver being adjusted in accordance with the results of the first series of tests. In the third and fourth series of tests the master reference system with the distortion networks in both the transmitter and receiver was compared with the standard cable reference system, the line of the master system serving as the adjustable element. These two series of tests were similar except that 24 miles of standard cable were used in one series of tests and 14 miles of standard cable in the other. The adjustments for the reference transmitter and reference receiver in these tests were those determined from the first and second series. From the results obtained in the third and fourth series of tests, the magnitudes were determined of the reflection gain at the junction of the standard cable line with either the reference transmitter or the reference receiver, and of the volume equivalent of 1 mile of standard cable in terms of db. The reference transmitter and reference receiver, each with its distortion network, were then readjusted in accordance with these data. The fifth series of tests served as a check on the results of the previous four series. In this fifth series, the master reference system with transmitter and receiver distortion networks and 24 db in the line was compared with the standard cable reference system with 24 miles of standard cable in its line.

In the sixth series of tests the adjustment of the reference receiver without distortion was determined to make it equivalent on a volume basis to the reference receiver with distortion. The reference transmitter with distortion and the reference line with 24 db formed the rest of the system during these comparisons. In the seventh series of tests the sound output of the master reference system without distortion was compared to the sound output of this same system with distortion networks in the reference transmitter and reference receiver, the reference transmitter being adjusted to obtain a balance. During these tests 24 db was kept in the reference line. The final series of tests, serving as a check on all of the above determinations, consisted of a comparison between the master reference system without distortion and the standard cable reference system, the line of the master system being adjusted in making this comparison.

In making voice tests to determine the above settings, the speaker, whose position with respect to the transmitters was kept constant, called standard testing sentences in a conversational tone. A given intensity of calling was maintained by watching the deflections on a volume indicator connected across the output of the transmitting element. An observer, located in a quiet room removed from the systems or instruments under test, determined when the two systems under comparison gave output sounds of equal loudness. Each testing team, consisting of a speaker and observer, made 12 balances. In order to attain a suitable precision in the final results of these tests, a large number of testing teams were used, the number being largest for the tests where the difference in the quality of the output sounds of the two systems under comparison was greatest. For example, for the first series of tests, six teams were used, for the fifth 25 teams, and for the eighth series, where the master reference system without distortion was compared with the standard cable system, balances were made with 37 teams. In all, over 2,000 individual balances were made. The standard deviation of the determination for each of the first five series is of the order of 0.5 db and for each of the last three series about 1 db.

The response characteristics of the transmitter and receiver elements of the master reference system, when adjusted on the basis of the results of the voice tests, to be equivalent on a volume or loudness basis to the corresponding parts of the standard cable reference system, are shown in Fig. 10. The mean values weighted from the standpoint of importance for volume are 0.027 volt per bar for the reference transmitter, 16 bars per volt for the reference receiver and 0.43 bar per bar for the complete master reference system with 0 db in the reference line. Further consideration is being given to the values of these response characteristics of the reference transmitter and receiver to be adopted as standards.

The response characteristics of the reference transmitter with transmitter distortion network No. 1 and of the reference receiver with receiver distortion network No. 1, when these elements are adjusted on the basis of the above voice tests to be equivalent on a volume or loudness basis to the corresponding parts of the standard cable reference system, are shown in Fig. 11.

Application of the System

The results of articulation tests over the master reference system when adjusted for optimum volume are practically equivalent to those obtained in direct air transmission in a quiet room. This system and replicas of it, are particularly adapted for use in making articulation studies, since they provide an approximately ideal system with which the loudness of the output sounds can be varied distortionlessly over a wide range and in which distortion networks of various types and controlled amounts of noise can be introduced. In this way the effects on articulation of various kinds of physical performance of a telephone circuit can be investigated.

The master reference system itself will be used chiefly for the important work of rating working standard systems and instruments. These working standards can be simpler than the master system and can be provided in any number required to handle the rating of commercial circuits and apparatus.

The working standard may be of several forms. It can be similar to the master reference system, simplified in its detailed construction but capable of calibration by the means employed for calibrating the master reference system. Such a system would probably find employment in laboratories and factories where the volume of testing is sufficient to justify the use of such apparatus. Another form may include electrostatic or electrodynamic instruments which are not capable of being measured by the calibration equipment of the master reference system. A third form which the working standard may take is that involving the use of transmitters, receivers and station sets such as have been used in the standard cable reference system. These latter types of working standards can be calibrated by volume comparisons with the master system or with the first type of working standard. They will find their chief field of usefulness at such points as shops for the repair and recovery of station apparatus, where the volume of work is not sufficient to justify the expense involved in maintaining more elaborate working standards.

European Master Reference System

In Europe the recommendation of technical standards for telephony is a function of the Comité Consultatif International des Communications Telephoniques a Grande Distance (C.C.I.), which is composed of representatives of the various European telephone administrations. In 1926, at the invitation of the C.C.I., representatives of the Bell System met in London with a committee appointed by the C.C.I. to consider the adoption of a transmission reference system. This committee recommended that the C.C.I. adopt as their master reference system a system essentially the same as the one described in this paper, and that such a system, which would be a replica of one in New York, be installed in Paris in the laboratory of the C.C.I. and be known as the European Master Reference System. This recommendation was adopted by the C.C.I.

Subsequently, some improvements were made in the system, and two duplicate systems, each with its associated calibrating apparatus, have been constructed. One of these is now in the Bell Telephone

Laboratories in New York and the other in the laboratory of the C.C.I. in Paris. The C.C.I. further recommended that primary and working standard systems, used in the telephone administrations adhering to the C.C.I., be calibrated in terms of the Master Reference System. The establishment of these two master systems insures the use of a common base line for the expression of transmission standards, and for the ratings of the transmission performance of telephone circuits in the two continents where the telephone system has had its greatest development.

Shielding In High-Frequency Measurements [1]

By J. G. FERGUSON

In this paper the purpose and usefulness of shielding in high-frequency measurement are outlined. General principles of electrostatic shielding are developed as applied to simple impedances and to networks of impedances, particularly to bridge networks. Practical applications of these principles to the shielding of adjustable impedances, and in the construction of actual bridge circuits, are described.

SHIELDING of high-frequency measurement apparatus has for its immediate object the control of certain electromagnetic and electrostatic couplings unintentionally introduced in the usual high-frequency circuit. These couplings are represented by stray admittances between the various parts of the system, either direct or to ground, and mutual impedances resulting from stray magnetic fields. In general, the control of these couplings is exercised for the purpose of attaining an accuracy of test that cannot be obtained so readily in other ways.

When we speak of electromagnetic and electrostatic coupling, it should be understood that these are simply component parts which together make up the total coupling which exists. They cannot be considered as existing independently of each other, and we cannot consider the shielding for one of these components without taking into consideration the effect on the other.

However, for the frequencies and impedances ordinarily used in communication work, at least, this interdependence is small enough to allow us to consider the shielding problem for each type by itself, without getting into practical difficulties due to this connection. As a result, two types of shielding which are known as electromagnetic, and electrostatic shielding have been developed.

It may be argued that by extensive separation of the physical parts of circuits and apparatus, any couplings can be decreased in value and in consequence errors caused by them can be reduced, thus eliminating any need for shielding. But there are obvious limits to the extent to which this method can be employed practically. In the case of electrostatic coupling to ground, it is scarcely of any value, and in any case excessive separation of the parts of a circuit introduces other errors due to the length of the wiring involved. Accordingly, it is usually necessary, where the maximum accuracy is desired, to have recourse to shielding.

[1] Presented before the A. I. E. E. Summer Convention, June 24–28, 1929.

The principles involved in the application of electromagnetic and of electrostatic shielding are quite different. In the case of electromagnetic shielding, the methods used have for their object the elimination of all couplings from the unit shielded to all other apparatus; thus, if perfect shielding were possible, the unit would have no coupling to any other parts of the circuit. It is never possible to accomplish this in the case of electrostatic shielding. Any electrical apparatus will have electrostatic coupling to any other apparatus in the vicinity and particularly to ground. The addition of shielding always introduces additional electrostatic coupling from the apparatus to the shield and the shield usually has more coupling to other equipment and to ground than the apparatus had before shielding it. Consequently, the principles of electrostatic shielding are mainly a matter of controlling this coupling in such a way that it has the least harmful effect in the circuit even at the expense of increasing its actual magnitude, rather than a matter of eliminating it entirely. For this reason electrostatic shielding requires much more extensive consideration and this paper is, therefore, devoted mainly to it, the principles of electromagnetic shielding being covered only briefly.

Principles of Electromagnetic Shielding

The necessity for electromagnetic shielding is limited practically to wound apparatus such as coils and transformers. It may be reduced to a minimum by using high permeability core material wherever possible in coils and transformers, and by using some form of closed core such as the toroidal type. By these means stray fields may be reduced to a relatively low figure. However, there are cases where the remaining coupling may be objectionable and it is then necessary to use shielding to reduce still further the amount of these stray fields.

Two types of shielding may be used. A high permeability material may be used for the purpose of short circuiting the stray field. The principles of this method of shielding are described fully in another paper and will not be considered further here.

In the case of air-core coils which are often of the solenoidal type, since the advantage of using the toroidal form is less in this case, and for coils used at very high frequency where heavy magnetic material is not so effective, shields of non-magnetic material may be used to confine the field by the effect of eddy currents. For these shields, a material of high conductivity is used, usually copper, and the principal consideration is the spacing of the shield from the coil rather than the thickness of the shield itself.

There is always a loss in efficiency due to the losses in the shield, and this loss is greater, the closer the shield is placed to the coil, that is, the stronger the field in which the shield is placed. However, even with solenoidal air-core coils very effective shielding may be attained by moderately thick copper shields spaced about the distance of a diameter from the coil.

Principles of Electrostatic Shielding

In both theory and practice all measurements assume that between different terminals or junction points of the system there are impedances having values known to a degree of definiteness consistent

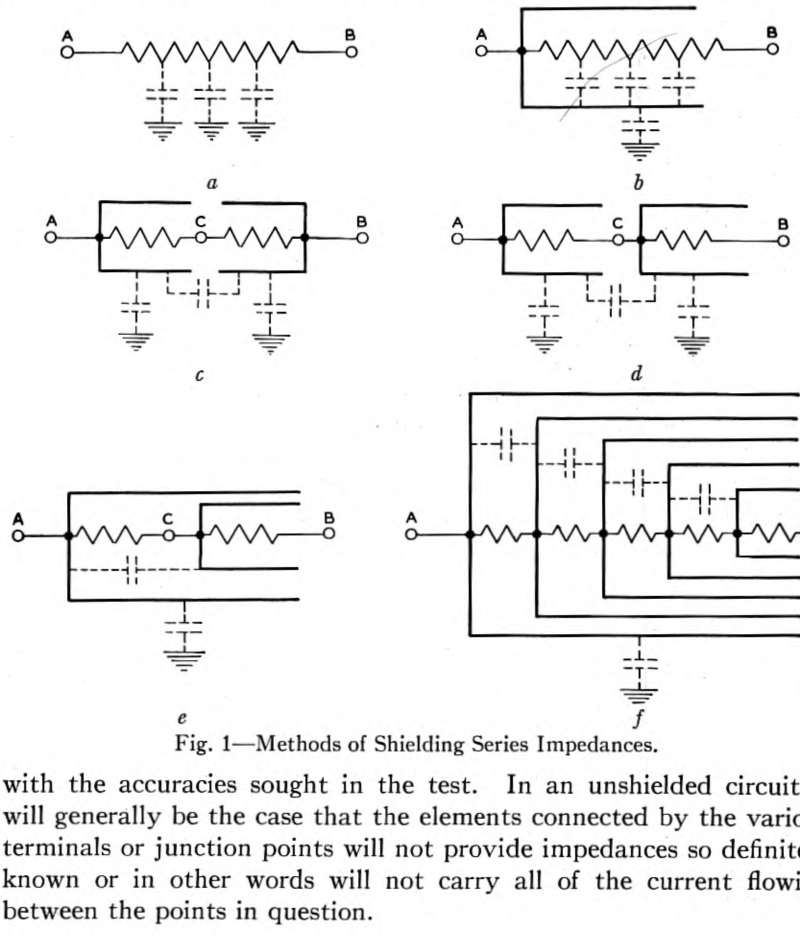

Fig. 1—Methods of Shielding Series Impedances.

with the accuracies sought in the test. In an unshielded circuit it will generally be the case that the elements connected by the various terminals or junction points will not provide impedances so definitely known or in other words will not carry all of the current flowing between the points in question.

Resistors

In the case of the simple resistor such as pictured schematically in Fig. 1*a* there are admittances from different parts of the conductor to other parts of the whole system and in particular to ground. These, of course, act to modify the effective impedance between the terminals and as they vary with the location of the resistor, the result is that its effective impedance is variable and known only for the location in which it has been calibrated. One of the first objects to be accomplished by shielding is to remedy this type of indefiniteness of value. This is done by mounting the elements within a shield of conducting material and in fixed space relation thereto, as shown in Fig. 1*b*. Thus, the circuit element has direct admittances only to the shield and as these are of fixed value the terminal to terminal impedance becomes independent of the location of the shielded element.

If, then, we connect the shield to any fixed point in the circuit element such as one terminal, all of the current transferred by the shield admittances passes to or from the circuit at this particular point. This concentration of admittance enables the ready evaluation of the effect produced by it when the element is used in conjunction with others in a complete measuring system. We may summarize all of this to form a fundamental rule of shielding, viz.: "the association of an element of a system with a shield so that all admittances from the element to other parts of the system or to ground are confined to one terminal."

If it is possible to connect such an element in a circuit so that the terminal to which the shield is connected is grounded, all variable admittances will be eliminated completely.

Series Impedances

In the case of two impedances in series as shown in Fig. 1*c*, shielding may be accomplished by connecting one shield to terminal A and the other shield to B. In addition to the effects described for a single impedance, there will then be admittance between the two shields which will depend on the position of the apparatus. This admittance is slightly more objectionable than admittance from shield to ground since, while we may ground either A or B, there will always be an admittance from one shield to ground which will be variable.

The shields may also be connected as shown in Fig. 1*d*, in which case the admittance between shields appears across the first impedance. Now if we extend the shield connected to A to include the other shield as shown in Fig. 1*e*, we have introduced a fixed admittance across AC and have variable admittances to ground from A. The admittance across AC is not objectionable in the case of a capacitor since it may be considered simply as an addition to it, but it has the effect of increasing the phase angle of a resistor and in the case of an inductor it increases the effective inductance and resistance variation with respect to frequency.

If this combination of impedances can be grounded at A we have a complete system having no variable admittances. The principle may be extended to include any number of series elements, the effect being to place admittances across all of the elements but one, and to enclose the whole system in one outer shield. Such a system for five elements in series is shown in Fig. 1*f*.

Parallel Impedances

The shielding of parallel impedances is comparatively simple since any number may be shielded individually and the shielding all connected to the same point. In reducing the shielding of multiple impedances to the simplest form the question arises whether it is sufficient to include them in a single shield or whether in addition

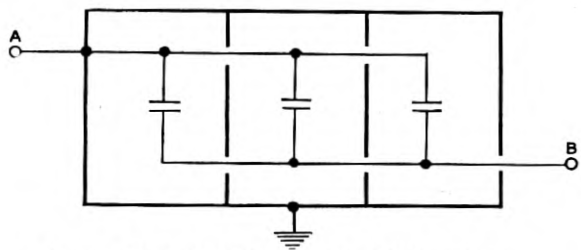

Fig. 2—Method of Shielding Parallel Impedances.

they should be shielded from one another. If they are not shielded from one another, there will be distributed admittances between them which may cause errors. Preferably each should be shielded individually. Fig. 2 shows such a shielding system for capacitors in parallel.

By following the procedure outlined above it is comparatively simple to apply shielding to any combination of impedances in series or in parallel in such a way that we will have all admittances to external conductors from the shielded elements concentrated at terminals or junction points of the system.

Circuit Shielding

In many cases it is impossible to connect the above combinations in a given circuit so that the outer shield is grounded. In such cases it is necessary to determine from the position of the network in the system the effect of admittances from the shield to other shields and to ground. To illustrate let us take the simple bridge circuit shown in Fig. 3. Each of the four impedances constituting the arms may be considered as any combination of individual impedances. With the shields connected as shown, the total admittances are reduced to three; namely, between *B* and *D* and from *B* and *D* to ground. These admittances do not affect the bridge balance and, therefore, are not objectionable. However, if we add input and output circuits and follow the same system of shielding, we get the result shown in Fig. 4. In this case it is impossible to concentrate all of the admittances at *B* and *D*. Neglecting for the present the ground at *D*, we have added variable admittances from *A* to *B*, to *D* and to ground. The only way of overcoming this difficulty is to use double shielding as

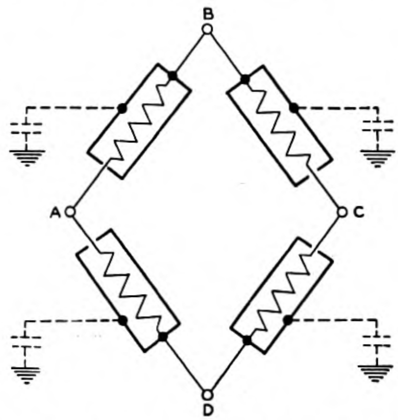

Fig. 3—Bridge Network Using Shielded Impedances.

shown, adding an outer shield to the impedance across *AC* and connecting it to *D*. This puts a fixed admittance across *AD*, but as we have not made any distinction between the four arms of the bridge, this admittance may generally be placed across an arm where it can be taken care of satisfactorily. If in addition we ground *D*, the admittances reduce to a single one from *B* to ground.

Admittance to Ground of Unknown Impedance

From the above it would appear that the general bridge circuit is susceptible of a simple complete solution, since the shielding shown in Fig. 4 is equally applicable to all cases. This would be true if the unknown impedance to be measured in the circuit had no admittance to ground. This is usually not the case. We generally have an additional requirement that the potential condition with respect to ground of the impedance during the measurement be defined in some way.

If the impedance can be connected across one arm of the bridge and its value is desired with one terminal grounded, the circuit shown is satisfactory. However, these are special conditions, and where the impedance to be measured forms only part of the total series impedance of an arm, or where the potential requirements are different, such as the requirement that the coil be measured with its terminals at equal potential to ground, the bridge shielding becomes a more serious problem.

In general, the question of selecting the most suitable system of electrostatic shielding for a specific test circuit, resolves itself into a determination of the most advantageous location of the admittances which, as described above, have been arranged to terminate at certain terminals or junction points. The facts which need to be taken into

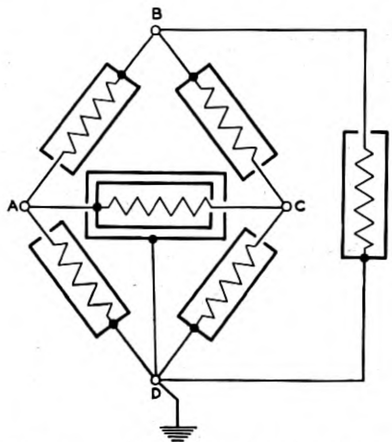

Fig. 4—Completely Shielded Bridge Network.

consideration are usually so varied that no general rules can be established. A few typical examples in which shielding is applied with considerable success will, therefore, be taken and the selection of suitable shielding for these circuits discussed.

Examples of Electrostatic Shielding

Adjustable Resistor

An adjustable resistor usually takes the form of a dial box in which there are from one to six dials arranged in series in decade formation. Each decade considered by itself is no more difficult to shield than a single resistor. The admittance of the shield, however, has a different effect at each step, which means that the phase angle varies with the setting of the dial. If the admittance to the shield is small, this effect will not be very great and in any case it is always the same for a given setting and hence may be included in a calibration.

In shielding several decades in series, admittances between decades are introduced. Effects due to these admittances can be taken care of completely by the use of nested shields as already shown in Fig. 1*f*. For a resistance box of five or six dials, this type of shielding becomes

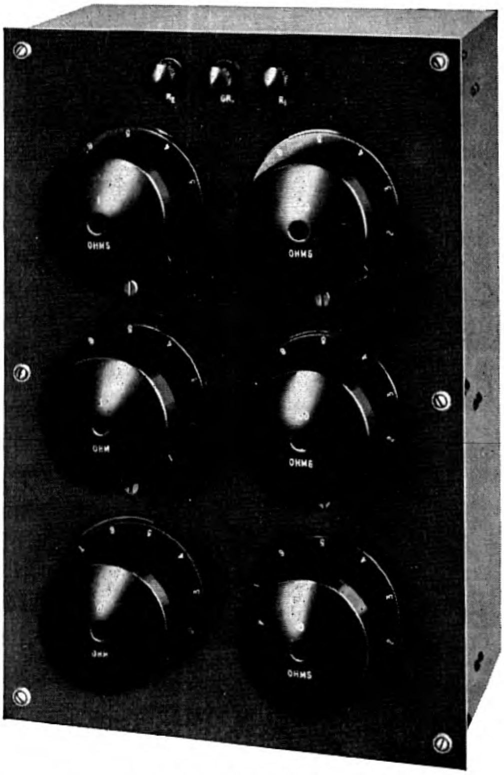

Fig. 5—Six-Dial Shielded Adjustable Resistor.

prohibitive from a size and cost standpoint and in consequence such shielding is usually not attempted. The use of a single shield for all decades of a resistor means that the impedance of two or more dial settings is not exactly equal to the sum of the impedances of each setting by itself. If the difference is appreciable the only alternative to the expensive type of shielding mentioned above is the use of a calibrated value for every combination of dial settings. This error in additions is smaller the lower the resistance, and usually may be neglected for values below 100 ohms.

The decades are ordinarily connected in series in ascending order of magnitude. The shield should always be connected to the low end, that is, to the terminal to which the decade of smallest value is connected. The reason for this may be explained as follows: the admittance from any decade to the shield is a function of the dimensions of the dial switch rather than of the resistance value. Consequently, all dials have approximately equal admittance to ground. It is desirable that the total admittance to ground be a minimum across the higher resistance settings. This requires that the low resistance dials be connected between the high dials and the shield, that is, the shield should be connected to the low end of the box.

In the actual constructon of such a resistor it is essential that the shielding be complete, particularly at the dials. Since the effect of the hands in operating the dials is more variable than any other coupling, it is of very little value to place an unshielded dial box in a metal shield which allows admittance from the hand of the operator to the circuit.

An example of a six-dial resistor in a complete single shield is shown in Fig. 5. The box itself and the panel are of metal, and the construction of the dials is such that there is a continuous metal shield between each dial head and the switch proper which it controls.

As stated earlier, the effect of the shield on the performance of the resistor is to increase the phase angle of the higher resistance values. In the case shown the admittance introduced by the shielding is of about the same value as the total admittance distributed in the coils themselves and from the coils to the switch parts.

Adjustable Inductor

The same considerations apply to an inductor as to a resistor except that on account of the larger physical size of the former, larger admittances are associated with it and for that reason it is usually necessary to use nested shields. Fig. 6 shows a standard inductor consisting of three decades and an inductometer using four shields. The three top panels have been removed showing the method of nesting the shields, and the construction used to bring the dial controls through the shields. The shielding of this unit is not complete in that the fourth shield (the outer one) does not extend over the top. This is allowable as the admittance from the third shield to ground is across the inductometer and any variation in it has little effect, particularly as the final balance is obtained with the inductometer, thus eliminating variations due to the hands of the operator, which occur in operating the other dials.

The admittance between shields is considerable but due to the method of construction the largest admittance is across the smallest inductance and there is no intershield admittance added across the highest decade. Accordingly, the effect is not as serious as might be thought at first glance.

In the case shown, the inductometer and the lowest decade are generally used only in combination with the higher dials and under these conditions they are not used at sufficiently high frequencies for the admittance shunting them to have much effect. The greatest effect of the admittance introduced by the shielding usually occurs when the second highest dial is used at a high frequency with the high dial set on zero. However, the admittance introduced across

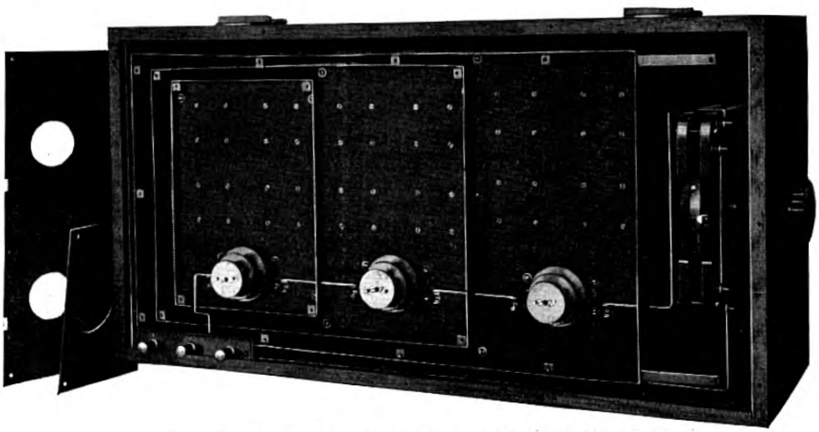

Fig. 6—Three-Dial Shielded Adjustable Inductor.

this decade is not appreciably larger than the distributed admittance across the coils. The shielding, therefore, does not limit the range of these inductance standards to any great extent.

Adjustable Capacitor

The units of an adjustable capacitor are practically always connected in parallel and the problem of shielding them is that of shielding a single capacitor. It is desirable to shield the decades from each other if the capacitances are small as this facilitates calibration and is easily effected. Where the capacitance is large, say over 10,000 $\mu\mu$f., this precaution is unnecessary. The capacitance introduced from the shield to the units has the effect of increasing slightly the value of each dial setting. The form of construction of the shielding is similar to that of the resistor shown in Fig. 5.

Bridge Circuits

The general principles of bridge shielding have been discussed by Campbell [2] and the equal ratio-arm comparison bridge has been discussed in detail by Shackelton.[3] The mechanical construction of the bridge itself exclusive of standards is simplified by the fact that there are comparatively few dials to be brought through the shielding.

This bridge with the standards described above may be used for a wide variety of measurements. A rather simple modification is the so-

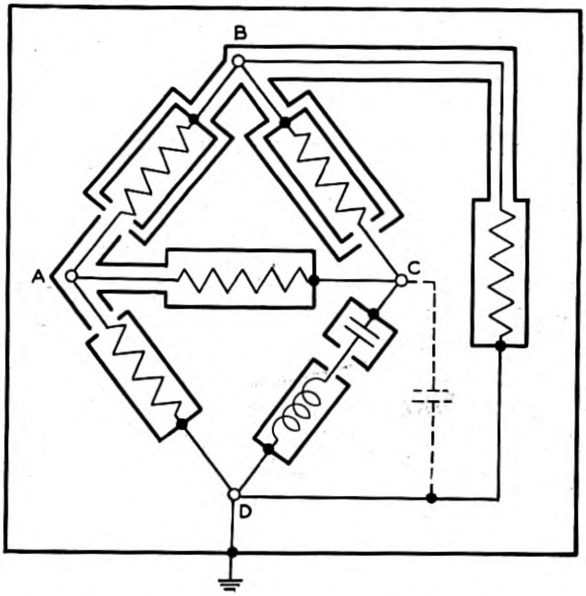

Fig. 7—Shielded Resonance Bridge Network.

called resonance bridge, in which the bridge unit is an equal ratio-arm comparison type, and a resistance is balanced in one impedance arm against a capacitance and an inductance connected in series in the other impedance arm. The balance is usually effected by adjusting the resistance and capacitance.

The shielded circuit of such a bridge is shown in Fig. 7. The capacitance from C to D introduced by the shielding may be compensated for in the usual way by the addition of an equal capacitance across AD. In this circuit the coil is usually measured under the

[2] G. A. Campbell, "The Shielded Balance," *Electrical World and Engineer*, April 2, 1904, p. 647.

[3] W. J. Shackelton, "A Shielded A-C. Inductance Bridge," *A. I. E. E. Journal*, Feb., 1927.

condition of one terminal at ground potential. Thus D is shown trapped to the ground shield. For this case, the shielding may be simplified considerably. Fig. 8 shows the mechanical construction of the combined resistance and capacitance standard used with the bridge unit for these measurements. The unit is shown with the top of the outer shield removed. The capacitance, in accordance with the shielding diagram, is double shielded, while the resistance requires only a ground shield.

Another bridge of the comparison type but using capacitance ratio arms is described by Kupfmuller [4] with a complete description of the shielding involved.

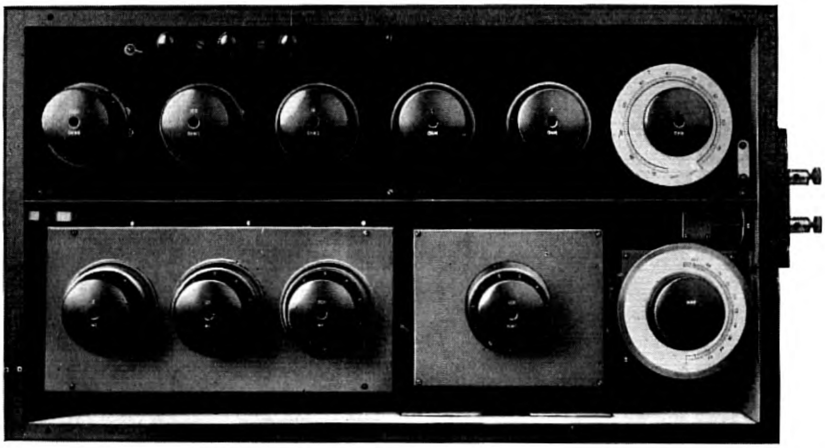

Fig. 8—Shielded Resonance Unit, Top Panel Removed.

A bridge of the general comparison type having self-contained standards of resistance and capacitance is shown with top panel removed in Fig. 9. It may be used for a wide variety of measurements such as series or shunt resonance, and direct comparison, by using the switches controlled by the small dials on the extreme left and right to throw the standards into various combinations.

Another bridge circuit which is interesting from the shielding point of view is the Owen bridge.[5] This is a skew bridge in which the ratio arms are 90° out of phase instead of being equal. For this reason any admittance introduced in one arm by the shielding cannot be compensated for by any equal admittance in another arm. Two

[4] Von K. Kupfmuller, "Über eine Technische Hochfrequenz Messbrucke," *Elek. Nach. Tech.*, September, 1925, pp. 263–270.

[5] D. Owen, "A Bridge for the Measurement of Self Inductance," *Proc. Phys. Soc. London*, October, 1914.

methods of taking care of this admittance may be used. It may be concentrated in the arm consisting of a capacitance and considered part of it, or an admittance across one impedance arm may be compensated for by a resistance across the other impedance arm. Both methods have been used in the construction of these bridges. A more detailed discussion of the shielding involved in this type of bridge is contained in a previous paper by the present author.[6]

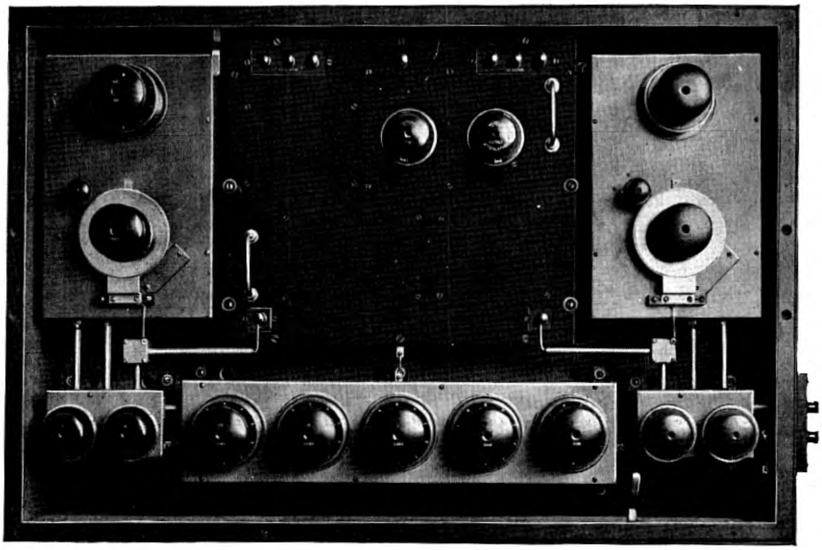

Fig. 9—Shielded Comparison Type Bridge, Top Panel Removed.

Details of Construction

We have discussed so far the admittance introduced by the shielding without going into details as to the form which this admittance takes although it has been broadly assumed that it is principally due to capacitance. Since it generally forms an integral part of the measuring circuit, it is obvious that as much consideration should be given to it as to the rest of the circuit. While the admittance is due essentially to capacitance, the necessary supports introduce a certain amount of conductance which causes some difficulty in obtaining compensation.

For instance, in the typical equal ratio-arm bridge circuit where the admittance across one arm requires compensation in the other arm, it is a simple matter to use an adjustable condenser for the compensation of capacitance. However, if the conductance is left un-

[6] J. G. Ferguson, "Measurement of Inductance by the Shielded Owen Bridge," *Bell System Technical Journal*, July, 1927, pp. 375–386.

compensated for it may cause considerable error, particularly in the measurement of high impedances at high frequencies. For this reason it is desirable that all shields be supported by insulating material of the highest quality such as hard rubber, glass or quartz and that only the minimum amount necessary for satisfactory mechanical support be used.

The wiring it will be noticed in Fig. 9 is shielded by brass tubing. This shielding is insulated from the conductor by means of bushings, only enough being used to insure that the conductor and shield do not change their relative positions with respect to each other. The insulating bushings used most generally are either hard rubber or glass beads.

Even after taking these precautions it has been found necessary for the highest precision work at the highest frequencies, to introduce a conductance compensator in the form of a small adjustable condenser in which the dielectric is an insulating material such as phenol fiber. By this means the amount of conductance in one arm may be varied to obtain correct compensation. The balance, once obtained, does not vary appreciably with frequency. Such an adjustment is used with the bridge shown in Fig. 9.

In bridge input and output transformers, which must generally be double-shielded, the shielding is rendered more difficult due to the requirement of a low conductance between shields. This demands a much more expensive construction than the simple requirement of complete electrostatic shielding.

Limitations of Shielding

Having discussed the uses and advantages of shielding, it may not be amiss to discuss briefly some of the limitations. As already brought out, the introduction of shielding always brings with it some additional admittance. Since this admittance is a function of frequency it is natural that shielding should introduce more trouble, the higher the frequency. However, it is also equally true that the stray admittances due to lack of shielding introduce more trouble, as the frequency is increased.

In general, it may be said that if shielding a circuit is found to have a definite advantage at moderately high frequencies, it will have an advantage up to the maximum frequency at which the circuit is used. The principles outlined already apply over the whole range of communication frequencies. Where shielding is found to result in frequency limitations, it is due to the added admittance introduced with it and not due to inherent defects in the principles involved.

The shielding may, in special cases, limit the maximum frequency at which the circuit will operate; but in such cases it can usually be taken for granted that even if the circuit would operate at higher frequencies without shielding, the accuracy of the results would be highly questionable. Examples of limitations of shielding may be given using the apparatus already described. Take the case of the resistor shown in Fig. 5. The admittance across the resistances results in objectionably high phase angles and an effective change in the resistances at very high frequencies. While this effect would be present even though no shielding were used, the shielding increases it and therefore limits the maximum frequency at which the apparatus can be used from the standpoint of this type of error. The same limitation occurs in the case of the inductance standards only it is more serious due to the large physical size of these standards. The exact type of limitation here is that the individual units increase in inductance due to the admittance across them to such an extent that the difference between them cannot be bridged by the next lower decade, thus rendering it impossible to obtain certain values of inductance by any dial combination.

In the case of a symmetrical bridge the principal limitation is the shunting effect of the admittance introduced across the impedance arms. This becomes so large that, at frequencies in the order of 100 kilocycles, difficulties are encountered in measuring the current through the unknown impedances by the method of measuring the total current input to the bridge. If the meter question is eliminated, the actual loss in sensitivity, which is the only other objectionable feature of this admittance, may be made of no serious consequence up to frequencies as high as 2,000 kilocycles. In all other respects, the shielding functions as satisfactorily at this frequency as at the ower frequencies.

Auxiliary Equipment

While auxiliary apparatus such as oscillators and detectors is not strictly speaking measuring apparatus, its operation is essential to the satisfactory operation of the measuring circuit and so a few words may be added regarding the shielding of this apparatus.

Provided they are separated sufficiently from the measuring circuit and from each other, there is no need to shield the oscillator or detector from the standpoint of operation of the measuring circuit. However, for maximum flexibility it is desirable that they be so constructed that no special precautions are necessary in placing them relative to the measuring circuit. If, as is usually done, the individual apparatus included in these circuits is adequately shielded it is only necessary to place the completed equipment in an electrostatic shield to avoid all coupling to the measuring circuit or from one to the other. This is usually done by mounting the apparatus on a metal panel and placing it in a wood box with a sheet metal lining. By this means it is possible to place the auxiliary apparatus as close to the measuring circuit as desired, without introducing errors.

As far as the internal shielding of the auxiliary apparatus is concerned, the same rules hold as for other apparatus described. However, in the case of vacuum tube equipment, wherever any gain is introduced, coupling between parts of the circuit must be reduced in proportion to the gain introduced between these parts. This is usually accomplished quite readily by suitable mechanical design and may be insured by placing each stage in a separate grounded shield, although this is seldom necessary.

Conclusion

It has been impossible to go into very great detail in this brief paper on the subject of shielding. The attempt has been made, therefore, to outline a few general rules and to give representative examples of typical measuring circuits. It will be noted that the examples have been limited largely to the bridge circuit. This is because our experience has shown that this circuit is the most flexible and accurate over the whole of the frequency range over which precise impedance measurements have been made, and because the problems of shielding it are sufficiently difficult and varied to give satisfactory examples of the solution of rather complicated problems. The principles of shielding given have been found to apply equally well at all frequencies and it has been found that up to the maximum frequency at which precision measurements have been made, the shielding methods developed for use with moderate frequencies require practically no modification as the frequency is increased. Experience with measurements and measuring circuits up to 2,000 kilocycles makes it appear probable that when precision measurements are made at still higher frequencies, the shielded bridge circuit will continue to remain the most satisfactory measuring circuit.

Fatigue Studies of Non-Ferrous Sheet Metals[1]

By JOHN R. TOWNSEND and CHARLES H. GREENALL

The paper describes the development of a fatigue test machine for sheet metals and gives results of fatigue tests on five alloys of alpha brass, one alloy of nickel silver, one alloy of phosphor bronze and Everdur.

The results indicate that cold work raises the endurance limit but not proportionally to the increase in tensile strength produced by the same cause.

Micrographs are shown indicating that fatigue failure of the metals investigated is transcrystalline.

Dispersion hardening of alpha brass by nickel silicide increases the endurance limit.

The ratio of endurance limit to ultimate tensile strength of these alloys varies from .12 to .36 depending on composition, heat treatment, and cold work. These ratios are much lower than similar ratios for steel.

THE materials referred to in this paper are those non-ferrous sheet metals that are employed in electromechanical devices such as telephone apparatus and includes a wide variety of equipment, such as switches, relays, jacks, contact springs,[2] etc. These metals are employed principally in springs used for electrical contacting purposes. In many cases these springs have precious metal contacts welded to them and in other cases the metal itself is used for the contact. Many of these springs are subjected to millions of cycles of stress and it is important, therefore, that the endurance limit of these materials be known in order that apparatus may be designed which will endure for its required service life. Very little precedent has been established in the design of fatigue machines for the testing of sheet metals and it was necessary, therefore, to develop a form of fatigue machine especially suitable for these materials.

Another joint paper by one of the authors describes these non-ferrous metals and explains various methods of test and the commercial limits developed for specification purposes.[3]

Sheet Metal Fatigue Specimen

The specimen shown by Fig. 1 was designed to simulate in its major dimensions the normal size of the springs used in telephone apparatus. It will be noted that the design of the specimen provides a section of uniform stress for 3/8 inch at approximately 1/2 inch from the clamped end of the specimen. This is accomplished by

[1] Presented before A. S. T. M. Convention, June 24–28, 1929.

[2] "Telephone Apparatus Springs," by John R. Townsend: *Proceedings A. S. M. E.*, 1928; *Bell System Technical Journal*, April, 1929.

[3] "Mechanical Properties and Methods of Test for Sheet Non-Ferrous Metals," by J. R. Townsend, W. A. Straw and C. H. Davis, presented before A. S. T. M. Convention, June 24–28, 1929.

designing a cantilever beam that will have a uniform bending moment for part of its length. The dashed lines indicate the shape of a beam of uniform bending moment; the heavy lines show the final shape of the specimen and how the portion of uniform bending moment has been connected by means of fillets. This is essential in order to eliminate the possibility of the clamping stresses affecting the applied stress as would be the case if a uniform rectangular cantilever beam specimen had been employed. The specimen is deflected at a point ½ inch from the operated end or, in other words, where the hypothetical beam of uniform bending moment terminates.

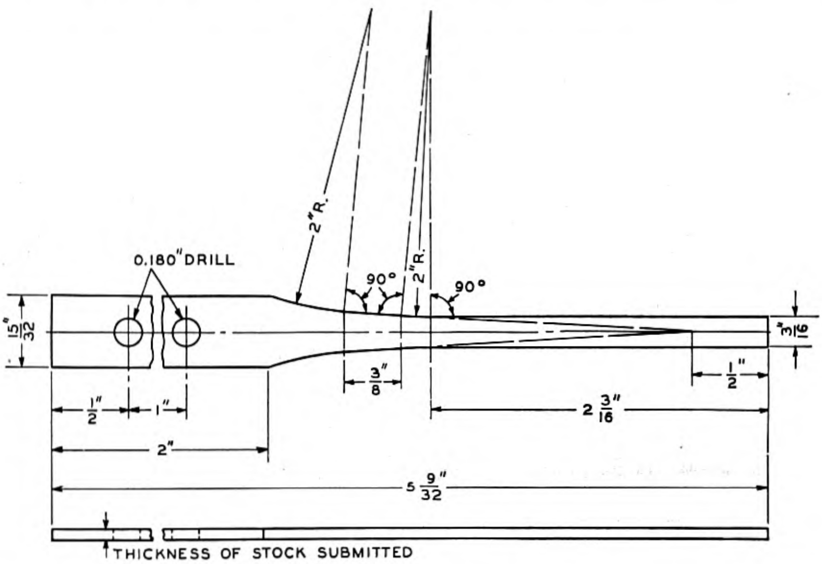

Fig. 1—Sheet Metal Fatigue Specimen.

The specimens are prepared by blanking rectangular samples which are clamped together and then cross milled with a form milling cutter in a manner similar to that described elsewhere for the preparation of tensile specimens.[4] The specimens were cut with the direction of rolling parallel with their length.

Sheet Metal Fatigue Machine

Referring now to Fig. 2, it is seen that the specimens (*S*) are clamped between phenol fiber blocks (*B*). This is done in order that reasonably rigid material will be provided and at the same time a material

[4] "Methods for Determining the Tensile Properties of Thin Sheet Metals," by R. L. Templin. *Proc. A. S. T. M.*, Part II, Vol. 27 1927.

sufficiently dissimilar to the metal to accomplish good clamping without scoring the surface of the clamped portion. Furthermore, the use of the phenol fiber blocks provides a means of automatically recording the breaking of the specimen since the specimen is insulated from the machine and may be employed to break an electrical monitoring circuit. The deflected end of this specimen is held between two fingers ($F_{1.2}$) which have a vertical cylindrical half section. The cylindrical portion is in contact with the specimen. This is necessary in order to compensate for the angular movement of the reciprocating arm (A) in relation to the specimen. One of these fingers (F_1) is fixed and the other is movable (F_2) but bears against the specimen with

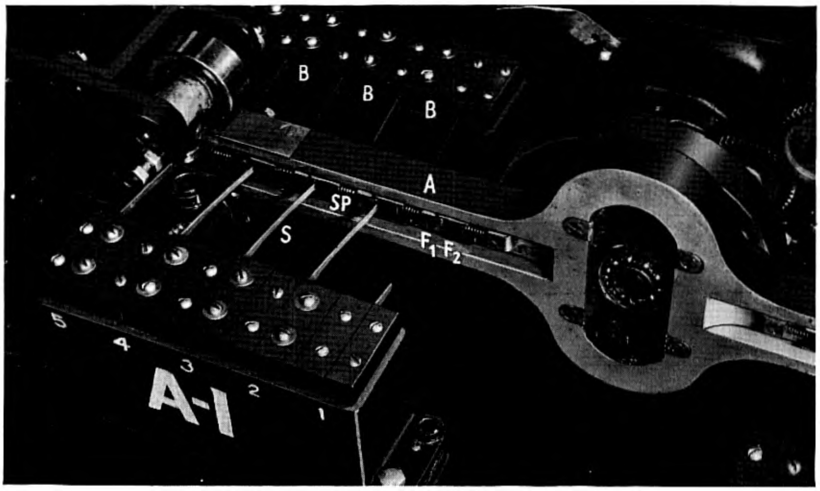

Fig. 2—Sheet Metal Fatigue Machine.

a tension provided by compression spring (S_p). This permits some slight movement of the specimen in relation to the fingers which is necessary by reason of the change in free length of the specimen as the reciprocating arm moves backward and forward. The deflection of the specimen is determined in two ways, first by measuring the movement of the reciprocating bar and also by observing the specimen in operation by means of a stroboscope. In this way the static and dynamic deflection of the specimen may be measured and for all practical purposes, these have been found to be the same within the range of deflection and speed used in this investigation.

The speed of the machine is approximately 1,500 r. p. m. It is necessary to adjust the speed of the machine to the material under test since if this is not done the machine may be operated near the

TABLE I

AVERAGE CHEMICAL ANALYSIS OF MATERIALS

Material *	Alloy	Copper	Lead	Iron	Zinc	Nickel	Manganese	Tin	Phosphorus	Silicon	Combined Carbon
[1] High Brass		65.09	0.02	0.03	Balance			0.00			
[1] Alloy "G" Brass		71.73	0.02	0.03	"	0.01					0.018
[1] Nickel Silver		55.23	0.005	0.06	"	18.38	0.11				
[1] Phosphor Bronze		91.84	0.02	0.03	0.00	0.00		8.08	0.03		
[1] Everdur		96.00							3.00	1.00	
Hardened Brass	33	Balance			9.89	2.32				.57	
	34	"			19.89	2.37				.57	
	35	"			30.12	2.36				.66	

* No graphite was present in any of the materials.
[1] Material and Analysis furnished by C. H. Davis, American Brass Co.

TABLE II

PHYSICAL PROPERTIES

Material	Heat Treatment	B & S Nos. Hard	Tensile Strength Psi	P Limit Psi	Mod. of Elasticity Psi × 10^6	% El. in 2″	Rockwell Hardness* 1/16″ Dia. Ball Red Figures	Endurance Limit Psi	Ratio Endurance Limit Ult. Tensile Strength
High Brass	600° C. Anneal	0	46,600	13,000	14.5	56	16	12,000	25.7
		4	77,200	32,000		6	79	13,500	17.5
		10	95,000	30,000		2	87	15,000	15.7
Alloy "G" Brass	600° C. Anneal	0	46,300			61	16	12,000	25.9
		4	81,600			6	84	18,000	22.0
		10	97,800			2	92	20,000	20.5
Nickel Silver		0	66,900			42	19	14,000	36.0
		4	98,700			2	69	18,500	17.4
		10	116,200	60,000	20	1.5	79	22,000	18.9
Phosphor Bronze		0	59,700			67	11	21,000	35.2
		4	95,500			14	71	22,000	23.0
		10	124,800	55,000	15	2	84	24,500	19.6
Everdur	"Spring Temper"		80,000	26,000	12.4	22	91	24,000	30.0
Hardened Brass Alloy No. 33	Quenched 800° C. aged 1 hour at 500° C.		90,000	44,500	19.8	14	86	14,000	15.5
Alloy No. 34	Quenched 850° C. aged 1 hour at 500° C.		85,800	37,200	17.2	21.5	85	12,500	14.6
Alloy No. 35	Quenched 800° C. aged 1 hour at 400° C.		85,400	38,000	16.5	28.0	79	16,000	17.3

* 100 kg. load for brass alloys and 150 kg. load used for nickel silver, phosphor bronze and Everdur.

natural frequency of vibration of the specimen and this may superimpose additional stresses upon it. This is determined by observing the operation of this specimen by means of a stroboscope and accurately setting the speed of the machine to a point where the vibratory motion of the specimen is uniform.

The machine has a capacity of forty specimens. Twenty specimens are tested on each end of the motor drive. The machine is statically balanced and is smooth in operation. It is customary to test at least five specimens of each material at each stress. The machine therefore, has a capacity of four alloys of five specimens each at two deflections. The practice of using five specimens for each deflection was adopted because it was seen from the results of previous experimenters in fatigue testing that a more accurate result might be provided by doing so. The capacity of the machine is sufficiently large to permit this being done.

Materials

The materials investigated consisted of five alloys of alpha brass, three of which had been hardened with nickel silicide and one alloy each of nickel silver, phosphor bronze and Everdur. The three alloys of hardened brass have been described previously.[5]

The chemical composition of these alloys is given in Table I and the tensile strength, proportional limit, modulus of elasticity, per cent elongation in 2 inches, Rockwell hardness and endurance limit are given in Table II. The heat treatments and amount of cold work expressed by number of B. & S. gauge reductions from standard anneal are shown also on Table II.

Fatigue Endurance Test

Method of Determining Stress in Specimen

The method of determining the stress in the specimen consists in clamping a specimen in the same manner as on the fatigue machine. The clamped specimen is mounted on the table of a Société Genevoise Star Comparator so that its large surfaces are parallel with the vertical plane, the axis being parallel to the table. By mounting the specimen in this manner its weight has no appreciable effect on its deflection. The stress in the specimen is determined from the load deflection curve obtained by applying dead weights ½ inch from the end of the specimen and measuring the amount of deflection for various units of load by means of a microscope mounted on the comparator in such a

[5] "Heat Treatment and Mechanical Properties of some Copper-Zinc and Copper-Tin Alloys Containing Nickel and Silicon," by W. C. Ellis and Earle E. Schumacher. *Proc. A. I. M. M. E.*, 1929.

manner that the rectangular coordinates of the deflected specimen may be read on the micrometer heads. Readings were taken to 1 micron. The stress per unit deflection is then calculated from the formula

$$S = \frac{6Pl}{bd^2},$$

where S = stress in pounds per square inch,
P = load in pounds,
l = length in inches,
b = width in inches,
d = thickness in inches.

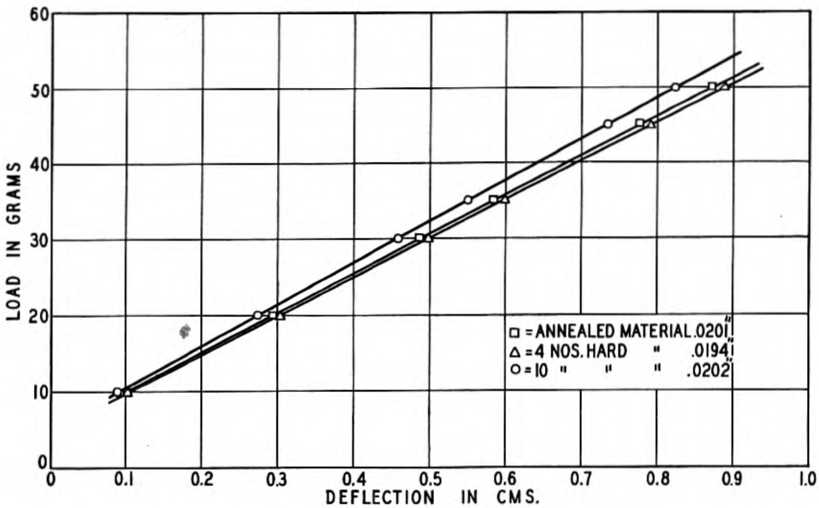

Fig. 3.—Relation of Load to Deflection, Alloy G Brass, No. 24 B. & S. Gauge.

The curve shown by Fig. 3 for alloy "G" brass sheet gives the load for uniform deflection of the specimen upon the fatigue machine. The various stresses are then obtained by varying the amount of deflection of the end of the specimen by adjustment of the roller bearing that operates the reciprocating bar.

Fatigue Endurance Results

The curves shown on Fig. 4 are for high brass sheet annealed and rolled four and ten numbers hard. Figs. 5, 6, 7 and 8 give similar results for alloy "G" brass, nickel silver, phosphor bronze and Everdur respectively for annealed material and rolled four and ten B. & S. gauges numbers hard. Fig. 9 gives the fatigue results for the alpha

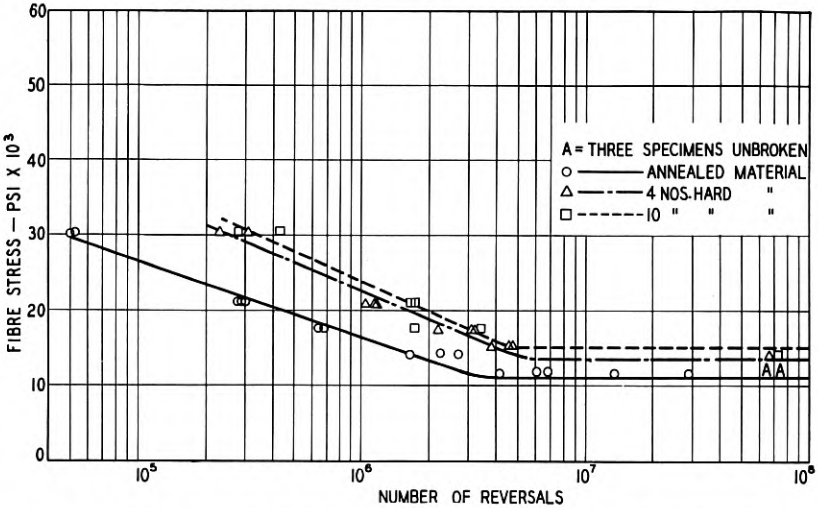

Fig. 4—Relation of Fibre Stress to Reversals, High Brass Sheet, No. 24 B. & S. Gauge.

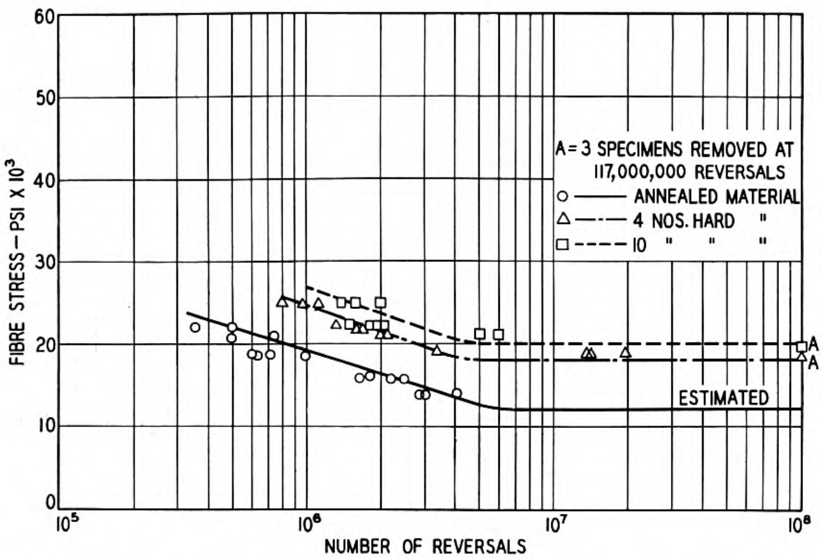

Fig. 5—Relation of Fibre Stress to Reversals, Alloy G Brass Sheet, No. 24 B. & S. Gauge.

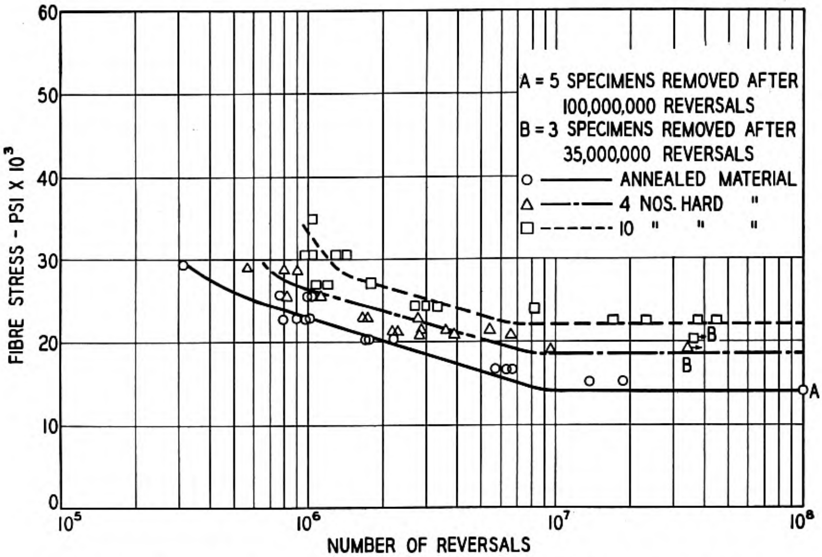

Fig. 6—Relation of Fibre Stress to Reversals, Alloy B Nickel Silver, No. 24 B. & S. Gauge.

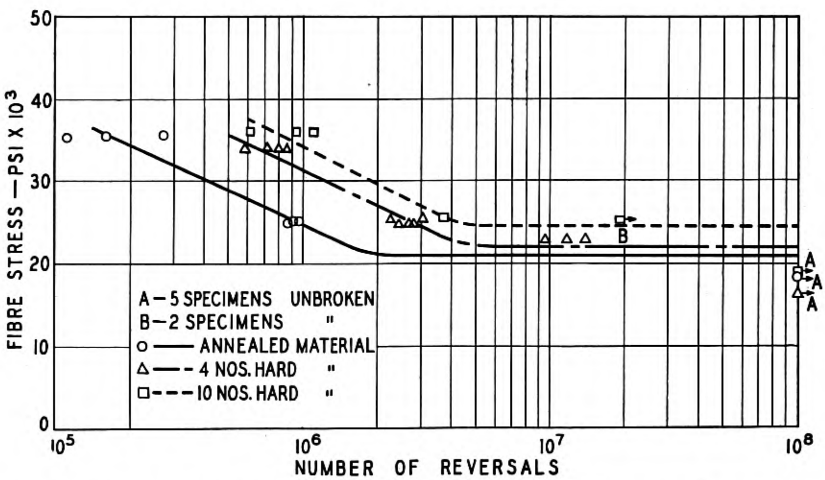

Fig. 7—Relation of Fibre Stress to Reversals, Alloy C Phosphor Bronze, No. 24 B. & S. Gauge.

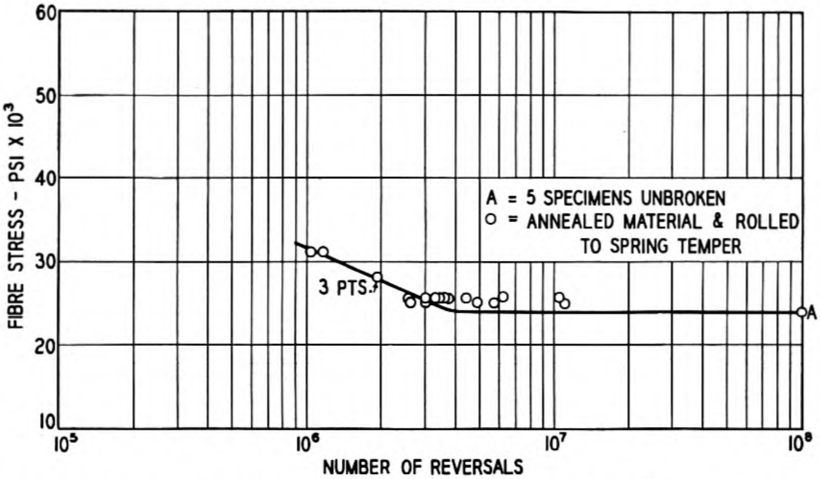

Fig. 8—Relation of Fibre Stress to Reversals, Everdur Alloy Spring Temper, No. 24 B. & S. Gauge.

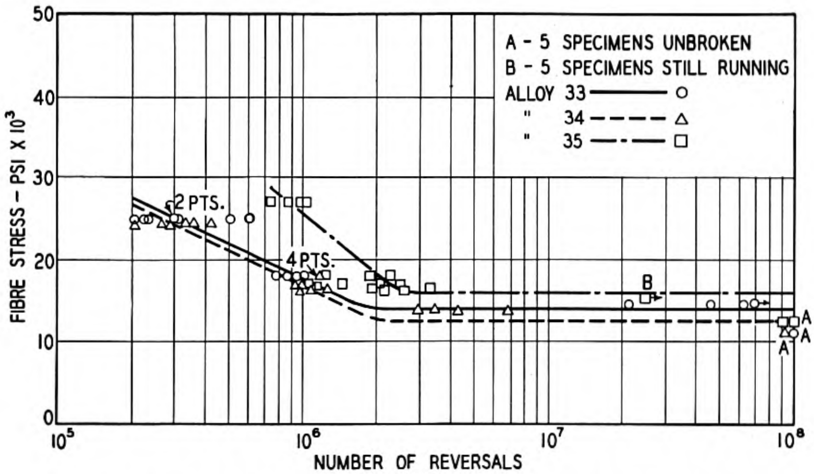

Fig. 9—Relation of Fibre Stress to Reversals, Dispersion Hardened Brasses, Alloys Nos. 33, 34 and 35, No. 24 B. & S. Gauge.

brasses hardened by nickel and silicon otherwise mentioned as alloys Nos. 33, 34 and 35 respectively.

Microstructure

Fig. 10 shows a photograph of a number of broken specimens. The regularity of the break is shown and in every case occurs within the uniformly stressed area. Photomicrographs shown by Fig. 11 are typical of the various alloys. In these cases incipient cracks are revealed within the uniformly stressed area. It is seen that these cracks are, without exception, transcrystalline and there

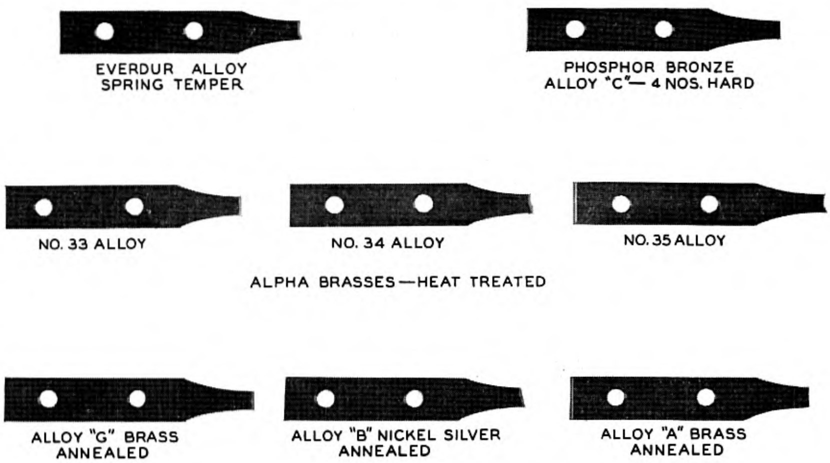

Fig. 10—Typical Broken Fatigue Specimens.

appears to be no distortion of the metal adjacent to the fractures. With regard to the typical structure of the hardened brass alloys reference is made to the previous paper.[6]

Discussion

Examination of the results shown by Table II reveals that the ratio of endurance limit to tensile strength for sheet non-ferrous metals is much lower than that reported for steel rod.[7] These ratios reported for plain carbon and alloy steels in all heat treatments vary from .35 to .67 averaging about .40 whereas for these sheet non-ferrous metals these ratios vary from .14 to .36.

[6] "Heat Treatment and Mechanical Properties of some Copper-Zinc and Copper-Tin Alloys containing Nickel and Silicon," by W. C. Ellis and Earle E. Schumacher. *Proc. A. I. M. M. E.*, 1929.

[7] "The Fatigue of Metals," by H. J. Gough, Scott Greenwood & Sons. Also "The Fatigue of Metals," by H. F. Moore and J. B. Kommers, McGraw Hill & Co.

A

B

C

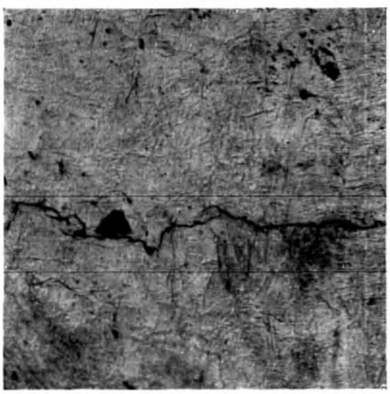

D

E

Fig. 11—Photomicrographs of Fatigue Specimens.

A. Nickel-Silver, 4 B. & S. Nos. Hard, Stress 28,750 Psi, 800,000 cycles, mag. 200.
B. Phosphor Bronze, 4 B. & S. Nos. Hard, Stress 25,500 Psi, 2,600,000 cycles, mag. 200.
C. Alloy G Brass, Annealed, Stress 15,750 Psi, 2,471,200 Cycles, Mag. 200.
D. Everdur, Spring Hard, Stress 25,500 Psi, 1,186,900 Cycles, Mag. 200.
E. Hardened Brass Alloy No. 33, Stress 18,200 Psi, 850,000 Cycles, Mag. 200.

Prepared by Miss A. K. Marshall

The improvement in the endurance limit due to cold rolling brass, nickel silver and phosphor bronze is not consistent with the increase in tensile strength produced by the same means. This is shown by Table II where in practically every instance material hardened by cold work shows a progressive decrease in the ratio of endurance limit to tensile strength.

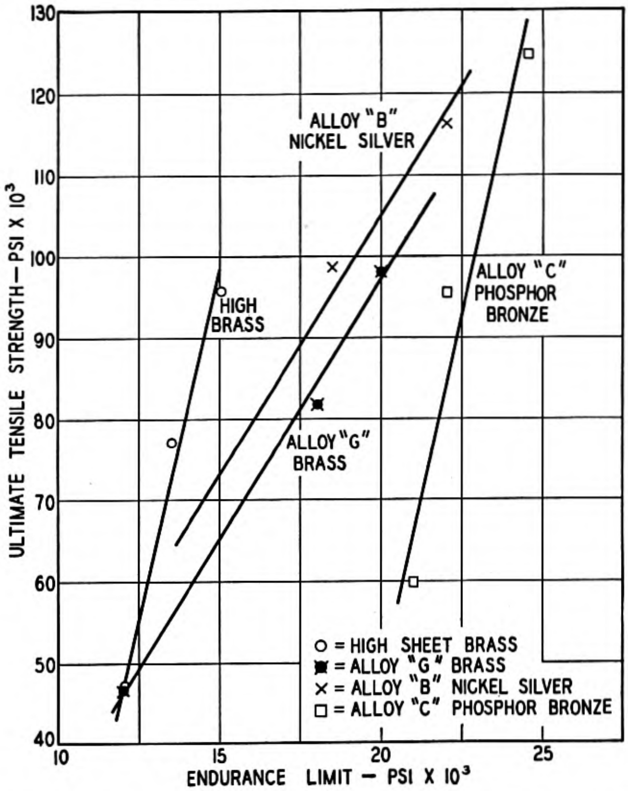

Fig. 12—Relation of Ultimate Tensile Strength to Endurance Limit, No. 24 B. & S. Gauge, Non-Ferrous Sheet.

Previous investigators have shown a close correlation between endurance limit and tensile strength for iron and steel. Fig. 12 fails to reveal such a general correlation for the sheet metals under test. For a particular alloy, however, there appears to be a progressive increase in endurance limit with increase in tensile strength due to cold work but the slope of the curves shown are widely different for the various alloys.

The results for alloy "G" brass and high brass show the effect of change in composition on the endurance limit. The greater improvement in fatigue endurance of alloy "G" brass due to cold work over high brass shows the superiority of this alloy for spring purposes. This was to be expected on the basis of its physical properties.[8, 9]

Alpha brass hardened by nickel and silicon shows considerable improvement in the endurance limit and also an improvement in the ratio of endurance limit to tensile strength. This offers a means whereby some non-ferrous alloys may be improved in this respect.

Attention is called to Fig. 6 which gives the stress cycle graphs for nickel silver in three tempers. It will be noted that the curves tend to turn sharply upward for the higher stresses. This indicates the effect of drastically overstressing the metal. The authors have observed this effect with other metals on the rotating beam machine. It seems that after a limiting stress value that the number of cycles to failure tends to become constant.

Conclusion

From the test results obtained on these non-ferrous metals it is seen that the fatigue endurance limit varies from approximately 12 to 36 per cent of the ultimate tensile strength, whereas the commonly accepted ratio of fatigue endurance to tensile strength of steel is in the neighborhood of 40 per cent of its ultimate tensile strength. In other words, it appears that the low endurance limit of these materials emphasizes the need for their careful selection for use as springs. High tensile strength or proportional limit are not sufficient guarantors that the material will perform satisfactorily in service.

Cold work raises the endurance limit but not in a manner proportional to the increase in tensile strength produced by the same cause. There is no correlation between tensile strength and endurance limit except for cold worked metal of a definite composition. For other compositions the correlation is different.

Precipitation hardening of alpha brass by nickel silicide increases the endurance limit.

The fatigue failure appears to be a result of a fracture across the crystals of the material. Photomicrographs are given showing incipient cracks that were developed in the uniformly stressed areas of the specimen.

[8] "Physical Characteristics of Copper and Zinc Alloys," Bassett and Davis. *Proc. Inst. Metals Div. A. I. M. M. E.*, 1928.

[9] The authors are indebted to Mr. L. E. Abbott for his assistance in obtaining laboratory data.

The curves given for fatigue endurance show the results for each specimen tested. The shape of the fatigue endurance curve for these metals is similar to those published previously for other metals.

A special form of fatigue machine has been developed to test sheet metals. This machine will accommodate forty specimens. Capacity is thereby provided so that as many as five specimens may be employed for each of four materials at two deflections under test.

An Application of Electron Diffraction to the Study of Gas Adsorption

By L. H. GERMER[1]

Under appropriate experimental conditions, electron scattering by a single crystal of nickel can give rise to diffraction patterns of four quite distinct types. We attribute one of these patterns to the space lattice of the nickel crystal, one to the topmost layer of nickel atoms, one to a monatomic layer of adsorbed gas atoms, and one to a thick layer of gas atoms. From these phenomena some conclusions concerning gas adsorption have been drawn. We have at hand a new and important method of crystal analysis.

IN the paper by Dr. C. J. Davisson and myself entitled "Diffraction of Electrons by a Crystal of Nickel,"[2] we published a variety of information concerning the gaseous contamination of the surface of our diffracting crystal. This information was obtained from a study of the modifications produced by adsorbed gas in the electron diffraction pattern. We have subsequently succeeded in obtaining some additional facts concerning adsorbed gas from a further study of our original data. Along with the presentation of these new facts, I am taking this opportunity to publish in greater detail the data upon which our original conclusions were based.

In our Physical Review paper we showed that the interaction of a beam of electrons with a single crystal of nickel gives rise to phenomena which, in their most essential characteristics, are similar to the diffraction phenomena which would be observed if the beam of electrons of adjustable speed were replaced by a beam of X-rays of adjustable wave-length. The diffraction patterns produced by electron scattering are, however, substantially more complicated than would be the corresponding X-ray diffraction pattern. We showed that electron scattering can give rise to diffraction phenomena of four quite distinct types. The diffraction patterns of two of these types arise from the nickel atoms in the crystal lattice, while the diffraction patterns of the other two types have their origins in the layer of gas adsorbed upon the surface. The relative intensities of the diffraction patterns of these four types are determined by the amount of gaseous contamination on the surface of the crystal, and also by the temperature of the surface.

The first publication of our discovery of electron diffraction was contained in a note in "Nature."[3] At the time of this first paper we had already discovered two of these types of electron diffraction, and had distinguished sharply between them. The first type, which we later

[1] Translation from "Zeitschrift für Physik," April 12, 1929, pp. 408–421.
[2] C. J. Davisson and L. H. Germer, *Phys. Rev.*, 30, 705 (1927).
[3] C. J. Davisson and L. H. Germer, *Nature*, 119, 558 (1927).

found to be predominant under all conditions, was the normal diffraction from the space lattice of the nickel crystal. The diffraction pattern of this type is analogous to a Laue X-ray pattern produced by the interaction of a beam of heterogeneous X-rays with a single crystal. The second type of diffraction pattern consisted of a curious but very simple assemblage of twelve electron diffraction beams which, at the time of their discovery, we designated "anomalous beams."

At the time of publication of the note in "Nature" the nickel crystal, with which we were experimenting, had not been heated after the bulb containing it was sealed from the pumps. Subsequently the crystal was heated many times by electron bombardment. The effect of these heatings was to destroy the diffraction pattern of the second type, made up of the so-called anomalous beams, and to intensify greatly the first type of diffraction pattern. Simultaneously patterns of two entirely new types appeared for the first time. These new diffraction patterns were comparatively short-lived. Both of them disappeared completely within a few hours after heating the crystal. After its initial increase in intensity, following such a heating, the diffraction pattern of the first type also became weaker with the passage of time, but at a rate very much less rapid than the rate at which these new patterns changed. After the lapse of some days the diffraction pattern of the second type was again found. At first the beams of this pattern could barely be detected, but they became progressively stronger as the diffraction pattern of the first type became weaker.

Experiments more or less similar to the experiment just described were performed many times. After the initial heating of the crystal the rapidity of occurrence of the changes in the diffraction patterns varied greatly, from one experiment to another. These changes occurred very slowly when the experimental conditions were such as to warrant the belief that the vacuum in the experimental tube was unusually high. The changes took place much more rapidly when the vacuum was known to be comparatively poor. We concluded that the changes in the diffraction patterns which were observed following a heat treatment of the crystal were caused by gas being gradually adsorbed upon its surface. The two new types of diffraction pattern must arise from a clean or nearly clean surface, and their complete disappearance seemed conclusive evidence that the surface had become covered by at least one layer of gas atoms.[4] The diffraction pattern of the first type was weakened only slightly at the time of their disap-

[4] We have not obtained any information regarding the nature of the adsorbed gas. In referring to this gas the word "atom" has been used to mean either atom or molecule.

pearance, and we therefore concluded that at the time when this pattern was itself greatly weakened the surface of the crystal was covered by *many layers* of gas atoms. Furthermore, we were able to conclude that the diffraction pattern of the second type had its origin in the film of adsorbed gas, and that *many layers* of gas were necessary for its formation.

In Figs. 1–4 are exhibited polar plots of typical electron diffraction beams belonging to the diffraction pattern of the first type. The curves of these figures show the effect of gaseous contamination of the crystal

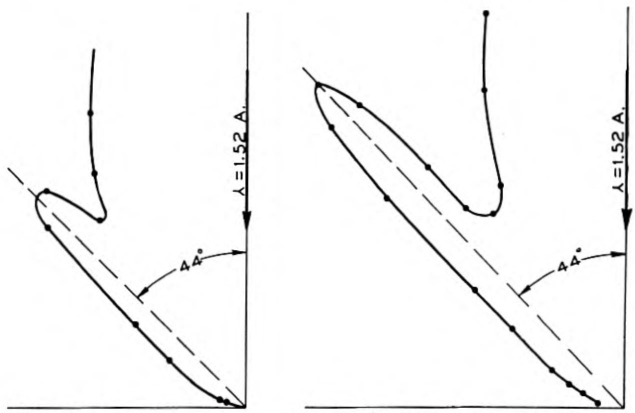

FIG. 1—Showing the effect of the removal of surface gas upon the intensity of the electron diffraction beam whose Miller indices are (422)

surface upon the intensities of diffraction beams arising from the space lattice of the crystal. In these figures the electron diffraction beams have been designated by their Miller indices in accordance with the conventional X-ray nomenclature. Since the refractive index of nickel for electron waves differs from unity by a quite appreciable fraction, in the wave-length range of our experiments, a knowledge of the values of this index was necessary before these Miller indices could be assigned. This knowledge has been supplied by our experiments [5] on electron reflection. (Although Bethe [6] and others deduced refractive indices correctly from the data which we published in the Physical Review (loc. cit.) and assigned the correct Miller indices to the diffraction beams which we observed, these deductions seem to us to have rested upon a rather inadequate experimental basis.)

[5] C. J. Davisson and L. H. Germer, *Proc. Nat. Acad. Sci.*, 14, 619 (1928).
[6] Bethe, *Naturwissenschaften*, 16, 333 (1928).

disappearance of X-ray diffraction beams under similar conditions. In other words, the wave-length resolving power of the crystal is not so good for electron waves as for X-rays of comparable wave-lengths. This is due to the fact that the penetration of electron waves into the metal is very much less than the penetration of X-rays of the same wave-length.[7]

It is, of course, just this slight penetrating power of electron waves which made the diffraction patterns arising from our nickel crystal sensitive to the presence of adsorbed gas, and caused the extraordinary complexity in the observed phenomena. The circumstance, that electron waves are scattered very efficiently by the surface atoms of the crystal and are consequently extinguished on penetrating into the crystal at a very rapid rate, opens up to us the possibility of the use of electron diffraction as a means of studying surfaces.

The first application of this new method of surface study was the analysis (*Phys. Rev.*, loc. cit.) of the two transient diffraction patterns which existed for only a short time after the crystal surface was cleaned by heating. The first of these patterns to appear after the heating was found as soon as the crystal was comparatively cool. This pattern I shall refer to as the electron diffraction pattern of the third type. It consisted of electron beams emerging near to grazing the surface in the principal azimuths of the crystal, occurring in each azimuth just as if the surface of the crystal were a plane diffraction grating. For each diffraction beam the grating constant was equal to the separation between the rows of atoms on the surface of the crystal normal to the azimuth of the beam. Figures showing beams of this type in the principal crystal azimuths were exhibited in our original paper (loc. cit., Figs. 14–16).

The change in intensity with time of a typical beam of this third type after the crystal surface was cleaned by heating is shown by the curve marked "Type-3" in Fig. 5. (The crystal was not cool until nearly twenty minutes after the heating.) From the positions of these "plane grating" (Type-3) beams near to grazing the crystal surface and from their behavior with time after the surface was cleaned, we concluded that, when the beams of this type were most intense, the crystal surface was completely free from adsorbed gas. We concluded also that, until these beams had become quite weak, the surface was not covered by so much as a single layer of gas atoms. The condition,

[7] The lower curves in Fig. 3 represent the data from which we calculated (*Phys. Rev.*, loc. cit.) the rate of extinction of 54 volt electrons ($\lambda = 1.67$ A.) on penetrating into the metal. A similar calculation cannot readily be made from the data of the lower curves in Fig. 4. These matters were considered in detail in our original paper and need not be discussed here.

which we recognize as a completely clean condition of the crystal surface, could be produced by a comparatively mild heating, to a temperature roughtly estimated to be about 900° C. The conclusion that such a mild heating was sufficient to clean the surface completely is of interest, as it appears to be in disagreement with similar evidence concerning gas on surfaces obtained from photoelectric and thermionic measurements.

Transient electron diffraction beams of another type appeared some time after the crystal had become cool following a heating. These beams constitute what I shall call the electron diffraction pattern of the

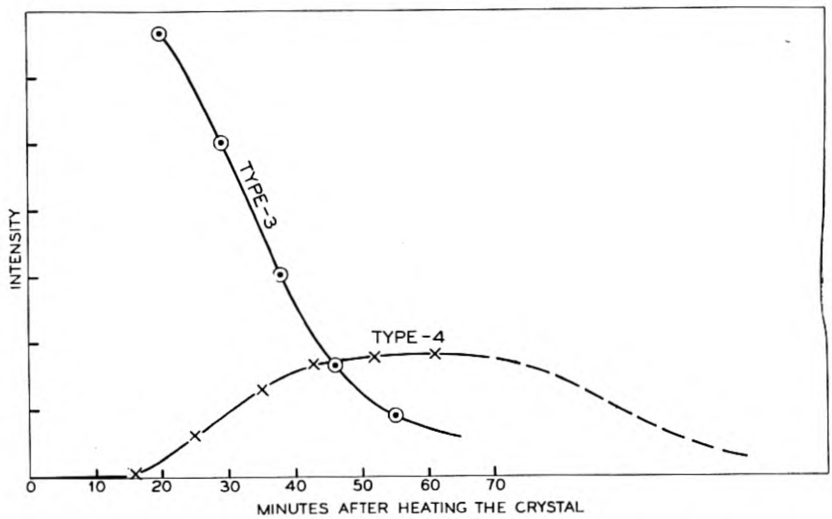

FIG. 5—Change in intensity of a typical "Type-3" beam and of a typical "Type-4" beam as gas settled upon a clean crystal surface. Measurements of the intensities of these two beams were made alternately over a period of an hour.

fourth type. They could not be detected until the diffraction pattern of the third type had become appreciably weakened, and did not attain their maximum intensities until the pattern of the third type had almost disappeared. The curve marked "Type-4" in Fig. 5 shows the life history of a typical beam of this type following a heat treatment of the crystal. In this particular experiment intensity measurements were not made after sixty-one minutes. The dashed continuation of the curve represents its general course as known from other experiments.

The two curves of Fig. 5 represent a single experiment which was carried out at a time when the vacuum condition of our experimental apparatus was intermediate between the best and the worst conditions which we were able to realize. Under our best vacuum conditions, the intensity changes took place more than twenty times more slowly than the changes shown in Fig. 5, and under our poorest vacuum conditions they took place so rapidly that the diffraction patterns of the third and fourth types could not be found.

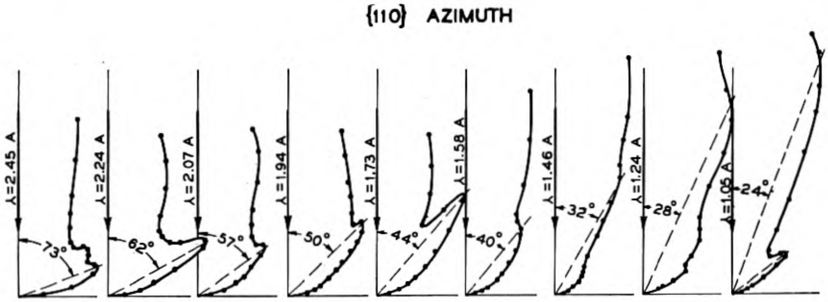

FIG. 6—Scattering curves in a (110) azimuth of the crystal showing the transient electron diffraction beams of the fourth type. On each arrow indicating the primary beam is printed the wave-length of the electrons giving rise to the curve.

The entire diffraction pattern of the fourth type is exhibited by the curves of Figs. 6–8.[8] These figures show a series of electron scattering curves in each of the principal azimuths of the crystal. When these

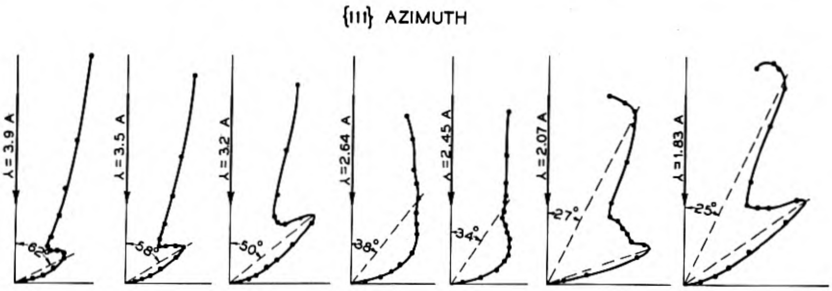

FIG. 7—Scattering curves in a (111) azimuth showing electron diffraction beams of the fourth type

curves were taken, the crystal surface was in the transient gas-covered condition corresponding to the maximum of the "Type-4" curve shown in Fig. 5. The vacuum condition of the apparatus was so good at this

[8] It will be remembered that we were bombarding normally a (111) face of a nickel crystal. Each azimuth of the crystal we designated by the Miller indices of the densest plane of atoms the normal of which lies in the azimuth and in or above the surface of the crystal. Diffraction beams were found only in the three most important azimuths, the designations of which are the (111) azimuth, the (100) azimuth, and the (110) azimuth. (Other azimuths were explored without finding diffraction beams.)

time that the intensities of the beams shown in these figures remained sensibly unchanged for several hours.

The scattering curves near the right-hand ends of these three figures show weakened diffraction beams of the third type, which we recognize readily. The curve second from the right in Fig. 8 shows also a diffraction beam of the first type, a beam arising from the space lattice of the nickel crystal. This is a (311) reflection according to X-ray terminology. The other electron beams shown in Figs. 6–8 can be most easily considered by correlating the wave-length of each beam with the sine of its co-latitude angle. This is the procedure which was followed in Fig. 17 of our original paper in considering the diffraction beams of the *first* type. (Loc. cit. Fig. 17.) Fig. 9 is

{100} AZIMUTH

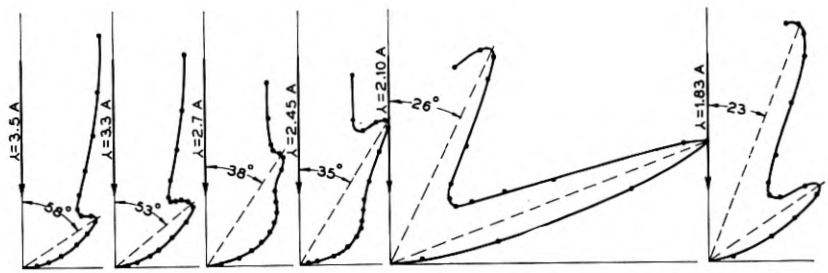

FIG. 8—Electron diffraction beams of the fourth type in a (100) azimuth

similar to Fig. 17 of the original paper. The diagonal lines in Fig. 9 are the plots in the various orders of the plane grating formula $n\lambda = d \sin \theta$, where in each azimuth the grating constant d is equal to the separation between lines of nickel atoms on the surface of the crystal normal to the azimuth. On this figure are plotted as dots all of the originally reported diffraction beams of the first type and as crossed circles the diffraction beams of the fourth type shown in Figs. 6–8.[9]

It is clear from Fig. 9 that the diffraction beams of the fourth type are "plane grating" beams of "one-half order." The obvious interpretation of the occurrence of such beams is that, for these beams, *the value of the grating constant is really 2d instead of d.*

It was known from the consideration of data similar to those shown in Fig. 5 that the diffraction pattern of the fourth type had its origin

[9] In Fig. 9 there is plotted a crossed circle for each of the separate curves shown in Figs. 6–8. In this respect the crossed circles of Fig. 9 are not similar to the dots. Each dot represents a diffraction beam of the first type *at its intensity maximum,* whereas the crossed circles represent all the beams of the fourth type which were found. The intensities of some of these were very small.

in a film of gas on the surface of the crystal, and that this film of gas was thin. The last figures show that this gas film consisted of only a single layer of atoms, and that these atoms were arranged in a crystalline structure similar to a parallel layer of nickel atoms but separated by distances twice as great as the separations of nickel atoms (*Phys. Rev.*, loc. cit., Fig. 20). This arrangement of gas atoms and surface nickel atoms is shown in Fig. 10.

Very interesting information was obtained by taking data similar to those represented in Fig. 5 with the crystal maintained slightly

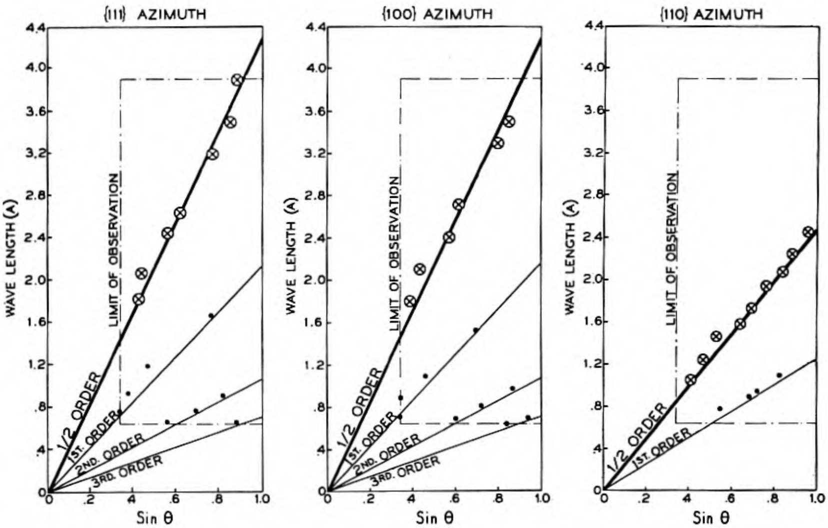

FIG. 9—Plots of the grating formulas in the principal azimuths of the crystal. Positions of electron diffraction beams of the fourth type are indicated by crossed circles and positions of beams of the first type by dots.

warm, at a temperature roughly estimated to be 150° C. For this slightly warm crystal the life history of a typical "Type-3" beam was substantially the same as that shown in Fig. 5. The "Type-4" beams, however, did not develop at all. We concluded that gas atoms settled upon the crystal when warm much the same as when cold, but that upon the warm surface they were unable to take up the regular arrangement which they assumed upon the cold surface. One is led to say that the temperature of 150° C. was above the melting point of the two dimensional "gas crystal." It would have been comparatively easy to have found out whether or not the gas crystal melted abruptly at some critical temperature, but this information was not obtained.

One of the most striking features of Figs. 6–8 is the marked change in intensity of the "Type-4" beams from one curve to another. In our original publication we pointed out a possible interpretation of these intensity differences. The data concerning these beams have now been more carefully studied, and it has turned out that this suggested interpretation gives quantitative results in agreement with the observations.

What we suggested was that the changes in the intensities of the "Type-4" beams were due to interference between the beams diffracted from the layer of gas atoms and the beams arising from the underlying

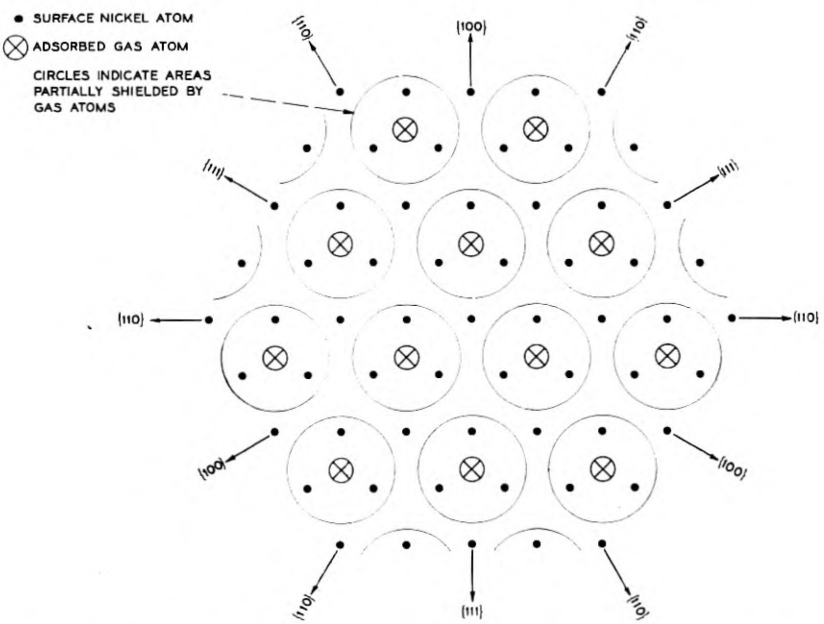

FIG. 10—The arrangement of gas atoms which gives rise to the "Type-4" diffraction beams. The designation of crystal azimuths is the one upon which the calculations of Table I are based.

nickel. That the nickel crystal can produce diffraction beams capable of interfering with the beams from the doubly-spaced layer of gas atoms arises from the fact that the gas atoms divide the surface nickel atoms into two classes. Three-fourths of the surface nickel atoms are adjacent to gas atoms and are presumably partially shielded by these atoms from the incident electron waves (Fig. 10). The other fourth of the nickel atoms on the surface, which are not so shielded, are arranged in a structure similar to that of the gas atoms and having the same scale factor. Thus it is that the surface layer of nickel atoms can give rise to differential diffraction beams capable of interfering with the "plane grating" beams from the gas atoms.

Believing that the intensity differences of the beams in Figs. 6–8 arise in this manner, one can hope to determine from the intensities of these beams the space relation existing between the layer of gas atoms and the surface layer of nickel atoms. In carrying out the plan of making this determination one naturally assumes a certain relative spacing, and upon this assumption calculates the wave-lengths (and angles) at which the diffraction beams from the gas layer are in phase with the differential beams from the surface nickel layer.[10] These wave-lengths are then compared with the wave-lengths in Figs. 6–8 at which the "Type-4" beams are found to be strong.

Calculations of this kind have been carried out, with the gas atoms placed as shown in Fig. 10, for each of a series of assumed separations between the plane of the gas atoms and the plane of the surface nickel atoms. In comparing the results of these calculations with the observations of Figs. 6–8, the azimuths are to be taken either as shown in Fig. 10 or with the (111) and (100) azimuths interchanged. As far as the first layer of nickel atoms is concerned the (111) and (100) azimuths are identical. When one must distinguish between these azimuths (as in Fig. 10), this distinction is equivalent to a certain definite location of the gas atoms relative to the *deeper layers* of nickel atoms. It turns out that, when the centers of the gas atoms are assumed to lie in a plane separated by 3.0 A. from the plane of the centers of the surface nickel atoms and when the azimuths are chosen as shown in Fig. 10, the calculated wave-lengths of the intensity maxima of the "Type-4" beams agree pretty well with the wave-lengths at which the beams are observed to become strong. These calculated wave-lengths of the intensity maxima are given in Table I.

TABLE I

Calculated Wave-lengths of the Intensity Maxima of "Type-4" Beams Assuming the Azimuth Designations of Fig. 10 and a Separation of 3.0 A. between the Plane of the Gas Atoms and the Plane of the Surface Nickel Atoms

(110) Azimuth (compare with Fig. 6)	(111) Azimuth (compare with Fig. 7)	(100) Azimuth (compare with Fig. 8)
2.20 A.	3.07 A.	3.53 A.
1.72	2.10	2.36
1.38	1.57	1.72
1.13		
0.96		

[10] One does not, of course, obtain in this simple manner the intensities of the diffraction beams, but one does obtain the positions and wave-lengths at which these beams reach intensity maxima.

They are to be compared directly with Figs. 6–8. Better agreement could not be expected in view of the fewness of the experimental data. For other assumed separations the calculated wave-lengths of the intensity maxima do not agree so well with the observations.

Designating azimuths as shown in Fig. 10 is tantamount to stating that the gas atoms locate themselves directly over nickel atoms of the third layer. This location appeals to one as inherently probable. The separation of 3.0 A.[11] is greater by about fifty per cent than the separation of layers of nickel atoms parallel to the surface (2.03 A.). This also seems reasonable in view of the fact that the gas atoms are separated laterally by distances twice as great as the separations of nickel atoms.

. . . .

Our analyses of the diffraction patterns of the first, third and fourth types seem to us to be fairly satisfactory. The study of the diffraction pattern of the second type has, however, turned out to be futile. This pattern consisted of twelve diffraction beams, one in each of the principal azimuths of the crystal (see Fig. 10). All these beams appeared at the same co-latitude angle of about 58° and for the electron wave-length 1.17 A. We know that this curious pattern had its origin in a heavy layer of adsorbed gas, but we have been unable to determine what were the crystalline regularities in this layer. Our present feeling is that these beams may really have reached their intensity maxima at slightly different angles and wave-lengths in the different crystal azimuths, and that perhaps there may have been other beams belonging to this pattern which we did not detect. We are inclined to believe that we shall not be able to obtain information concerning the crystalline arrangement of a heavy gas layer until further experimental data are available.

. . . .

Looking back over the information recorded here concerning gas upon a crystal surface, one should think of it as information which has been obtained by a new method of diffraction analysis. Thinking of it in this way I realize that the observations are of a rather elementary nature. The facts which we have discovered are by no means comparable in complexity with the elaborately detailed information concerning crystal structure which is so readily obtained by X-ray analysis.

Electron diffraction is, however, a new field. At the time when the

[11] Logically this value of 3.0 A. should perhaps be changed by a few per cent to take into account a refractive index slightly different from unity.

experimental data described here were obtained, we could have learned a great deal more concerning gas upon our crystal surface with comparatively little effort. In the above pages there are many suggested continuations which were not followed up. When our measurements were made our interests were quite naturally centered upon the phenomenon that electrons are diffracted, and we neglected many lines of physical investigation which were open to us. The work described here must be regarded as only the very first application of what may possibly develop into a useful method of crystal analysis, occupying a field entirely distinct from the field of X-ray analysis.

Abstracts of Technical Articles From Bell System Sources

Relation of Nitrogen to Blue Heat Phenomena in Iron and Dispersion-Hardening in the System Iron-Nitrogen.[1] R. S. Dean, R. O. Day and J. L. Gregg. It has been generally observed that iron, as an outstanding exception among metals, increases its hardness and strength by low-temperature annealing after cold work, and also by increase of testing temperature to the range of 150° C. to 300° C. This investigation was made with the object of ascertaining if similar phenomena were observed in high purity iron and, if not, to the presence of which impurities these phenomena could be traced. After describing the tests made and giving the results, the authors come to the conclusion that commercial irons owe their property of hardening by reheating after cold work, as well as their increase in tensile strength in the range 100° C. to 300° C., to the solution of small amounts of iron-nitride present.

Heat Treatment and Mechanical Properties of Some Copper-Zinc and Copper-Tin Alloys Containing Nickel and Silicon.[2] W. C. Ellis and Earle E. Schumacher. The addition of nickel and silicon to the copper-zinc and copper-tin systems results in alloys which can be hardened by heat treatment. The heat treatment, in general, consists of a quench from 800° C. followed by hardening at 400° C. to 500° C. The dispersion-hardening effect of nickel and silicon in these alloys opens a considerable field in the manufacture of high strength brasses. The mechanical properties in the rolled condition of the hardened brass containing 30 per cent of zinc and 3 per cent of nickel plus silicon are in general similar to those of high brass sheet in the spring temper. The endurance limit in reversed flexure for this alloy in the hardened condition is, however, approximately 20 per cent higher than that of high brass sheet in the same temper.

A Metallographic Study of Tungsten Carbide Alloys.[3] J. L. Gregg and C. W. Küttner. This paper gives the results of an investigation of the structure of five of the tungsten-carbon alloys by means of microscopic and X-ray methods, the samples studied being small tools or wire-drawing dies. After a general discussion of the constituents of tungsten-carbon alloys, the preparation of the samples is described, and the structures found are shown in twenty-one figures accompanying the text.

[1] *Mining and Metallurgy*, Vol. 10, March, 1929, p. 163 (abstract).
[2] *Mining and Metallurgy*, Vol. 10, March, 1929, p. 162 (abstract).
[3] *Mining and Metallurgy*, Vol. 10, February, 1929, p. 94 (abstract).

Motion Pictures in Relief.[4] HERBERT E. IVES. In this article Dr. Ives describes the method by which stereoscopic motion picture projection can, theoretically at least, be attained. The method is relatively complicated and has severe practical limitations. It appears to be theoretically sound and capable of realization, at least on an experimental scale.

The Absorption of Oxygen by Rubber.[5] G. T. KOHMAN. The work reported in this paper was planned for the purpose of determining the part played by oxygen absorption in the natural aging of rubber. To do this, the effects of a number of factors known to influence natural aging on rates of oxygen absorption were studied. A piece of apparatus, developed for determining these rates, which involves special means for keeping the oxygen pressure surrounding the sample constant is described. The results obtained lead to the conclusion that oxygen absorption is the predominating factor in the natural aging of rubber and that rates of oxygen absorption are of value in predicting the natural life of rubber.

An Electrical Test for Tin Coating on Copper Wire.[6] H. M. LARSEN and C. M. UNDERWOOD. The method described is essentially a deplating process. The wire samples are placed in an acid solution and a current of suitable value applied to effect the deplating. The weight of tin on the wire surface and that alloyed with the copper are determined separately, the measuring means being two graduated tubes containing electrodes (sometimes called voltameters). The gas evolved in these voltameters is proportional to the current and hence to the tin being removed. As soon as the copper surface is exposed, an auxiliary electrode in the deplating bath actuates a relay which brings into operation the second voltameter, permitting determination of the tin alloyed with the copper.

Very simple formulæ permit determining the amount of tin from the volume of gas accumulated in the two voltameters. The method is said to save time and permit the use of relatively unskilled operators as compared with the usual chemical tests applied to tin coatings.

Further Observations on the Microstructure of Martensite.[7] FRANCIS F. LUCAS. This paper is a further contribution by Dr. Lucas on the microstructure of martensite. It describes a number of quenching and

[4] *Journal of the Optical Society of America and Review of Scientific Instruments*, Vol. 18, February, 1929, pp. 118–122.
[5] *Journal of Physical Chemistry*, Vol. 33, February, 1929, pp. 226–243.
[6] *Wire & Wire Products*, Vol. 4, April, 1929, pp. 118–119, 140.
[7] *Transactions of the American Society for Steel Treating*, Vol. 15, February, 1929, pp. 339–364.

tempering experiments in which commercial high quality tool steels were used. Representative structures found in the quenched and various tempered conditions are illustrated and discussed.

Technique of the Talking Movie.[8] DONALD MACKENZIE. In this article the talking movies are described in some detail as to mechanical features, production and exhibition. The author tells some interesting things about producing these pictures and the human reactions that must be considered in preparing a picture with sound record so that it will seem natural and the changes that producers will have to make to satisfy the public.

Some Long Distance Transmission Problems.[9] H. MOURADIAN. This paper discusses the transmission properties of high voltage power transmission lines with incidental reference to telephone transmission. The method of improving the performance of power lines by means of synchronous condensers at the ends and at intermediate points is discussed and compared with a proposed method in which neutralizing networks are neutralized at intervals. Each network consists of a pi whose series and shunt elements neutralize the corresponding elements of the line at the frequency of transmission. It is stated that the synchronous condensers increase the power transfer limits of the line but decrease the transmission efficiency, while the neutralizing networks increase both the power transfer limits and the efficiency. Illustrative numerical examples are given for a 220,000-volt line, 500 miles long. Some possibilities of a transcontinental power transmission line are discussed.

Electrical Conduction in Textiles. Part II—Alternating Current Conduction.[10] E. J. MURPHY. This paper shows the variation of the equivalent parallel capacity and conductance of cotton and silk with relative humidity and frequency (for a small range). It also shows the effect of changes in the amount of electrolytic material in the textile. The main results are: At high humidities the capacity is greatly reduced by a reduction in the amount of electrolytic material in the textile. The a.c. and d.c. conductivities of cotton approach each other as the humidity is increased and become equal at humidities greater than 80–85 per cent (that is, dielectric loss is entirely due to direct current conductivity in this range). At humidities lower than this a large part of the dielectric loss is not due to d.c. conduction, but this

[8] *Journal of the Western Society of Engineers*, Vol. 34, February, 1929, pp. 95–102.
[9] *Journal of the Franklin Institute*, Vol. 207, February, 1929, pp. 165–192.
[10] *Journal of Physical Chemistry*, Vol. 33, February, 1929, pp. 200–215.

part of the dielectric loss is also strongly affected by the amount of electrolytic material in the textile. These characteristics can be explained if the textile is regarded as an electrolytic cell in which the absorbed water and dissolved salts form the electrolyte and the solid constituents of the textile act as a container which determines the volume, geometric form and specific conductance of the electrolyte. The capacity at high humidities is regarded as due chiefly to the electrolytic polarization capacity of this electrolyte.

Electrical Conduction in Textiles. Part III—Anomalous Properties.[11] E. J. MURPHY. This paper deals with the increase of conductivity with increasing applied voltage (the Evershed effect), and with the residual electromotive forces and changes in resistance produced by the passage of current through the textile. The results point to the conclusion that the Evershed effect is due to two factors, a back-e.m.f. due to electrolytic polarization, and an increase, caused by the increase in voltage, in the amount to which the ions adsorbed by the interface between the aqueous solutions and the solid material of the textile contribute to the total conductivity. The characteristics of the residual e.m.f. change with humidity; at high humidities the e.m.f. is apparently caused by chemical changes in the aqueous solutions due to their electrolysis. It was found that the passage of a current through a textile causes its resistance to become non-uniformly distributed, the distribution depending on the nature of the electrode material; this is interpreted as due to changes in the chemical composition of the solutions in different parts of the textile. The anomalous properties can be explained in terms of the electrolytic cell mechanism suggested in the preceding paper by attributing to the solid in which the aqueous conducting paths are contained the properties of adsorbing ions and of hindering the equalization of concentration differences in the solutions by diffusion. Thus, all of the properties of conduction in textiles observed in this investigation can be explained in terms of a single general mechanism which appears to be a probable consequence of the colloidal structure of the materials.

Study of Weller Brittleness Test for Paper.[12] R. L. PEEK, JR. and J. M. FINCH. On the assumption that paper possesses certain basic properties, an expression is theoretically obtained relating the results of the Weller brittleness test to these basic properties, the dimensions of the sample, and the conditions of testing. Experimental data are presented which show that the effect of the sample dimensions and the

[11] *Journal of Physical Chemistry*, Vol. 33, April, 1929, pp. 509–532.
[12] *Paper Trade Journal*, Vol. 88, February 7, 1929, pp. 56–62.

conditions of testing are substantially as indicated by the theoretical expression. The theory is then employed to interpret the results of the test and to indicate the best form in which these may be expressed. The general question of testing for flexibility and brittleness is considered in the light of this study.

Diffusion of Water through Rubber.[13] EARLE E. SCHUMACHER and LAWRENCE FERGUSON. This article gives data on the diffusion of water through thirteen rubbers of different compositions. The mathematical derivation of a simple formula for calculating the rate of diffusion has been given. The diffusion measurements have shown: (*a*) that the rate of diffusion of water through a rubber membrane is inversely proportional to the square of the thickness: (*b*) that the rate of diffusion decreases greatly with increase in hardness; (*c*) that the effect of saturating the rubber with water is to increase the rate of diffusion through it, due probably not only to an increase in the water vapor pressure within the rubber, but also to a decrease in hardness; (*d*) that there is no intimate relationship between rate of diffusion and minor variations in the composition of the rubber.

Effect of Arsenic on Dispersion-Hardenable Lead-Antimony Alloys.[14] K. S. SELJESATER. Arsenic has no solid solubility in lead and is known to form a continuous series of solid solutions with antimony. Therefore, immediately after annealing and quenching the antimony is in solid solution in the lead, and there is a certain amount of eutectic between the lead-antimony solid solution and arsenic. After quenching, the lead-antimony solid solution is supersaturated (the same as if arsenic were not present) and minute crystals of antimony separate. Since arsenic is soluble in antimony, some of the arsenic present will be concentrated in the surface layer of the minute antimony particles, which will then possess surface conditions different from those of pure antimony particles. The condition of the alloy at this stage is analogous to a suspension in a liquid which has been partly stabilized by a third constituent. Agglomeration and precipitation will occur, but at a much slower rate than if the third constituent were not present. Arsenic, therefore, is to be considered as a retardant for the agglomeration of minute antimony particles in the lead matrix. The length of the stabilization time decreases at elevated temperatures. The offered explanation is in agreement with the fact that the increase in hardness is practically independent of the percentage of arsenic within limits investigated. The addition of a third constituent insoluble in the

[13] *Industrial and Engineering Chemistry*, Vol. 21, February 1, 1929, pp. 158–162.
[14] *Mining and Metallurgy*, Vol. 10, February, 1929, p. 94 (abstract).

solvent and forming a continuous series of solid solutions with the solute, might be of advantage to other kinds of age-hardenable binary alloys.

A Precision Regulator for Alternating Voltage.[15] H. M. STOLLER and J. R. POWER. In this paper a recently developed precision voltage regulator for use with alternating current is described. It will maintain its output voltage constant to within 0.03 per cent over an input voltage range of 10 per cent and a load range of from zero to full load.

This regulation is accomplished by means of a small transformer inserted in one of the lines which boosts or bucks the impressed voltage by the required amount. The transformer is controlled by a vacuum tube circuit acting through an inductance bridge.

[15] *Journal of the A. I. E. E.*, February, 1929, Vol. 48, pp. 110–113.

Contributors to this Issue

C. J. Davisson, B.Sc., University of Chicago, 1908; Ph.D., Princeton University, 1911; Instructor in Physics, Carnegie Institute of Technology, 1911–17; Engineering Department of the Western Electric Company, 1917–25; Bell Telephone Laboratories, 1925–. Dr. Davisson's work since coming with the Bell System has related largely to thermionics and electronic physics.

G. W. Elmen, B.Sc., University of Nebraska, 1902; M.A., 1904; Research Laboratories of the General Electric Company, 1904–06; Engineering Department of the Western Electric Company, 1906–25; Bell Telephone Laboratories, 1925–. Mr. Elmen's principal line of work has been magnetic investigations. He is the inventor of the permalloy alloys. For this he was awarded the John Scott Medal in 1926 and the Elliott Cresson Medal in 1928.

J. G. Ferguson, B.Sc., University of California, 1915; M.Sc., 1916; Research Assistant in Physics, 1915–16; Engineering Department, Western Electric Company, 1917–25; Bell Telephone Laboratories, 1925–. Mr. Ferguson's work has been in connection with the development of methods of electrical measurement.

L. H. Germer, A.B., Cornell, 1917; M.A., Columbia, 1922; Ph.D., Columbia, 1927; Engineering Department, Western Electric Company, 1917–1925; United States Army, 1917–1919; Bell Telephone Laboratories, 1925–. Dr. Germer has been engaged chiefly upon work in thermionics and electron scattering.

C. H. G. Gray, B.Sc., Massachusetts Institute of Technology, 1918; Instructor, Electrical Engineering, Massachusetts Institute of Technology, 1918–19; Engineering Department, Western Electric Company, 1919–25; Bell Telephone Laboratories, 1925–. Mr. Gray, in addition to his work on the master reference system, has been engaged in the development and application of machine testing methods for the inspection of transmitters and receivers.

Charles H. Greenall, M.E., Lehigh University, 1922; Engineering Department, Western Electric Company, 1922–25; Bell Telephone Laboratories, 1925–. Mr. Greenall's work has involved investigation of telephone apparatus, and testing methods as applied to specification requirements and development of metallic materials.

F. R. Lack, B.Sc., Harvard, 1925; Engineering Department, Western Electric Company, 1913–22; First Lieutenant, Signal

Corps, A.E.F., 1917–19; Harvard, 1922–25; Bell Telephone Laboratories, 1925–. Mr. Lack has been engaged in experimental work connected with radio communication.

W. A. Marrison, Royal Flying Corps, later Royal Air Force, Canada, 1917–18; B.Sc., Queens University, Canada, 1920; A.M. in Physics and Mathematics, Harvard University, 1921; Western Electric Company, 1921–25; Bell Telephone Laboratories, 1925–. Mr. Marrison is engaged in the study of picture transmission and methods for the production of constant frequency.

W. H. Martin, A.B., Johns Hopkins University, 1909; B.Sc., Massachusetts Institute of Technology, 1911; American Telephone and Telegraph Company, Engineering Department, 1911–19; Department of Development and Research, 1919–. Mr. Martin's work has related particularly to transmission of telephone sets and local exchange circuits, transmission quality and loading.

W. O. Pennell, B.Sc., Massachusetts Institute of Technology, 1896; Instructor, Lafayette College, 1896–1898; Equipment and Traffic Engineer, Bell Telephone Company of Philadelphia, 1898–1902; Engineering Department, American Telephone and Telegraph Company, 1902–03; Chief Engineer, Missouri and Kansas Telephone Company, 1903–12; Southwestern Bell Telephone Company, 1912–29, and for the last eleven years their Chief Engineer. In addition to his activities as an engineer, Mr. Pennell has from time to time contributed articles of a mathematical nature to various technical publications.

J. R. Townsend, Engineering Department, Western Electric Company, 1919–25; Bell Telephone Laboratories, 1925–. Mr. Townsend has been largely concerned with the testing of telephone apparatus and more recently with the development of requirements of test for metallic materials.